THE DYNAMIC BEHAVIOR OF PARTICULATE SYSTEMS INVOLVING SIMULTANEOUS NUCLEATION AND GROWTH

by

BARRY LISS

A dissertation submitted to the Graduate Faculty in Engineering in partial fulfillment of the requirements for the degree of Doctor of Philosophy, The City University of New York.

1975

This manuscript has been read and accepted for the Graduate Faculty in Engineering in satisfaction of the dissertation requirement for the degree of Doctor of Philosophy.

Aug 17 75
date

Chairman of Examining Committee

Aug 18, 1975
date

Executive Officer

Robert A. Graff

Harry Soodak

Supervisory Committee

The City University of New York

TABLE OF CONTENTS

Heading	Page
ACKNOWLEDGEMENTS	i
LIST OF TABLES	iii
LIST OF FIGURES	iv
NOMENCLATURE	vi
INTRODUCTION	1
I - CONTINUOUS CRYSTALLIZATION	3
FORMULATION OF SYSTEM EQUATIONS FROM PHYSICS	11
I-I AREA DEPENDENT NUCLEATION AND GROWTH	11
I-II NUMBER DEPENDENT NUCLEATION	14
STEADY STATE ANALYSIS	15
STEADY STATE DEPENDENCE OF B AND G FOR DIFFERENT MODELS	17
LINEARIZED STABILITY ANALYSIS	24
CASE I B(c, a/ϵ), G(c, a/ϵ): Area Dependent Nucleation and Growth	24
CASE II B(c, n) G(c): Number Dependent Nucleation	29
CASE III Bennett, Fieldelman & Randolph Model	30
SUMMARY AND DISCUSSION	35
II - CONTINUOUS PRECIPITATION POLYMERIZATION	37
INTRODUCTION	37
DERIVATION OF THE SYSTEM EQUATIONS	41
STEADY STATE ANALYSIS	52
DYNAMIC ANALYSIS	64
APPENDIX	90
APPENDIX I-A	90

Table of Contents (cont.) Page

DEVELOPMENT OF AN AREA DEPENDENT NUCLEATION AND GROWTH MODEL 90

APPENDIX I-B 94

UNIQUENESS OF STEADY STATE FOR AREA DEPENDENCE .. 94

UNIQUENESS CONDITIONS FOR NUMBER DEPENDENT NUCLEATION 97

APPENDIX C 100

LINEARIZED STABILITY ANALYSIS: B(c, a/ϵ), G(c, a/ϵ) 100

LINEARIZED STABILITY ANALYSIS: B(c,n), G(c) 106

APPENDIX D 109

APPENDIX II-A..... 116

BIBLIOGRAPHY 121

VITA 128

ACKNOWLEDGEMENTS

In the spirit of true gratitude, I would like to acknowledge the many people that have aided me in their various ways in completing this thesis.

First of all, to Cyndee Rosen Liss who has been my closest companion through virtually all my college years. She has taken the brunt of my previous inability to complete things. She has perservered with me magnificently.

My life would not be what it is if it were not for my having met and worked with Stanley Katz. He inspired me and was responsible for the cohesive energy that went into my resolution of the higher mathematics involved in the work. He will always be remembered for leading me to a space from which I could think clearly and "see how things are."

If it were not for the patience and understanding that Reuel Shinnar has shown me, in particular since Stanley left us, I could not have completed this work. Along with his patience, his high level of intuitiveness into the underlying principles of physical phenomena supported this work and for both I will be forever grateful.

I would like to acknowledge that I was supported in this work by a University Fellowship, a NSF Grant, and a NASA predoctoral traineeship.

I would especially like to express my gratitude to Lou Cox in acknowledgement for the safe space he has given me to grow in.

Edward T. Coles also must be acknowledged for his patience with me. I am delighted and excited to be working with him on a project in which I can draw on the principles underlying the dynamic behavior of a complex particulate system which involves simultaneous nucleation and growth. I dedicate my present energies to steady progress in this direction.

I would also like to acknowledge Kathy Price and Rozetta Simmons who put their personal energy out in helping me complete the typing of this manuscript.

Finally, I acknowledge Melanie Liss, for all that she has given me and for being herself.

LIST OF TABLES

Table		Page
I-1	Nucleation and Growth Dependence Parametric Study	20
II-1	Equations Governing Dynamic Behavior of Precipitation Polymerization Reactors	51
II-2	Equations Governing Steady State Behavior Precipitation Polymerization Reactors	56
II-3	Expressions for Leading Moments of Radical and Polymer Size Distribution and Monomer Equilibrium	70
II-4	Limiting Values of Growth Sensitivities to Reactor Variables	76
II-5	Limiting Values of Nucleation Sensitivities to Reactor Variables	77

LIST OF FIGURES

Figure		Page
I-1	Representation of Data Obtained by Rosen.....	5
I-2	Apparent Growth Rate Versus Particle Size From Figure I-1, G(r) versus r.....	6
I-3	Model of Matz.....	7
I-4	Mean Particle Size Versus Residence Time for Cases of Table I-1.....	21
I-5	Nucleation Rate Versus Growth For Cases of Table I-1.....	21
I-6	Stability Limits for Surface Dependent Nucleation and Growth in b*, g*, plane with m as a Parameter.....	26
I-7	Asymptotic Stability Limits for a Continuous Crystallizer With Surface Dependent Nucleation and Growth Kinetics.....	27
I-8	Stability Limits for Systems with Number Dependent Nucleation Kinetics in b*, g*, plane with b_n as a Parameter.....	31
I-9	Minimum Values of g* for Stability in Systems with Number Dependent Nucleation Kinetics.....	32
I-10	Asymptotic Stability Limits for a System with Number Dependent Nucleation Kinetics.....	33
II-1	Surface Area Concentration of Precipitated Particles Variation with Residence Time for Growth and Coalescence Models.....	62
II-2	Comparison of Nucleation Versus Growth Rate for Growth and Coalescence Models.....	63
I-A-1	Particle Size Distribution for System with Area Dependent Nucleation and Growth.....	93
I-B-1	Graphical Representation of Equation I-(8)	95
I-B-2	Graphical Locus of Points in which R. H. S. = L. H. S. from Equation I-(8) and Figure I-B-1....	95

List of Figures (cont.) Page

I-B-3	Graphical Representation of Equation I-(9)	96
I-B-4	Graphical Locus of Points in which R. H. S. = L. H. S. from Equation I-(9) and Figure I-B-3	96
I-B-5	Graphical Representation of Uniqueness of (I-11) and (I-10)	98
I-(D-1)	Locus of Stable Region for Area Dependent Nucleation and Growth Kinetics with m < -4	112
I-(D-2)	Locus of Stable Region for Area Dependent Nucleation and Growth Kinetics with m > -4	113
I-(D-3)	Locus of Stable Region for Area Dependent Nucleation and Growth Kinetics is with m = -4	114

NOMENCLATURE

Latin

a..... Surface concentration of stable particles..... surface/volume

A..... Surface area of a particle size L ..... surface

$b_c(v)$... Cluster formation rate ..... number/(volume-volume)

b ..... A nucleation sensitivity parameter ..... dimensionless

b_Θ..... Slope of log B versus log G ..... dimensionless

b_c..... Nucleation sensitivity to solute concentration..... dimensionless

b_I..... Nucleation sensitivity to initiator concentration....dimensionless

b_m.... Nucleation sensitivity to monomer concentration... dimensionless

b_n..... Nucleation sensitivity to particle concentration ....dimensionless

b_r.....Nucleation sensitivity to mean volume/surface ratio. dimensionless

b^*.....Nucleation stability parameter..... dimensionless

B^o.....Appearance rate of nucleators..... number/(volume-time)

B..... Nucleation rate.....number/(volume-time)

B_c..... Nucleation by cluster coalescence.....number/(volume-time)

B_g.....Nucleation rate for growth model..... number/(volume-time)

B_p.....Nucleation by radical growth..... number/(volume-time)

B_T..... Nucleation by radical termination ..... number/(volume-time)

c..... Solute concentration in system ..... moles/volume

c_f..... Solute concentration in feed..... moles/volume

c_s..... Solute equilibrium concentration..... moles/volume

$E(M_L)$ Langmuir type equilibrium function.....moles/surface

$f(L)$ Particle size distribution function .....number/(volume-size)

g..... A growth sensitivity parameter.....dimensionless

g_c.....Growth sensitivity to solute concentration..... dimensionless

gm..... Growth sensitivity to monomer concentration..... dimensionless

g_I..... Growth sensitivity to initiator concentration.....dimensionless

L..... A characteristic size ..... length

L_c..... Critical nuclei size ..... length

$\mathcal{L}$..... Avogadro Number ..... number/ mole

m.... Area dependent stability parameter ..... dimensionless

m_I.... Parameter defined on page 55 ..... dimensionless

M_L.... Monomer concentration in liquid ..... moles/volume

M_o.... Monomer concentration in feed ..... moles/surface

M_T.... Slurry density ..... mass/volume

n..... Particle concentration ..... number/volume

n_f..... Particle concentration in feed ..... number/volume

$p_L(x)$ Liquid polymer size distribution ..... moles/(volume - d. p.)

$p_s(x)$ Solid polymer size distribution ..... moles/(surface - d. p.)

P_c... Cluster size distribution parameter ..... dimensionless

P^*.... Stability boundary polynomial ..... dimensionless

q..... Parameter defined on page 55 ..... dimensionless

$r_L(x)$.. Liquid radical size distribution ..... moles/(volume - d. p.)

$r_s(x)$... Solid radical size distribution ..... moles/(surface - d. p.)

r..... Characteristic crystal size ..... length

r_c.... Critical nuclei size ..... length

r_D.... Dominant mean crystal size ..... length

r_o..... Nucleation size ..... length

r_θ..... Slope of log r versus Log θ ..... dimensionless

$S(\Psi)$... Function derived from cluster size distribution dependence ..... dimensionless

g_1^*, g_2^*, g_3^* Roots of stability boundary P^* ..... dimensionless

g_θ .... Slope of log G versus log θ ..... dimensionless

G..... Growth rate ..... length/time

Gc.... Capture contribution to growth rate

G_L ... Growth rate contribution of cluster capture..... length/time

G_M ... Growth rate contribution of solute mass transfer... length/time

G_P.... Propagation contribution to growth rate..... length/time

h, h_c.. Mass transfer coefficients ..... length/time

I ..... Initiator concentration in system ..... moles/volume

I_o .... Initiator concentration in feed ..... moles/volume

$I_0(Z)$, $I_1(Z)$ Modified Bessel functions ..... dimensionless

j..... Dimensionless monomer equilibrium constant..... dimensionless

j_1.... Langmuir constant ..... length

j_2.... Langmuir constant ..... volume / mole

J.... Dimensionless Langmuir function ..... dimensionless

k..... Parameter defined on page 55..... dimensionless

k^o..... Nucleation rate constant ..... in Part I

K^1.... Nucleation rate constant ..... in Part II

k_i .... Initiator decomposition rate constant ..... 1 / time

k_{pL}... Propogation rate constant in liquid..... volume/(mole-time)

$k_p s$.... Propogation rate constant on surface ..... surface /(mole-time)

k_ϕ..... Parameter defined on page 65 ..... dimensionless

k_{TL}.... Terminal in rate constant in liquid ..... volume/(mole-time)

k_{TS}.... Terminal in rate constant on surface..... surface/(mole-time)

k_ϕ..... Parameter of cluster size distribution ..... dimensionless

l_p..... Parameter defined on page 55 ..... dimensionless

l_T.... Parameter defined on page 55 ..... dimensionless

s.... Complex parameter 1/time

t.... Time ..... time

u.... Parameter defined on page 55 .....dimensionless

v_c.... Critical nuclei size .....volume

v_I..... Molar volume of initiator ..... volume/mole

v_m.... Molar volume of monomer .....volume/mole

v_o ... A parameter defined on page 51

x .... Degree of polymerization .....d.p.

x_{cr}... Critical nuclei size of radical molecule ....d. p.

x_{cp}.... Critical nuclei size of polymer molecule .... d.p.

y..... Degree of polymerization .....d.p.

Y.... Dimensionless reactor variable .....dimensionless

Z..... Dummy size variable .....volume

α	Liquid to solid volume fraction ..... volume/volume
β	Nucleation sensitivity to area ..... dimensionless
β_c	Coalescence rate constant ..... dimensionless
γ	Growth sensitivity to area ..... dimensionless
$\Delta(x)$	Heavy side - sides step function ..... dimensionless
$\delta(x)$	Dirac delta function ..... length
$\delta(\ )$	Perturbation variable ..... dimensionless
ϵ	Liquid volume fraction ..... volume/volume
χ	Particle shape factor ..... dimensionless
Θ	Mean residence time ..... time
λ_{0L}	Total liquid radical concentration ..... moles/volume
λ_{1L}	Total volume of liquid radicals ..... volume/volume
λ_{0S}	Total solid radical concentration ..... moles/volume
λ_{1S}	Total volume of solid radicals ..... volume/surface
λ_ϕ	Parameter construct ..... dimensionless
λ_ω	Parameter construct ..... dimensionless
ρ	Particle density ..... moles/volume
σ	Parameter of cluster distribution ..... dimensionless
σ_S	Ratio of solid to liquid monomer..... dimensionless
σ_L	Ratio of reacted to unreacted monomer ..... dimensionless
$\bar{\phi}(v)$	Subcritical particle size distribution ..... number/volume-time
ϕ	Solute resource function in system ..... moles/volume
ϕ_f	Solute resource function @ feed condition ... moles/volume
ψ	Microcrystallite size distribution ..... number/volume-size
ψ^*	Stability function ..... dimensionless
ω	Measure of radical termination to capture rate ..... dimensionless

INTRODUCTION

This dissertation considers the dynamic behavior of complex particulate systems involving simultaneous nucleation and growth processes. Initially, the specific problem of the extreme sensitivity of continuous precipitation polymerization to reactor conditions was investigated through the setting up of mathematically treatable nucleation models. Subsequent development of the mathematical machinery for the study of the stability led to results which are broadly applicable to many continuous particulate processes. The analysis was applied to continuous crystallization. It specifically accounts for cycling in systems of low apparent kinetic order. . The method of this analysis can easily be extended to continuous fermentation, emulsion polymerization, coal conversion and many other continuous particulate processes.

The thesis is presented in two separate and distinct sections. The first portion is essentially the paper presented at the 67th Annual Meeting of the American Institute of Chemican Engineers in Washington, D. C. on December 5, 1974. In this paper stability criteria are determined for the operation of an MSMPR crystallizer in which particle nucleation and growth depend on properties of the existing crystal magma. Systems with surface dependent nucleation and growth, and systems with number dependent nucleation, are shown to be potentially highly unstable. Mechanisms for nucleation and growth are discussed in which the existence of micro-coalescence can be mathematically modeled by surface dependence. The results of these analyses account for low apparent values of $\frac{d\ln B}{d\ln G}$ in dynamically sensitive systems and also provide an alternate interpretation of growth rate data generated in stirred tanks.

The second portion is essentially the paper delivered before the 163rd meeting of the American Chemical Society in Boston in April, 1972. The paper considered the dynamic behavior of precipitation polymerization reactors. Different models for the nucleation of precipitated polymer

particles are presented: one in which the nuclei are formed in the liquid by propagation and termination past a critical size, others in which the nuclei are formed by the physical coalescence of subcritical particles. In all the models, the growth of precipitated particles is partly by propagation in the solid phase, and partly by physical capture of polymer from the liquid.

Kinetic analyses based on "steady state" approximation show that the growth and nucleation rates of the precipitated particles may be regarded as functions of initiator and monomer concentration and of the ratio of particle surface to liquid volume.

With these "steady state" kinetic approximations, linearized stability analyses are carried out for a continuous stirred tank reactor. To a good approximation, the stable limits can be expressed in terms of three kinetic sensitivity parameters: the first carrying essentially the dependence of particle nucleation rate on monomer and initiator: the second, the dependence of particle growth rate on monomer and initiator; and the third, the dependence of the nucleation and growth rates on particle surface.

The upshot of this study is the resulting awareness that systems in which nucleation occurs in situ can be extremely dynamically sensitive. It will be shown that interpretation of particle kinetics from steady state data is risky in that simple growth mechanisms can be indistinguishable in form from complex coalescence processes. In such cases only dynamic testing would lead to further knowledge of the kinetics.

I - CONTINUOUS CRYSTALLIZATION

INTRODUCTION

Cyclic variations in stirred tank product quality and yield have been observed in continuous crystallization (27, 37, 39, 40), fermentation (10), precipitation polymerization (44, 13, 5), and emulsion polymerization (11, 13, 28, 29, 30).

Up to the present, mathematical treatments of the dynamic behavior and stability of complex particulate systems have dealt mainly with crystallizers. (1, 15, 18, 19, 35, 37, 42, 43, 45) The dynamic behavior of precipitation polymerization reactors has been studied recently (20).

The underlying physical properties common to all these particulate systems, which produces cyclic instabilities, is the occurrence of competitive simultaneous nucleation and growth of particles with a considerable time lag from nucleation to growth to the mean particle size.

In most of the treatments of the stability of continuous crystallizers, simple functions for the nucleation and growth kinetics have been used, typically dependence on supersaturation. Limiting cases of size dependent growth rates have been handled. (1, 42)

With the forms for B and G specified, one can obtain the steady state behavior and compute stability criteria based on a linearized stability analysis. These methods have been used effectively to predict and correlate the steady state performance of crystallizers. The models also correctly predict the destabilizing effect of classification, the effect of classification on size distribution, the effect of staging and in limiting cases, the effect of size dependence of the growth rate on stability.

There are two places where the present state of the art falls short from accounting for actual system performance. The classical linearized stability analyses (37, 35, 42) will only predict the unstable behavior of a mixed suspension mixed product removal (MSMPR) crystallizer for systems in which the ratio of nucleation to growth sensitivity to perturbation in supersaturation is very high $\left\{\frac{d\ln B}{d\ln G} > 21\right\}$. Many systems

have a low apparent $\frac{d\ln B}{d\ln G}$ (typically between 1 and 5) and still exhibit cyclic instabilities.

A second problem is in correlating the measured crystal size distribution of a MS MPR crystallizer with the size dependent growth rates of individual crystals. If the particle size distribution is known, one can compute G(r) from the relation

$$f(r) = \frac{B}{G(c,r)} e^{-\int \frac{dr}{\Theta G(c,r)}}$$

where f(r) is the number distribution.

When the growth rate is size independent, a semi-log plot of the number distribution is expected to be linear. The slope can then be used to obtain a size independent growth rate. Many particle size distribution data for a MSMPR crystallizer, however, exhibit some curvature concave upward, see Figure I-1 (9, 31, 37, 45, 38), and in many instances a tendency toward downward concave at large particle sizes.

Data in the form of Figure I-1 at first glance seem to imply that the form of G(r) is that of Figure I-2 where small particles have an apparent growth rate significantly lower than the large particles. This implication is counter to classical mass transfer theory where the growth rate for small particles is significantly larger than the growth rate of the large particles (26). The data of Matz (24) is illustrated in Figure I-3. To account for the shape of the particle size distribution, Rosen and Hulburt (38) suggested that the large crystals could withstand high energy impacts while smaller crystals would shatter. This was treated mathematically by hypothesizing a critical size above which crystals would not shatter.

The data represented in Figure I-1 is of the same form hypothesized by Randolph and Larson (36) for a MSMPR crystallizer with fines destruction (r_c here being the maximum fines size). It has been suggested that there may be internal fines destruction by localized regions of unsaturation. If we assume that particles below 100μ have a high chance to coalesce

Figure I-1: Representation of data obtained by Rosen (Figure 10 in reference 38).

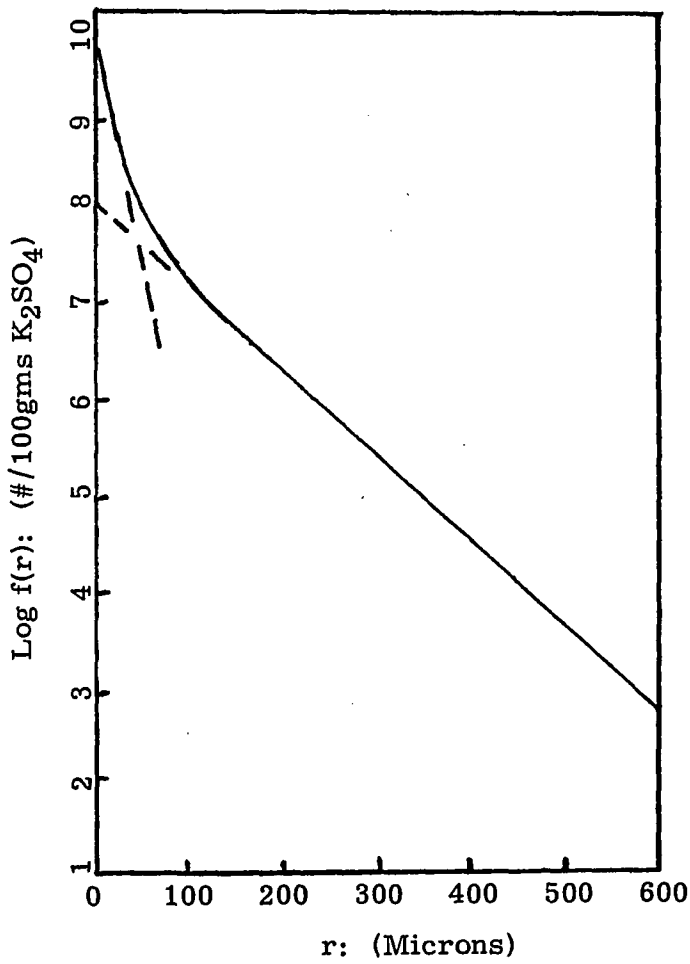

Figure I-2: Apparent growth rate versus particle size from Figure I-1, G(r) versus r.

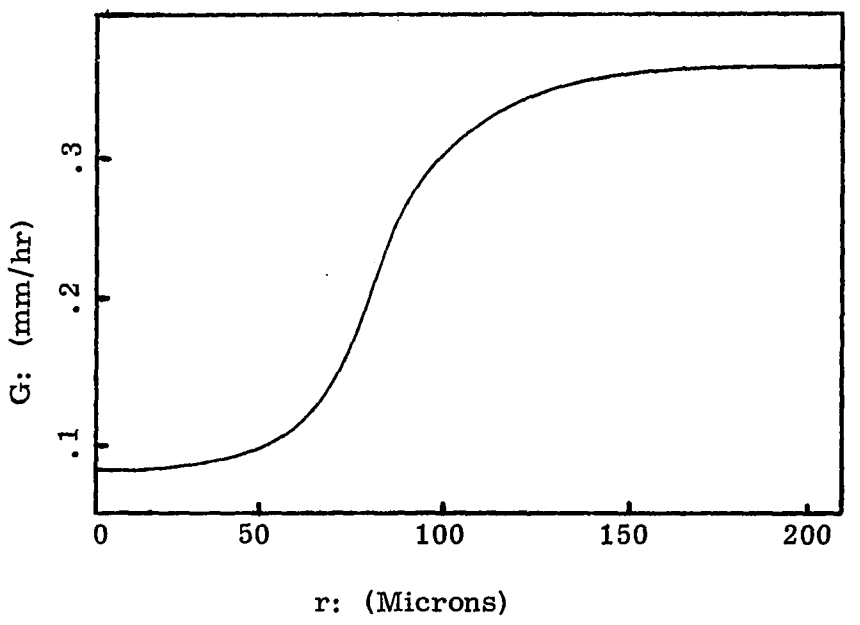

Figure I-3: Model of Matz (24) G(r) versus r/r_c for NaCl in H_2O.

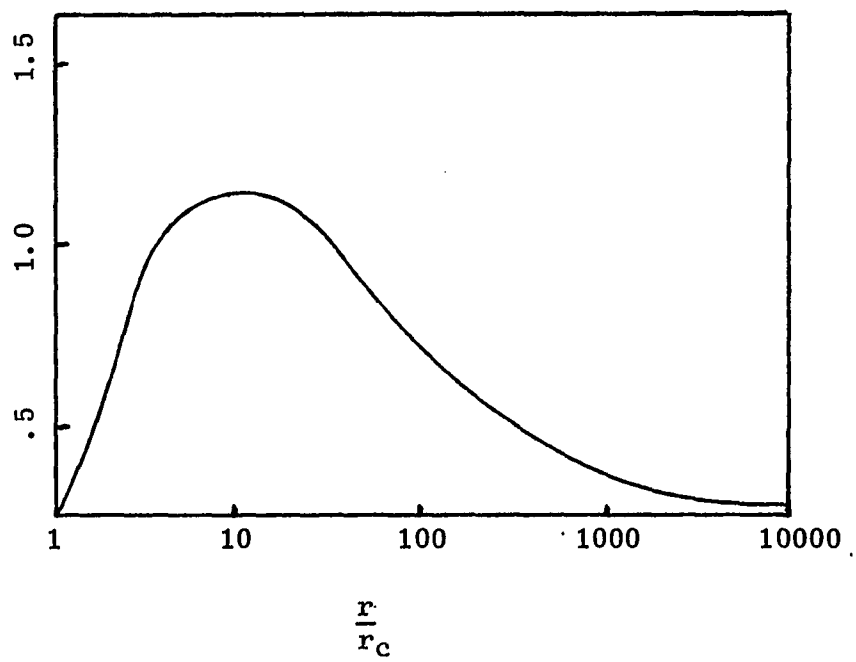

whereas large particles are stable, we would obtain such a distribution. Curvature in the large size range may be accounted for by non-ideal product withdrawal as well as a lower surface integration rate.

It is well known that the standard assumptions underlying the conventional analysis of both steady state and dynamic behavior of crystallizers (35, 37, 42, 45) contain some very strong simplifying assumptions. The effect of size dependent growth rate has already been investigated (1, 42) and has been found to be small. The major effect that until now has been virtually neglected is the effect of the properties of the magma on both nucleation and growth.* In the previous references the only feedback that the magma exercises on these processes is via the supersaturation. We know, however, that other feedbacks are possible and have been suggested in the literature. One well known effect is secondary nucleation in which nuclei formation is enhanced by the presence of existing crystals (7, 16, 31, 32, 34, 46, 47). Several investigators have suggested nucleation mechanisms due to attrition or secondary nucleation enhanced by collisions(3, 31, 32, 17, 6). Bennett (4) has recently summarized some of these methods. In all of the aforementioned cases, it is possible to approximate the dependence of the nucleation rate on the properties of the magma by a relation $B = B(c-c_S, \mu n)$ where μn are the moments of f(r).

$$\mu_n \triangleq \int_0^\infty r^n f(r) dr$$

The hydrodynamic conditions can be included in the constants or form of $B(c-c_S, \mu n)$. Instead of $c-c_S$ we also can use an average growth rate G. Thus the model of Bennett and Randolph for secondary nucleation in the impeller region becomes

$$B = k G M_0 \left(\frac{M_3}{M_2}\right)^4$$

*A recent paper by Larson et al. (3) has brought attention to the need for definition of nuclei survival.

Dependence of nucleation on one or several of the leading moments arises in other complex particulate systems. In emulsion polymerization nucleation dependence on area arises from the surface requirements of soap to produce stable emulsified particles. In biological processes such as continuous fermentation, dependence of new microorganism formation is widely accepted as being dependent on existing number. Number dependence might be useful in some systems to approximately model the dependence of the size distribution of the existing suspension on nucleation from crystal-impeller or crystal-crystal collisions.

Thus it makes sense to look, in general, at how the dependence of nucleation rate on the moments of the size distribution effects the behavior of a crystallizer. Such is the object of this paper. For generality, we also include a possible dependence of G on μ_n, which is especially important for systems in which growth occurs due to coalescence (2).

Most of the cases mentioned until now deal with situations in which the dependence of B on the moments is either linear or at least not highly non-linear. $\left\{\frac{d\ln B}{d\ln G} < 5\right\}$

A much stronger dependence was encountered in a study of precipitation polymerization. In this case it has been shown (21) that small particles are unstable and coalesce either between themselves or with larger particles. Coalescence between two particles above a critical size is very slow. Such systems exhibit cyclic instabilities very similar to those of a crystallizer (21). In this case nucleation is highly dependent on the area of stable particles present and can be approximated by

$$B = k e^{-k' \frac{M_2}{G}}$$

Depending on the value of the exponent, $\frac{d\ln B}{d\ln \mu_2}$ can be very large.

As such models have properties very similar to those of a crystallizer

(low values of $\frac{d\ln B}{d\ln G}$ and a high degree of instability), an investigation was carried out to see if some crystallizers would not have similar properties. It was found that Glassner (12) has proposed a very similar mechanism for some crystallizations, and we will, therefore, discuss this model in detail.

Glassner's observations in crystallization are consistent with the basic properties of the models for precipitation polymerization. Briefly stated, it is assumed that particles above a critical size will not coalesce. This is consistent with Smoluchoski's equations where the collision efficiency drops 10-50 orders of magnitude in an order of magnitude of particle size (typically around .1 mm!) (41). Smaller particles may coalesce with one another or be captured by the particles above the critical size. Here we have a non-thermodynamic critical size referring to probability of effective coalescence and not to stability with respect to dissolution. It is in this sense that large crystals might act as a fines trap accounting for the shape of crystal size distributions typically observed. Independent of whether nucleation is homogeneous or heterogeneous, the total surface area of suspended particles can clearly decrease the survival probability of a growing nuclei and thereby be a controlling factor determining the effective nucleation rate. Mechanisms in this class result in nucleation and growth rates that will decrease with increasing surface. In the case in which secondary nucleation predominates, a large surface induces nucleation through some type of collision-attrition or breeding mechanism. (7, 17, 31)

Note that these models contain either the zeroth moment (total number) or the second moment (total surface) and this presentation will concentrate on those two cases, though one other case (4) will also be considered.

FORMULATION OF SYSTEM EQUATIONS FROM PHYSICS

(I-I) Area Dependent Nucleation and Growth

In this mathematical analysis of the behavior of the isothermal well mixed crystallizer, three assumptions are made.

a. The crystallizer is ideally mixed and the product removed will be a representative fraction of the dispersion inside the crystallizer.

b. The crystal growth rate is a function of supersaturation, is independent of particle size, but may be dependent on the moments of the particle size distribution - here, specifically, the area of crystals per unit liquid volume.

c. The nucleation rate is a function of the supersaturation and may depend, as the crystal growth rate, on the area of crystals per unit liquid volume.

Based on these assumptions, one may set down the governing equation describing the behavior of such a crystallizer.

With the crystals taken to be geometrically similar solids, the growth kinetics are described in terms of a characteristic linear dimension, r, as $G = dr/dt$; a constant.

The dispersion of crystal sizes may be characterized by a number density $f(r,t)$ where $f(r,t)\,dr$ is the number of crystals, in a unit volume, lying in the size range r, r + dr at a time t.

The volume of a particle of size r is taken to be kr^3 where k is the particle shape factor. Thus, the volume fraction of solids can be computed as $k\int_0^\infty r^3 f(r,t)\,dr$, and hence the liquid fraction $\epsilon(t) = 1 - k\int_0^\infty r^3 f(r,t)\,dr$. The area of solids may be computed given f(r,t) as: $a = 3k\int_0^\infty r^2 f(r,t)\,dr$

and thus the ratio of solids area to liquid volume "a/ϵ" may be computed given f(r, t).

The nucleation kinetics is taken to apply to the liquid phase or at the interface, hence B, the nucleation rate, is defined such that $\epsilon \cdot B$ is the total number of crystals per unit time per unit reactor volume formed at a vanishing small size (i.e., nuclei size is small compared to the mean crystal size). The nucleation and growth rates are taken to be functions of the supersaturation and also the ratio a/ϵ.

B may be an increasing or decreasing function of a/ϵ. In the region where nucleation is primarily a secondary effect such as breeding, one might expect B to increase with increasing a/ϵ. Alternatively, we can assume that a large surface of crystals per unit liquid volume provides a sink (an internal "fines trap") for potential nuclei in the liquid. The resulting capture of such potential nuclei reduces effective nucleation. Thus where contact nucleation may be occurring in the impeller region, the survival of the nuclei produced will be strongly a function of the existing state of the magma. If the residence time of subcritical sized particles in the bulk is a function of the capturing surface available, the growth rate of the stable particles can be a strong function of area in that the mass accumulated by the subcritical sized aggregates contributes to the growth rate. A simplified model leading to this type of dependence is considered in Appendix (I-A). Note that such modelling accounts for the shape of particle sized distribution data typically obtained.

Here, our presentation follows the method of Hulbert and Katz (48). Assuming , the crystal density, to be constant, and cf to be the solute inlet concentration in the clear feed, an overall material balance may be written at a given residence time θ.

$$\text{I-(1)} \qquad \frac{d\{\epsilon(t)\cdot C(t)+(1-\epsilon(t))\cdot\rho\}}{dt} = \frac{1}{\theta}\cdot C_f - \frac{1}{\theta}\{\epsilon(t)\cdot C(t)+(1-\epsilon(t))\cdot\rho\}$$

A balance of particles of size r may also be written:

$$\text{I - (2)} \quad \frac{\partial f(r,t)}{\partial r} + G(c,a/\epsilon)\cdot\frac{\partial f(r,t)}{\partial r} = \epsilon(t)\cdot B(c,a/\epsilon)\cdot\delta(r) - \frac{1}{\Theta}\cdot f(r,t)$$

where the left hand side represents accumulation of particles of a given size r and the growth rate of particles past the given size r, respectively. The right hand side represents accumulation of particles of a given vanishing small size r→o, and the particle take off rate respectively. (i.e., We are not overly concerned with the size distribution of subcritical sized crystals at this level of analysis; we are only concerned with the rate at which stable crystals are formed from the subcritical sized aggregates, it is only necessary to assume that the mass of the newly nucleating crystals is small compared to the total magma mass; the nucleation rate can then be written based on a "quasi steady state" approximation for the size distribution of subcrits in a manner similar to that used in the analysis of precipitation polymerization. See Appendix I-A.

The particle balance can be rewritten with the term representing the fact that all new crystals are formed at a vanishingly small size taken as a boundary condition. One now has a self contained set of equations for the determination of c(t) and f(r, t) in terms of the functional relationships B(c, a/ϵ) and G(c, a/ϵ) which are assumed to be known.

The governing equations are:

$$\text{I - (1a)} \quad \frac{d\{\epsilon\cdot C + (1-\epsilon)\cdot\rho\}}{dt} = \frac{1}{\Theta}\cdot C_f - \frac{1}{\Theta}\cdot\{\epsilon\cdot C + (1-\epsilon)\cdot\rho\}$$

$$\text{I - (2a)} \quad G(c,a/\epsilon)\cdot f(r,t) = \epsilon\cdot B(c,a/\epsilon)\ ;\ r = 0$$

$$\frac{\partial f(r,t)}{\partial t} + G(c,a/\epsilon)\cdot\frac{\partial f(r,t)}{\partial r} = -\frac{1}{\Theta}\cdot f(r,t)\ ;\ r > 0$$

where:

$$a = 3k\int r^2 f\,dr$$

$$\epsilon = 1 - k\int r^3 f\,dr$$

(I-II) Number Dependent Nucleation

Consider a crystallizer operating in a range in which the nucleation kinetics may be taken to be a function of the supersaturation level and n the existing number of particles. Here the particle growth rate is taken to depend on supersaturation alone and also be size independent. With B(c, n), the number of particles formed per unit time per unit crystallizer volume, and $G(c) = \frac{dr}{dt}$, both assumed to be known functions, we can write down the equation for the particle size distribution function as

$$\frac{\partial f(r,t)}{\partial t} + G(c) \cdot \frac{\partial f(r,t)}{\partial r} = B(c,n) \cdot \delta(r) - \frac{1}{\Theta} f(r,t)$$

Rewriting the particle distribution equation with the delta function in the boundary condition and using the same form as in the previous case for the crystallizable material balance, one is left with the following equations governing the dynamic behavior of continuous crystallizers with number dependent nucleation kinetics:

I -(1b)
$$\frac{\partial f(r,t)}{\partial t} + G(c) \cdot \frac{\partial f(r,t)}{\partial r} = -\frac{1}{\Theta} \cdot f(r,t) \quad ; \quad r > 0$$

$$G(c) \cdot f(r,t) = B(c,n) \quad ; \quad r = 0$$

I -(2b)
$$\frac{d\{\epsilon(t)\, c(t) + (1-\epsilon(t))\cdot\rho\}}{dt} = \frac{1}{\Theta} \cdot C_f - \frac{1}{\Theta} \cdot \{\epsilon(t) \cdot c(t) + (1-\epsilon(t))\cdot\rho\}$$

with:
$$n(t) = \int_0^\infty f(r,t)\, dr$$

$$\epsilon(t) = 1 - K \int_0^\infty r^3 f(r,t)\, dr$$

STEADY STATE ANALYSIS

It is now possible to study the steady state behavior of an isothermal mixed crystallizer based on the equations developed in the preceding section.

Let us first consider the case where B and G are functions of the total surface. Setting the time derivative in the particle balance equal to zero yields the following steady state equation:

$$G(c, a|\epsilon) \cdot f(r) = \epsilon \cdot B(c, a|\epsilon) \qquad ; r = 0$$

$$\text{I-(3)} \quad G(c, a|\epsilon) \cdot \frac{\partial f(r)}{\partial r} = -\frac{1}{\Theta} \cdot f(r) \qquad ; r > 0$$

where a and ϵ are given by the following relations:

$$a = 3K \int_0^\infty r^2 f(r) dr$$

$$\epsilon = 1 - K \int_0^\infty r^3 f(r) dr$$

The solution for the steady state particle number density is:

$$\text{I-(4)} \quad f(r) = \epsilon \cdot \frac{B(c, a|\epsilon)}{G(c, a|\epsilon)} \cdot e^{\frac{-r}{\Theta G(c, a|\epsilon)}}$$

Having obtained the steady state particle distribution, a and ϵ can be obtained by direct calculation of the moments. This computation yields:

$$a = 6K\epsilon \frac{B}{G} (\Theta G)^3$$

$$\epsilon = 1 - 6K\epsilon \frac{B}{G} (\Theta G)^4$$

Combining these results yields the surface to volume ratio of the crystals:

$$\text{I - (5)} \qquad \frac{a}{1-\epsilon} = \frac{1}{\Theta G}$$

By rearranging the second relationship yields an expression for the voidage

$$\text{I - (6)} \qquad \epsilon = \frac{1}{1 + 6K \frac{B}{G} (\Theta G)^4}$$

Turning now to the overall material balance and setting the time derivative to zero yields:

$$\text{I - (7)} \qquad C_f = \epsilon \cdot C + (1-\epsilon) \cdot \rho$$

Thus the voidage ϵ may also be written as:

$$\epsilon = \frac{\rho - C_f}{\rho - C}$$

Bringing this result to equations (5) and (6) yields the following equations respectively:

$$\text{I- (8)} \quad \Theta \cdot G \cdot a/\epsilon = \frac{C_f - C}{\rho - C_f}$$

$$\text{I - (9)} \quad 6K \frac{B}{G} (\Theta G)^4 = \frac{C_f - C}{\rho - C_f}$$

The solution to the steady-state equations I-(3) and I-(7) for the quantities c and a/ϵ will depend on the solutions to equations I-(8) and I-(9). With c and a/ϵ known, ϵ can be calculated from the overall material balance or from either equation I-(6) or I-(7) and the full distribution f(r) is then known. Thus the steady state behavior can be computed with a form for $B(c, a/\epsilon)$ and $G(c, a/\epsilon)$ specified. Uniqueness criteria

for the solution of I-(8) and I-(9) are presented in Appendix I-B.

One can easily modify this solution for the case where B depends on the total number. The steady state solution with number dependent nucleation kinetics is obtained by setting the time derivatives in (1b) and (2b) equal to zero. The steady state size distribution is found by direct integration to be

$$f(r) = \frac{B(c,n)}{G(c)} e^{\frac{-r}{\theta G(c)}}$$

With this result ϵ can be computed as a function of c and n and eliminated leaving the following two equations governing the steady state below:

I-(10) $$n = B(c,n) \cdot \theta$$

I-(11) $$n = \left(\frac{\rho - c}{c_f - c}\right) \frac{1}{6k\{\theta G(c)\}^3}$$

Given specific forms for B(c, n) and G(c), the steady state solution could then be obtained. Reasonably broad sufficient conditions for a unique steady state which should cover basic cases of interest are considered in Appendix I-B.

Steady State Dependence of B and G for Different Models

While it is not possible to uniquely determine the mechanism of secondary nucleation from steady state MSMPR data (35) nor can the nucleation and growth sensitivity to parametric variations in the system variables (i.e. $\frac{d\ln B}{d\ln c}$, $\frac{d\ln B}{d\ln a/\epsilon}$, $\frac{d\ln G}{d\ln c}$, etc.) be uniquely determined, it is possible to test whether data taken over a residence time range is consistent with a given model for nucleation and growth.

Nucleation and growth rates can be computed at a first level of approximation by measuring the suspension density and mean particle

size at a given residence time and computing B and G based on the relationships:

I-(12) $$G = \frac{\langle r_j \rangle}{j \cdot \Theta} \qquad \text{where } \langle r_j \rangle = \frac{M_i}{M_{j-1}}$$

$$B = \frac{j^3 \cdot M_T}{6K \langle r_j \rangle^3 \Theta}$$

When particle size distribution data is available, B and G can be computed from the intercept and slope, respectively. For the standard case, this is written as

$$\frac{d\ln r}{d\ln \theta} = \frac{\frac{d\ln B}{d\ln G} - 1}{\frac{d\ln B}{d\ln G} + 3}$$

First consider the cases in which nucleation and growth depend on supersaturation and surface concentration of crystals. Using equations (3, 9, 12) it is possible to develop an explicit expression for $\frac{d\ln r_j}{d\ln \theta}$ in terms of the partial derivatives of the nucleation and growth rates with respect to solute and area concentrations at any given steady state in question. It is these partial derivatives that carry with themselves the essential properties of the model that determine the slope of the steady state as well as the dynamic behavior of such systems. An expression for $r_\theta = \frac{d\ln r_j}{d\ln \theta}$ can be written as follows:

I-(13) $$r_\theta = \frac{d\ln\langle r_j \rangle}{d\ln \Theta} = \frac{(b^* - (1-m)g^* + (1-m))}{(1+\gamma)(b^* + \alpha g^* + m)}$$

$$b^* = \alpha\left\{(1+(\tfrac{\rho-c}{c})b_c)(1+\gamma) - \beta((\tfrac{\rho-c}{c})g_c + 1)\right\}$$

$$b^* = (\tfrac{1-\epsilon}{\epsilon})\left\{(1+(\tfrac{\rho-c}{c})\tfrac{\partial \ln B}{\partial \ln c})(1+\tfrac{\partial \ln G}{\partial \ln a/\epsilon}) - \tfrac{\partial \ln B}{\partial \ln a/\epsilon}((\tfrac{\rho-c}{c})\tfrac{\partial \ln G}{\partial \ln c} + 1)\right\}$$

$$g^* = \alpha\left\{(\tfrac{\rho-c}{c})g_c - \gamma(\tfrac{1+\alpha}{\alpha})\right\} = (\tfrac{1-\epsilon}{\epsilon})\left\{(\tfrac{\rho-c}{c})\tfrac{\partial \ln G}{\partial \ln c} - \tfrac{\partial \ln G}{\partial \ln a/\epsilon}(\tfrac{\epsilon}{1-\epsilon})\right\}\Big/(\tfrac{\epsilon}{1-\epsilon})\Big\}$$

$$m = \beta - \gamma = \frac{\partial \ln B}{\partial \ln a/\epsilon} - \frac{\partial \ln G}{\partial \ln a/\epsilon}$$

$$\Gamma \qquad \frac{\partial \ln a/\epsilon}{\partial \ln a/\epsilon}$$

In considering the asymptotic range of $g_c \gg 1$ and looking at the area independent growth case, a simplified expression results from which insight into the present analysis can be gained.

For $g_c \gg 1$ and $\gamma = 0$

I-(14) $$\frac{d \ln \langle r_j \rangle}{d \ln \theta} = r_\theta \sim \frac{\frac{b_c}{g_c} - 1}{\frac{b_c}{g_c} + 3 - \beta}$$

Several points ought to be made concerning this result. First of all, in cases in which nucleation and growth sensitivity to supersaturation are equal, the mean particle size ought not to vary significantly with residence time. Several systems are reported to exhibit such behavior. Also, from equation I-(14) it is clear that a large negative area dependence has a flattening effect on the steady state mean particle size slope. (Values of $(-50 < \beta < -10)$ are obtained in the model in which nuclei survival is a factor.) Conversely, models for secondary nucleation that assume effective nucleation increases with surface are equivalent to low positive values of β and asymptotically have little effect on the slope r_θ.

A similar expression for r_θ is obtained for the case of number dependent nucleation and growth.

I-(15) $$r_\theta \sim \frac{\frac{b_c}{g_c} - 1}{\frac{b_c}{g_c} + 3(1 - b_n)} \quad ; \quad g_c \gg 1$$

Compared here are the effects of modelling a continuous crystallizer over a narrow range of operating conditions. Data is typically available at high fractions of crystallization (.80 - .98). The product quality considered here is the dominant mean particle size $\langle r_j \rangle = \langle r_3 \rangle = 3 G \theta \frac{\mu_3}{\mu_2}$ The steady state performance of the following empirical models (See Table I-1) are presented in Figures I-4 and I-5.

Table I-1: Nucleation and Growth Dependence Parametric Study

CASE	β	γ	$\frac{bc}{gc}$	r_Θ	$\frac{b_\Theta}{g_\Theta}$
1	0	0	2.5	.27	2.5
2	-1	0	2.5	.23	2.2
3	1	0	2.5	.33	3.0
4	0	-1	2.5	-.5	5
5	-18	0	18	.44	4.1
CASE	b_n		$\frac{bc}{gc}$	r_Θ	$\frac{b_\Theta}{g_\Theta}$
6	1		2.5	.60	7.0
7	2		2.5	-3.0	-2.0

Figure I-4: Mean particle size versus residence time Log (r) versus Log θ for cases of Table I-1

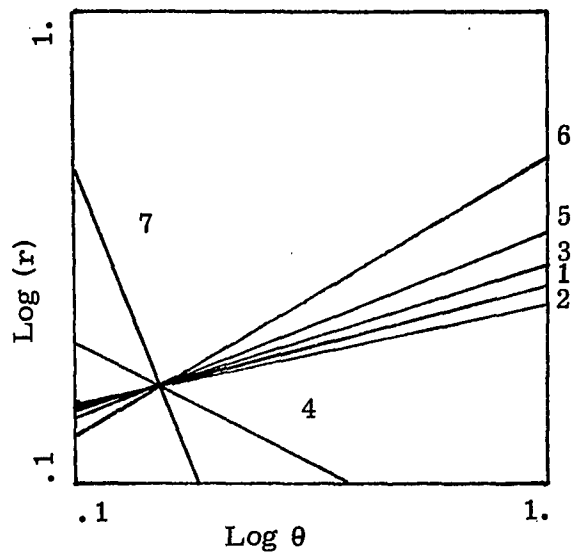

Figure I-5: Nucleation rate versus growth rate Log b versus Log G for cases of Table I-1

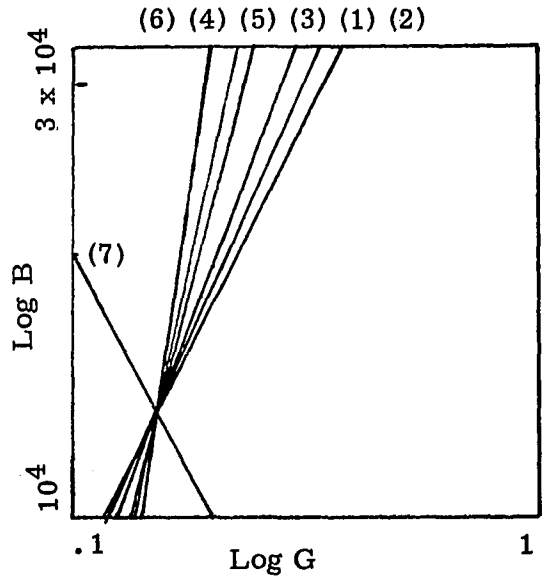

In their computation of stability criteria, Randolph and Larson use plots of log B vs. log G to obtain the stability parameter $\frac{d\ln B}{d\ln G}$ which in their analysis is essentially $\frac{\frac{d\ln B}{d\ln c}}{\frac{d\ln G}{d\ln c}}$. Where it has been assumed B and G to be functions of supersaturation and surface concentration a/ϵ, One must consider steady state data in terms of a total differential. That is, if one plots log B vs. log G taken at various residence times and obtaines a slope $\frac{d\ln B}{d\ln G}$, this ratio is in reality $\frac{\frac{d\ln B}{d\ln \theta}}{\frac{d\ln G}{d\ln \theta}}$. The slope

$\frac{b_\theta}{g_\theta} = \frac{d\ln B}{d\ln G}$ is then expressed as follows:

$$\frac{d\ln B}{d\ln G} = \frac{b_\theta}{g_\theta} = \frac{\frac{b_c}{g_c} + \frac{\beta}{g_c}\frac{d\ln a/\epsilon}{d\ln c}}{1 + \gamma \frac{d\ln a/\epsilon}{d\ln c}}$$

where

$$b_c = \frac{\partial \ln B}{\partial \ln C}$$

$$g_c = \frac{\partial \ln G}{\partial \ln C}$$

$$\beta = \frac{\partial \ln B}{\partial \ln a/\epsilon}$$

$$\gamma = \frac{\partial \ln G}{\partial \ln a/\epsilon}$$

Using equations I -(8, 9) it is possible to obtain an expression for $\frac{d\ln a/\epsilon}{d\ln c}$ in terms of the steady state parameters:

$$\frac{d\ln a/\epsilon}{d\ln c} = \left(\frac{3 + 3\alpha + \alpha\left(\frac{\rho - c}{c}\right) g_c - \alpha\left(\frac{\rho - c}{c}\right) b_c}{\beta - \gamma - 4} \right) \frac{1}{\alpha\left(\frac{\rho - c}{c}\right)}$$

In the asymptotic working range $g_c \gg 1$ the equation for $\frac{b_\theta}{g_\theta}$ may then be written as:

$$\frac{b_\theta}{g_\theta} = \frac{b_c}{g_c}\left\{\frac{4+\gamma}{4+\gamma\frac{b_c}{g_c}-\beta}\right\} - \left\{\frac{\beta}{4+\frac{b_c}{g_c}-\beta}\right\}$$

From this expression it can be seen how survival mechanisms involving surface (i.e. $\beta \ll 0$ a large negative surface dependence) yield low measured slopes of b_θ/g_θ even if the b_c/g_c ratio is high. This fact is part of the difficulty in establishing mechanisms from steady state data.

For the number dependent nucleation case, the measured slope $\frac{b_\theta}{g_\theta} = \frac{d\ln B(c,n)}{d\ln G(c)}$ can be expressed as a simple function of b_c/g_c and bn . In the range $(g_c \gg 1)$ this expression is:

$$\frac{b_\theta}{g_\theta} \sim \frac{4\frac{b_c}{g_c} - 3b_n}{4-3b_n}$$

It is clear from this form that measured slopes of log B vs. log G data may have large positive values and may also result in a negative slope, depending on the actual number dependence as well as the dependence on supersaturation. The above example uniquely demonstrates that in the case where B or B and G depend on the moments of the size distribution, data on $\langle n_j \rangle$ versus θ or B versus G give little insights as to the mechanism or kinetics of the crystallization. This fact has previously been illustrated (35, p. 232).

LINEARIZED STABILITY ANALYSIS

Case I. B(c, a/ϵ), G(c, a/ϵ): Area Dependent Nucleation and Growth

The equations governing the dynamic behavior of an MSMPR crystallizer with surface dependent nucleation and growth kinetics are rewritten in the following form:

$$\frac{d\,\phi(t)}{dt} = \frac{1}{\theta}\cdot\phi_f - \frac{1}{\theta}\cdot\phi(t)$$

$$G(c,a|\epsilon)\cdot f(r,t) = \epsilon(t)\cdot B(c,a|\epsilon)\ ;\ r=0$$

$$\frac{\partial f(r,t)}{\partial t} + G(c,a|\epsilon)\cdot\frac{\partial f(r,t)}{\partial r} = -\frac{1}{\theta}\cdot f(r,t)\ ;\ r>0$$

where

$$a = 3k\int r^2 f(r,t)\,dr$$

$$\epsilon = 1-k\int r^3 f(r,t)\,dr$$

$$\phi = \epsilon\cdot c + (1-\epsilon)\cdot\rho$$

$$\phi_f = c_f$$

In Appendix I-C the above equations are linearized and a formal spectral analysis is performed on the resulting linear operator. Application of the Routh - Hurwitz criteria to the resulting characteristic equation results in conditions for stability that may be expressed as:

$$-\left\{3g^*+1-m\right\} < b^* < \left\{\frac{21g^{*3}+(87-3m)g^{*2}+(128-2m)g^*+(64-m)}{(g^*+4)^2}\right\}$$

I-(16)

$$g^* > -2+\sqrt{-\left(\frac{m+4}{4}\right)}\ ;\ \text{for } m\le -5$$

$$g^* > -\frac{2}{3}\left(2+\left(\sqrt{-\left(\frac{m+4}{4}\right)}\right)^2\right);\ \text{for } m\ge -5$$

The stability conditions are plotted in the (b*, g*) plane for various values of m in Figure I-6. The derivation of the conditions is given in Appendix I-D. The lower limits have not previously been acknowledged in the literature and there may be systems in which mechanisms resulting in such nucleation and growth sensitivities are to be considered.

Note that the case where nucleation and growth are not a function of the area concentration of solids is equivalent to the results for m = 0. Also $b^* \sim b$ and $g^* \sim g$ which is equivalent to the results previously obtained. (37)

Although the presentation of the stability criteria in Figure I-6 is in a compact analytic form, it does not readily lend itself toward physical interpretation and prediction. To facilitate analytic simplification as well as to relate to actual physical cases, we now restrict ourselves to the case of $g^* \gg 1$. This can be seen from a quick order of magnitude analysis of the terms in g*. The dependence of the growth rate on supersaturation can usually be expressed as

$$G(c) = k_g (c - c_s)^p \qquad \text{such that} \qquad \frac{\partial \ln G}{\partial \ln c} = p \cdot \left(\frac{c}{c - c_s}\right) \gg 1$$

For a broad class of crystallizers, this is the working range. Since α and γ are typically 0 (1) one may rewrite the stability criteria for surface dependent nucleation and growth as follows:

$$\text{I-(17)} \qquad \left(\frac{-3+\beta}{1+\gamma}\right) < \frac{b_c}{q_c} < \left(\frac{21+\beta}{1+\gamma}\right)$$

$$\text{for } q_c \gg 1,\ q_c \gg |m|,\ \gamma > -1$$

This criteria for stability may be expressed graphically in the $\left(\frac{b_c}{q_c}, \beta\right)$ plane with γ as a parameter. See Figure I-(7). To simplify discussion let us first consider the case where $\gamma = 0$, that is, where the growth rate of the suspended particles is independent of the total area of the crystal suspension. $\left(-3+\beta < \frac{b_c}{q_c} < 21+\beta \right)$.

Figure I-6: Plot of stability limits for systems with area dependent nucleation and growth kinetics given by equation I-(16) in b*, g* plane with m as a parameter.

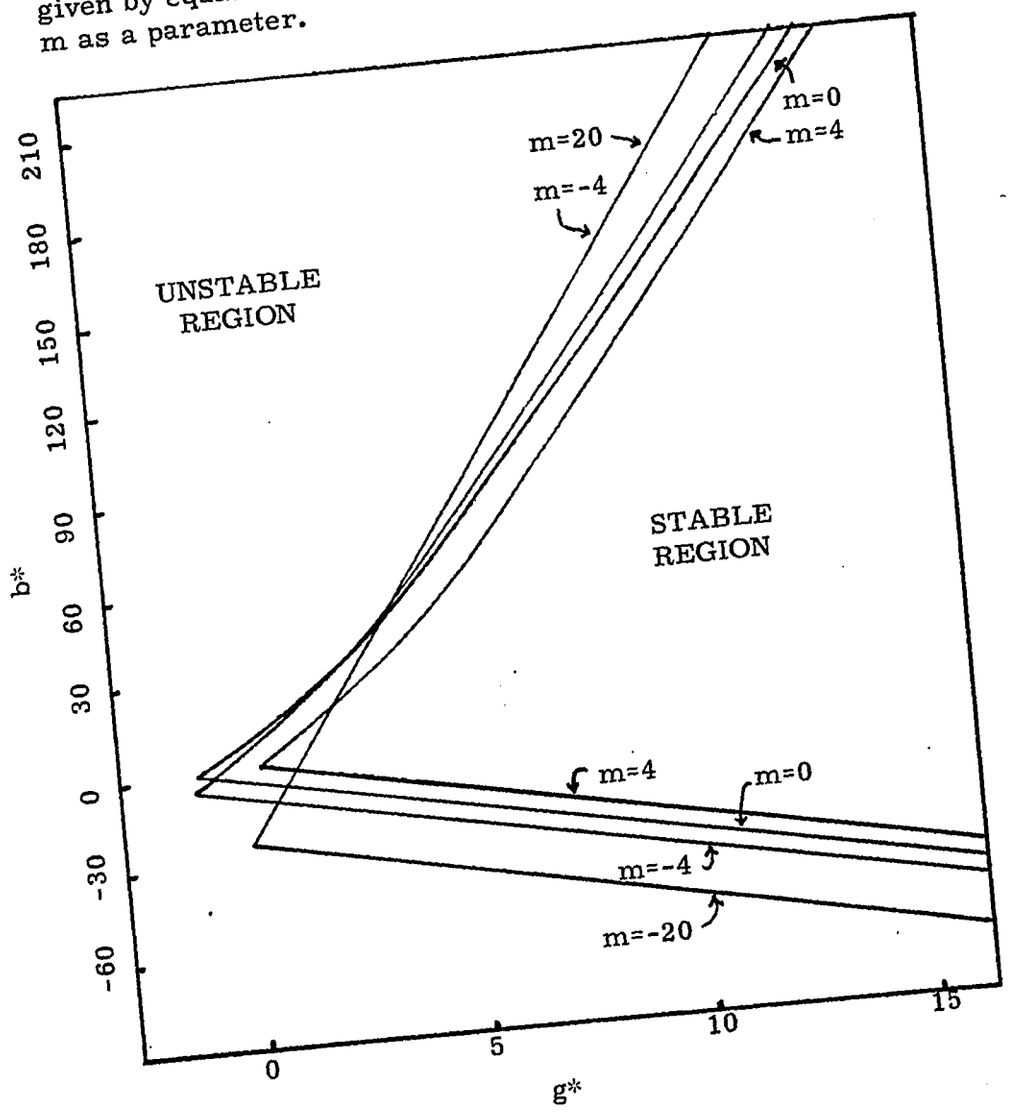

Figure I-7: Asymptotic stability limits for a continuous crystallizer with surface dependent nucleation and growth kinetics. $\frac{b_c}{g_c}$ versus β with γ as a parameter for $g_c \gg 1$.

Equation I-17: $\left(\frac{-3+\beta}{1+\gamma}\right) < \frac{b_c}{g_c} < \left(\frac{21+\beta}{1+\gamma}\right)$

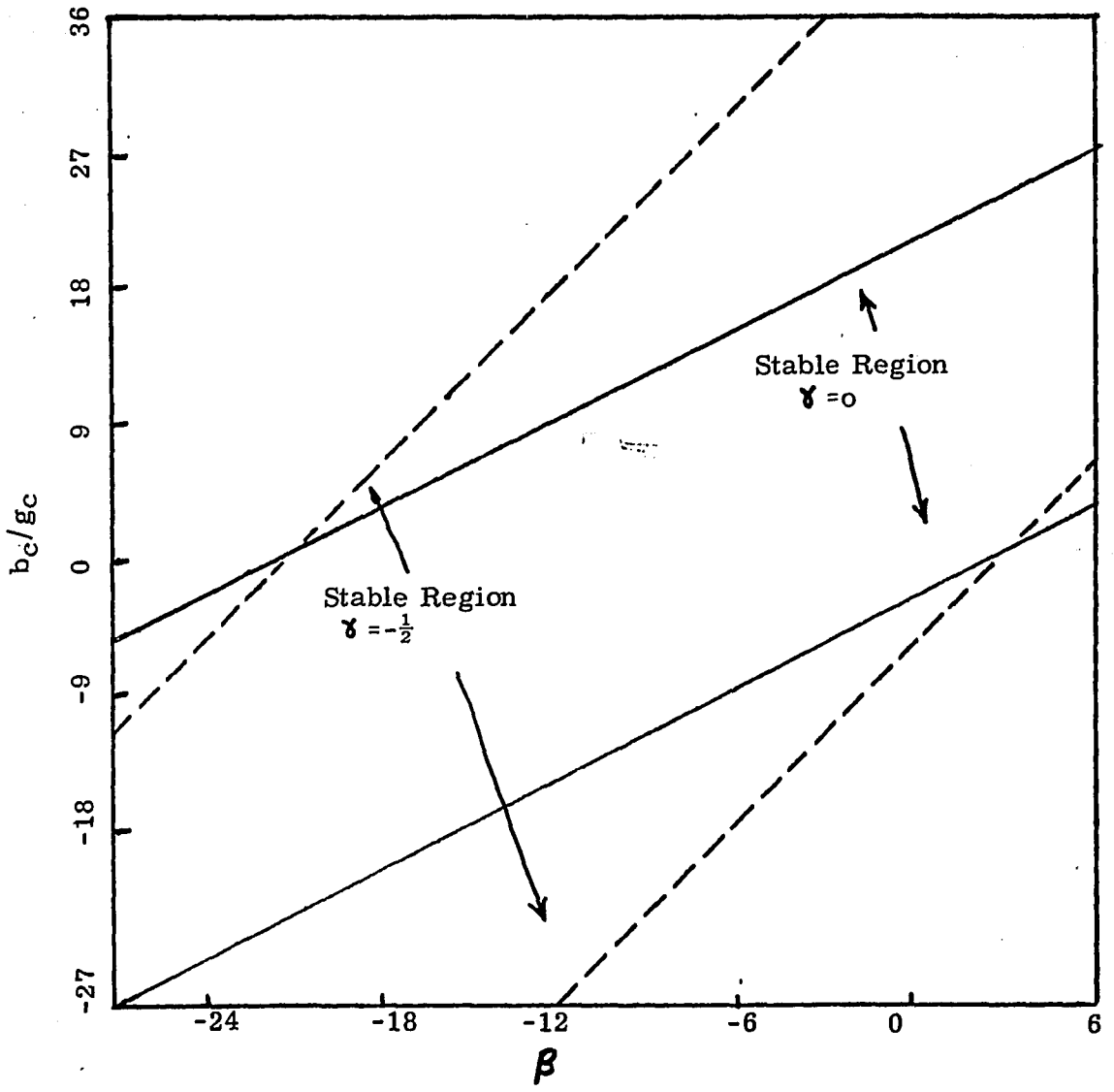

The stability criteria predicts an increase in upper and lower stability limits of $\frac{b_c}{g_c}$ for $\beta > 0$ relative to the area independent case. Conversely, $\beta < 0$ has an unstabilizing effect on the system dynamics.

Consider a system in which increasing the total particle surface increases the nucleation rate, i.e. $\beta > 0$. Assume that it is operating at its steady state operating point. A small perturbation in supersaturation will instantly cause many new particles to form. These particles initially do not greatly increase the total surface which would auto-accelerate the nucleation rate. Rather, these new particles cause an adjustment of the supersaturation by depleting the solute concentration in the liquid phase. Another point of viewing the stabilizing effect of a positive β is to consider a cycling system. The point in a limit cycle at which area is a maximum corresponds to the point of lowest supersaturation. Thus if $\beta > 0$ the large surface will form new particles at the low supersaturation, thereby self-regulating the system.

At the other extreme of the cycle, one has a small surface but a high supersaturation. Here, too, a $\beta > 0$ has a stabilizing effect, as the small surface counteracts the effect of high supersaturation.

If a continuous crystallizer is operating in a region where nucleation is suppressed by an increasing surface, i.e. $\beta < 0$, the largest b_c/g_c sustainable without cycling would be lower than the case where nucleation is independent of area, i.e. $\beta = 0$. This point may also be seen qualitatively by viewing the two potential extreme points of a limit cycle. The nucleation rate will be low at the extreme point in the cycle at which supersaturation is low. This point corresponds to a large surface area. Thus, if $\beta < 0$, the lowering of the nucleation rate is reinforced, thereby making the system less stable. (i.e. It drives the system further away from the steady state.). At the other extreme of the cycle, the total surface is low and supersaturation

high. Here, the area dependence of nucleation has the effect of reinforcing the high nucleation rate.

Thus, depending upon the actual mechanism of nucleation, the nature of the area dependence may have a stabilizing or unstabilizing effect.

Case II. B(c,n), G(c) : Number Dependent Nucleation

The equations governing the dynamic behavior of an MSMPR with number dependent nucleation kinetics are rewritten in the following form:

$$\frac{d\phi(t)}{dt} = \frac{1}{\Theta}\phi_f - \frac{1}{\Theta}\phi(t)$$

$$G(c)\cdot f(r,t) = B(c,n) \; ; \; r = 0$$

$$\frac{\partial f(r,t)}{\partial t} + G(c)\frac{\partial f(r,t)}{\partial r} = -\frac{1}{\Theta} f(r,t) \; ; \; r > 0$$

with

$$n(t) = \int_0^\infty f(r,t)\,dr$$

$$c(t) = 1 - k\int_0^\infty r^3 f(r,t)\,dr$$

In Appendix I-C the above equations are linearized and a formal spectral analysis on the resulting linear operator yields a characteristic equation. Application of the Routh-Hurwitz criteria results in conditions for linear stability.

These conditions are equivalent to:

$$\text{I-18)} \quad -(1-b_n)(1+3g^*) < b^* < \left\{ \frac{(21-15b_n+3b_n^2)g^{*3} + (87-81b_n+27b_n^2-3b_n^3)g^{*2} + (128-148b_n+62b_n^2-15b_n^3)g^* + (64-96b_n+48b_n^2-8b_n^3)}{(g^*+4-b_n)^2} \right\}$$

and

$$g^* > \left| \sqrt{\left(\frac{4-b_n}{2}\right)^2 - \left(\frac{20-15b_n+3b_n^2}{4-b_n}\right)} \right| - \left(\frac{4-b_n}{2}\right) \; ; \; b_n \geq 4$$

$$g^* > -\left(\frac{4-3b_n}{6-3b_n}\right) \; ; \; b_n \leq 2$$

These results are plotted in the (b*, g*) plane in Figure I-8 for various values of b_n. Note, there are no stable points in the range $2 < b_n < 4$, independent of the supersaturation dependence. In Figure I-9 the minimum stable values for g* are plotted as a function of b_n. It is also of interest to consider the asymptotic forms of the stability criteria of equation (18). In Figure I-10 the value of b_c/g_c at the critical stability limits are plotted as a function of b_n. Although the right hand stable region does not seem to fit any known physical cases, it is included for completeness. To understand the unstabilizing effect of a positive b_n we consider the effect of a pulse disturbance in supersaturation on a system operating at its steady state point. The short term increase in supersaturation results in the production of nuclei in excess of that necessary to sustain the steady state. These new particles contribute an immediate increase in the number of particles being formed. In fact for $b_n = 2$ (which is like second order mass action kinetics for nucleation) the disturbance tends to autoaccelerate itself explosively. In general within a mean residence time, this increase in n over its steady state depletes the supersaturation. The resulting lowering of the supersaturation then lowers the instantaneous nucleation rate and cycling proceeds as the existing particles grow at the expense of new particle formation.

Case III. Bennett, Fieldelman & Randolph Model

Although this model is not useful as a kinetic form for correlation of data, it was presented (4) as a display of the competing factors that stabilize secondary nucleation in an operating crystallizer. The equation $*B_e = k n^o \rho G \left[\frac{T \rho_s g}{T_0}\right] L_D^5$ can be related directly in terms of the leading moments by noting $L_D = \frac{\mu_3}{\mu_2} = 360$ and $n^o = \mu_0/\theta G$ as follows: $B = k \mu_0 \left(\frac{\mu_3}{\mu_2}\right)^4 G$ where k includes the hydrodynamic variables. A linearized stability analysis based on $B(G, \mu_0, \mu_3/\mu_2)$

*Defined in reference (4)

Figure I-8: Plot of stability limits for systems with number dependent nucleation kinetics given by equation I-(18) in b*, g* plane with b_n as a parameter.

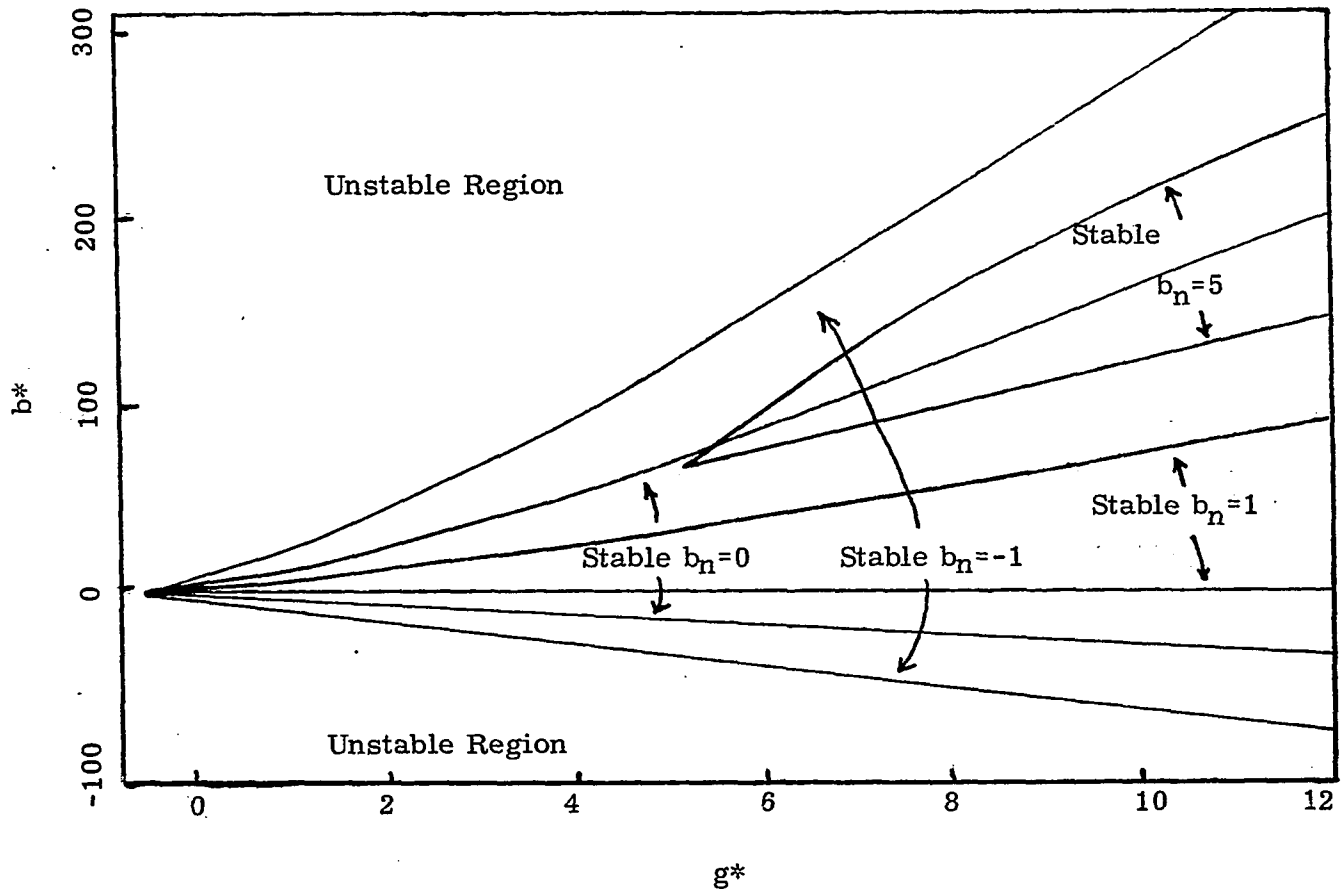

Figure I-9: Minimum values of g* for stability in systems with number dependent nucleation kinetics.

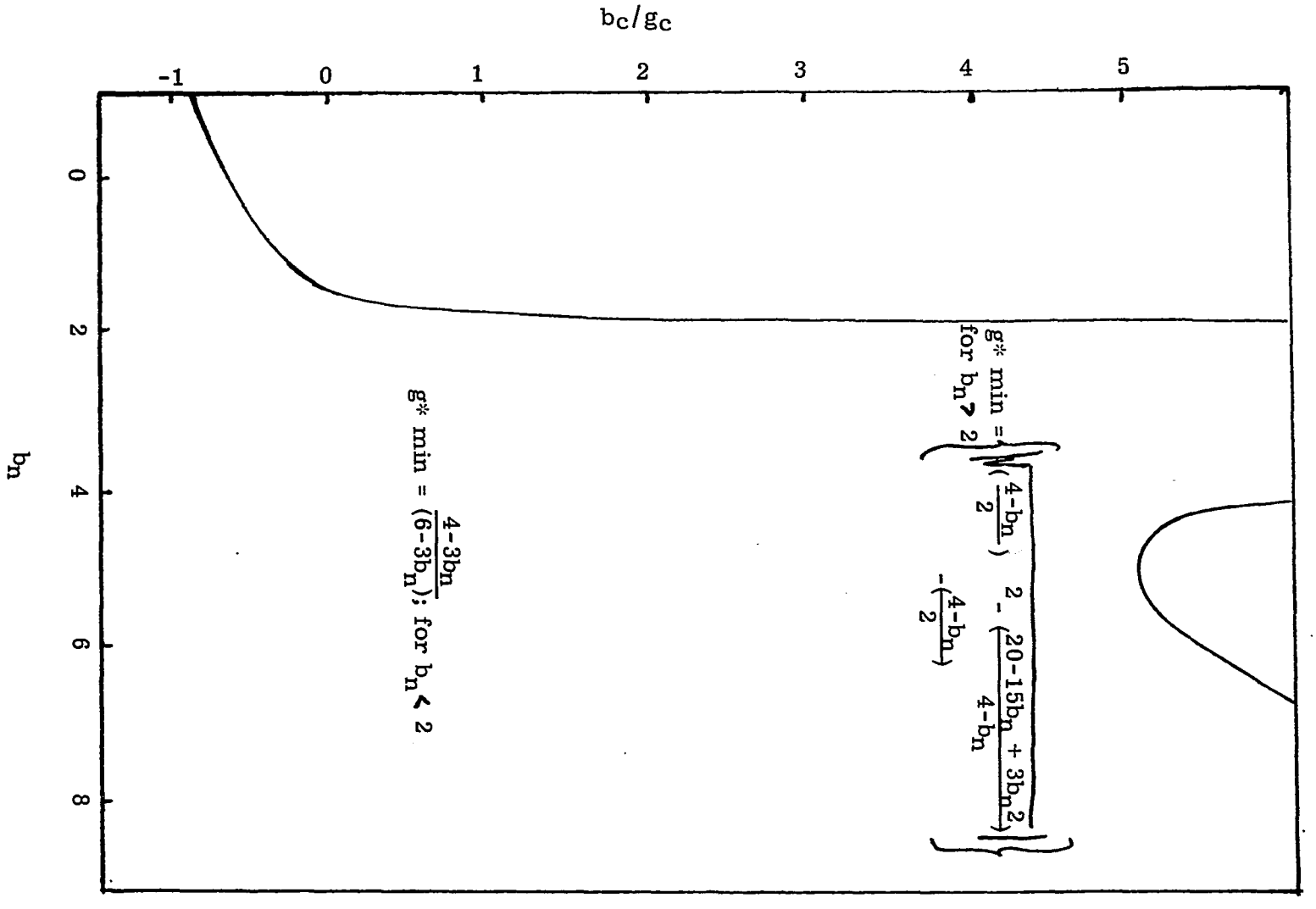

Figure I-10: Asymptotic stability limits for a system with number dependent nucleation kinetics.

Equation I-18: $-3(1-b_n) < \frac{b_c}{g_c} < 3(7-5b_n + b_n^2);\ g_c \gg 1$

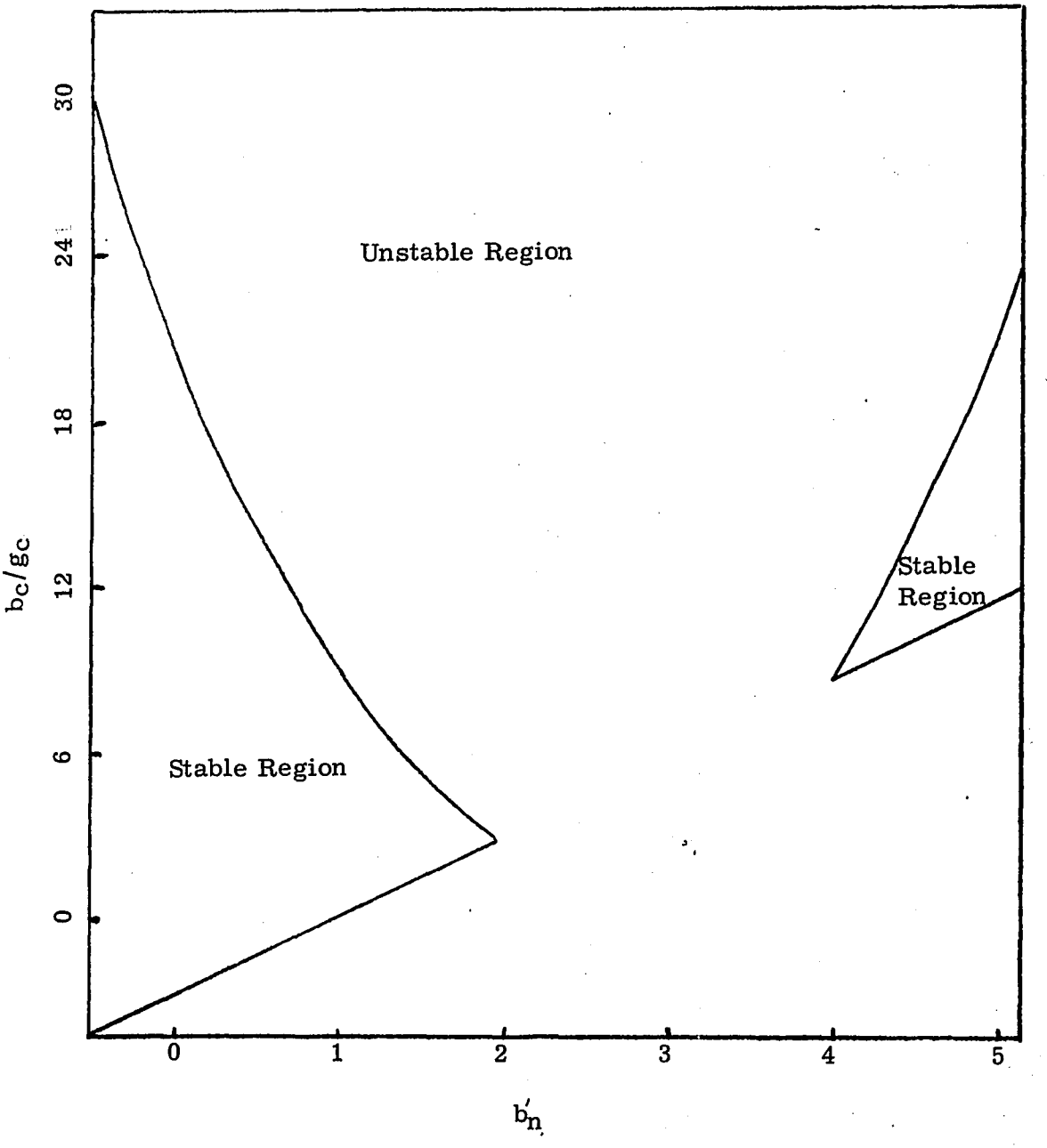

can provide criteria to test the stability of such a model.

The stability criteria for this model was computed based on the functions $B(c, n, \mu_3/\mu_2)$ and $G(c)$. The linearized stability analysis based on these variables results in the following expression for the critical stability limits in the asymptotic region $g_c \gg 1$:

$$\text{I - (19)} \qquad -b_r - (3 - b_n) < \frac{b_c}{g_c} < (21 - 15 b_n + 3 b_n^2) - b_r$$

where

$$b_n = \frac{\partial \ln B}{\partial \ln n}$$

$$b_r = \frac{\partial \ln B}{\partial \ln \mu_3/\mu_2}$$

In this model for nucleation in the impeller region $b_c/g_c = 1$, $b_n = 1$ and $b_r = 4$. Thus, based on a linearized stability analysis, this model does not predict instabilities in a MSMPR crystallizer. Other nucleation models treated by Bennett et. al. are related by M_T or M_4 for which the stability criteria developed by Randolph and Larson (35) indicate these models are linearly stable.

SUMMARY AND DISCUSSION

An analysis of two cases has been presented in which the nucleation and growth rates of a crystallizer depend on the total area or total number of crystals present. The main results of this analysis can be summarized as follows: A number or area dependence of the nucleation rate will have a strong effect on the steady state behavior, especially the dependence of the average particle size on residence time. Interestingly enough, the resulting plots of lnB versus lnG which have been used to study kinetics remain fairly linear over wide ranges of residence times. This has one important implication. It simply means that this type of measuring kinetics is useless in predicting dynamic behavior of crystallizers. This is an important conclusion, as such methods have been strongly promoted for this purpose. It is impossible from steady state behavior to draw any definite conclusions as to the detailed kinetics.

The same applies to the dynamic behavior, for which there are much less data available. We cannot really confirm any model. For this, we need detailed kinetics such as (3, 12, 34, 46). We can, however, draw some conclusions. First of all, we would expect that no mechanism will fit all crystallizing systems. Many crystallizations never exhibit strongly nonlinear dynamics or oscillating behavior. We can, however, draw some conclusions for those that do. Most of these systems have a relatively low value of dlnB/dlnG. The only cases we found that are unstable for overall values of dlnB/dlnG were the cases of strongly negative area dependences. It was possible to show that there is at least one physical nucleation mechanism that corresponds to an

exponentially inverse dependence on the area. That does not prove in any way that such systems really have a nucleation mechanism in which small particles are captured at a surface. Other physical mechanisms might have similar properties. In that case this method does not work. (Integrals involving only the tails of the size distribution function lead to characteristic equations which are not polynomials and cannot be treated by simply applying the Routh-Hurwitz criterion.) But a simple heuristic argument shows that this case is similar to a negative area dependence. In most crystallizers μ_3 is almost constant and varies only slightly. The presence of large particles is strongly correlated to the higher moments. An increase in the number of large particles causes both μ_4/μ_3 and μ_3/μ_2 to increase. As μ_3 is fairly constant, an increase in μ_4 occurs with a decrease in μ_2 . (i.e. As there tends to be more mass in the tail, the total surface decreases.) While there are methods of dealing directly with such cases (1, 42, 43), they are outside the scope of this work. These results should however, have wide applicability not only for crystallizers but for other processes such as polymerization, fermentation, coal conversion and other systems involving population balances in which growth and nucleation depend on the properties of the particles present.

II CONTINUOUS PRECIPITATION POLYMERIZATION

INTRODUCTION

At the present time, there are still many polymerization reaction systems that are difficult to scale up on a continuous basis. One problem common to many heterogeneous polymerizations, as well as to complex particulate processes, is to insure stability of the steady state operation of such systems. The property common to all such systems is the occurrence of competitive simultaneous nucleation and growth of particles. In this paper we focus our attention on the continuous production of precipitating polymers for its mathematical simplicity, although the methods and concepts presented in this paper may be applied to continuous emulsion polymerization, continuous crystallization, in continuous coal conversion, and other particulate processes involving simultaneous nucleation and growth.

In batch and continuous precipitation polymerization, the quality of the polymer product and the control of the plant are sensitive to the formation rate of the precipitated particles (1, 2). The mean particle size of the polymer product is a strong function of the nucleation rate, and particle size exerts a strong controlling effect on the molecular weight distribution. (Mean particle size is often in the micron range in commercial operation.) Continuous precipitation polymerization is known to exhibit cyclic behavior (2, 15) and even in the stable range is sensitive to small disturbances. In this respect, the process is quite similar to that of continuous crystallization in which limit cycle variation in mean particle size is known to occur (3, 16) This similarity is not surprising. The limit cycles in continuous crystallization are a result of the non-linear dependence of the nucleation rate on reactor conditions and the lag in time necessary for significant particle growth (10).

Nucleation in precipitation polymerization is highly non-linear. (11)

In setting up a physical model for the nucleation process in precipitation polymerization, one needs to consider that due to surface energy and colloidal charge effects, large particles do not coalesce, and therefore, it is necessary to view the need for potential nuclei to reach a stable or critical nuclei size. (4, 5) A large available surface in the crystallizer may either promote new particle formation via secondary nucleation effects or suppress nucleation through capture of potential nuclei. A large surface of precipitated particles in precipitation polymerization inhibits nucleation in two ways: One is through the increased rate of capture of potential nuclei prior to their reaching the stable nuclei size; the other is by the lowering of the polymerization rate in the liquid (this lowers the probability that a growing nuclei will acquire sufficient mass to reach the critical size prior to capture). This strong inhibiting effect of surface on nucleation has been demonstrated in batch experiments where after sufficient surface is present nucleation virtually ceases. Even further addition of initiator will not induce new particle formation. (6)

The dynamic behavior of precipitation polymerization reactors is viewed here in terms of the complex competition between the nucleation and growth of the precipitated particles. A small disturbance in reactor conditions may instantly produce a large increase in the number of stable nuclei being generated; these new particles do not instantly increase the available surface significantly. There is a considerable time lag (on the order of magnitude of the mean residence time) for new particles to grow to the size range where they significantly increase the total available surface. Therefore, as the nucleation rate leads the production of new available surface, cyclic variation of the mean particle size may occur.

In this section mathematically treatable simplified models are used for the nucleation and growth processes so as to obtain insight into the nature of their complex interactions. Although the processes considered

here occur simultaneously, in most cases a specific mechanism will predominate. For convenience and clarity the mechanisms are separated into two models. The first is a simplified form of the nucleation mechanism suggested by Dainton (7). In this coalescence model, terminated polymer molecules in the liquid are taken to aggregate via physical coalescence. When a cluster of such molecules in the liquid reaches a stable critical nuclei size, nucleation via precipitation of a stable solid particle is taken to have occurred. Here stability refers to the fact that particles above the critical size will not coagulate with one another although they may continue to collect subcritical aggregates from the liquid. From batch experiments with polymer hydrosols, Fitch et. al (4) concur that particle formation must be a nucleation-precipitation process. Sonshine, Klepfer and Shinnar (8) have previously formulated this mechanism mathematically using discrete variables and obtained approximate solutions to the steady state equations using moment closing techniques. This problem has since been reformulated and several nucleation models have been applied. (11) Here the governing equations are written in terms of continuous variables from which a closed exact set of equations can be written and exact solutions obtained.

Baxendale (9) suggested that particle formation occurs from coagulation and growth of colloidal macroradicals. The mathematical complexity of the equations governing the physics of a macroradical coagulation model is beyond the scope of this paper, and a presentation in full detail shall not be made at this time. A brief discussion of what may be referred to as the averaged coalescence model (11) is presented in Appendix II-4.

A second mechanism to be investigated is a simplified model in which coalescence of polymer molecules in the liquid phase shall be neglected entirely. A similar model has been proposed by Fitch (5) in which termination of radicals in the liquid phase was neglected.

Roe (13) suggests this may be the mechanism of particle formation in some emulsion polymerization systems. In this simplified model, nucleation is taken to occur when a single liquid radical grows via monomer addition past a critical nuclei size or when two growing liquid radicals terminate via combination to form an inactive polymer molecule above the critical nuclei size. The stable particles may collect, via physical capture, radicals and polymer from the liquid. Polymerization proceeds in the adsorbed state near the surface of these precipitated stable particles.

This mechanism shall be referred to as the growth model for nucleation in precipitation polymerization. Although there is no sound physical reason to neglect the effect of coalescence, the growth model is studied for its mathematical simplification. There could also be physical situations in which it applies.

The nucleation rate for the growth model can be computed analytically under steady state operating conditions as a function of initiator, monomer and area concentrations in the liquid. The nucleation rate for the coalescence model and the macroradical coagulation model can only be expressed in terms of a complex collision integral whose form prohibits analytical simplification. The underlying behavior is not greatly altered by use of the growth model and insight into the complex interaction between the nucleation and growth processes is obtained. The significance of this analysis is broader than the application to precipitation polymerization. The dynamics of nucleation in many complex particulate systems are governed on the microscopic level by some type of coalescence or coagulation process. The mathematical formulation and treatment of a nucleation process presented here may indeed be useful in considering such systems.

Goldstein and Amundson have previously investigated the dynamic behavior of two phase polymerization systems. (12) In this present analysis, we find that the potential for instabilities exists aside from the classical auto-acceleration resulting from an inbalance in heat

generation and removal as previously considered. (12)

The dynamic behavior of complex particulate systems involving surface dependent nucleation and growth processes has previously been investigated. (10) Formulation of the governing equations in a similar form permits the stability criteria based on a linearized stability analysis previously developed (10), to be applicable to continuous precipitation polymerization reactors. These criteria will be used to test the stability of steady state operating conditions obtained for the nucleation models developed. The qualities and properties of the nucleation models can be studied from the expressions developed for nucleation sensitivity to reactor variable fluctuation. These sensitivities are the essential terms in the stability parameters developed. The effects of initiator and monomer concentration in the feed on system stability are studied, providing qualitatively the criteria needed to control both reactor dynamics and product quality.

Derivation of the System Equations

The steady state behavior of the continuous production of precipitation polymers in a stirred tank reactor has previously been discussed. (11) Here we present a brief summary for the underlying physics and chemistry needed to model the dynamic behavior of such systems.

Consider the following processes occurring in a stirred tank. Monomer, initiator, and solvent are fed continuously into the reactor. In the solvent rich liquid phase, the following processes are taken to occur:

Initiator molecules decompose forming primary free radicals;

$$I \xrightarrow{k_I} 2 \cdot r_1(0)$$

where k_I is the decomposition rate constant for the initiator and $r_L(o)$ is the concentration of primary free radicals in the solvent rich phase.

A radical at a degree of polymerization x grows in the liquid phase by monomer addition:

$$r_L(x) + M_L \xrightarrow{k_{pL}} r_L(x+1)$$

Where k_{pL} is the propagation rate constant in the liquid and the (x+1) represents the fact that each addition of a monomer increases the degree of polymerization of the growing radical by 1.

Termination by combination occurs forming inactive polymer molecules;

$$r_L(x) + r_L(y) \xrightarrow{k_{tL}} p_L(x+y) \iff \phi\{v(x+y)\}$$

where k_{tL} is the termination rate content in the liquid. (It is assumed that k_{pL} and k_{tL} are independent of d.p.) $\phi\{v(x+y)\}$ represents the fact that as single polymer molecules are formed they are indistinguishable from what shall be referred to as a subcritical particle cluster formed at a volume equivalent to the degree of polymerization of the polymer molecule.

Subcritical particle clusters coalesce with one another in the liquid;

$$\phi(z) + \phi(v-z) \xrightarrow{\beta_c} \phi(v)$$

where β_c is a coalescence rate constant. (β_c is also taken to be size independent.)

It is assumed that radicals do not coalesce with polymer clusters in the liquid. This model shall be referred to as the pure coalescence model. The possibility of there being growing radicals associated with the subcritical polymer clusters is accounted for in the summary of the averaged coalescence model considered in Appendix II-A.

Radicals, polymers, and their clusters are captured by the existing stable particles. The rate of capture is given by the following:

Rate of radical capture = $h\,a\,r_L(x)$

Rate of polymer capture = $h\,a\,p_L(x)$

Rate of cluster capture = $h\,a\,\phi(v)$

where h is a mass transfer coefficient, a is the total surface area of the precipitated particles per unit reactor volume, $r_L(x)$ and $p_L(x)$ are molar concentrations of radicals and polymer molecules in the liquid at a d.p. of x and $\phi(v)$ is the concentration of polymer aggregates in the liquid at the molecular volume V. (Capture probabilities have been assumed size independent.)

We assume that the polymerization in the solid phase occurs exclusively at the solid surface. The monomer concentration at the surface is assumed to be in equilibrium with the monomer in the liquid. Here, we use a Langmuir type isotherm to relate the concentration at the surface to the monomer concentration in the liquid;

$$M_S = E[M_L] = \frac{j_1 \cdot M_L}{1 + j_2 \cdot M_L}$$

Radicals at the surface continue to grow by propagation;

$$r_S(x) + M_S \xrightarrow{k_{ps}} r_S(x+1)$$

where k_{ps} is a surface propagation rate constant. (k_{ps} is taken to be independent of x.)

Termination proceeds on the solid surface by combination of two growing radicals;

$$r_S(x) + r_S(y) \xrightarrow{k_{TS}} p_S(x+y)$$

where k_{ts} is a surface termination rate constant that is size independent.

The system is assumed to be well mixed and therefore the reactor effluent has the same composition as the reactor.

Before proceeding to set down the resource balances, a description of the physics and chemistry of the nucleation processes is presented.

When a radical grows past the critical size or when two growing radicals terminate to form a polymer above the critical size, nucleation of a stable precipitated particle occurs;

$$r_L(x_{cr}-1) + M_L \xrightarrow{k_{pL}} r_L(x_{cr}) \Longrightarrow \text{formation of a stable nucleus} \quad ; y_c \geq x_{cr}$$

$$r_L(x) + r_L(y_c - x) \xrightarrow{k_{TL}} p_L(y_c) \Longrightarrow \text{formation of a stable nucleus} \quad ; y_c \geq x_{cr}$$

Here stability refers to the fact that particles above the critical size will not coalesce with one another. This mechanism for nucleation has been referred to as the growth model.

If a cluster of inactive polymer molecules grows by coalescence with other sub-critical aggregates past the critical size, nucleation will occur.

$$\phi(z) + \phi(v-z) \xrightarrow{\beta_c} \phi(v) \Longrightarrow \text{formation of a stable nucleus} \quad ; v \geq v_c$$

This mechanism has been referred to as the coalescence model.

At this point material balances for initiator, monomer, liquid and solid radicals and polymers can be written as follows. (The contributions of nucleation to the radical and polymer balances, taken to be negligible):

II-(1): Initiator Balance

$$\frac{d\{\epsilon \cdot I\}}{dt} = \frac{1}{\Theta} I_0 - \frac{1}{\Theta} \epsilon I - \epsilon k_I I$$

II-(2): Monomer Balance

$$\frac{d\{\epsilon M_L + a M_S\}}{dt} = \frac{1}{\Theta} M_0 - \frac{1}{\Theta}\{\epsilon M_L + a M_S\} - \epsilon k_{pL} M_L \int_0^\infty r_L(x)\,dx - a k_{ps} M_S \int_0^\infty r_s(x)\,dx$$

II-(3): Monomer Equilibrium

$$M_S = E[M_L] = \frac{j_1 M_L}{1 + j_2 M_L}$$

II-(4): Liquid Radical Balance

$$\frac{\partial\{\epsilon r_L(x)\}}{\partial t} + k_{pL} M_L \frac{\partial\{\epsilon r_L(x)\}}{\partial x} = \epsilon_2 k_I I \delta(x) - h_a r_L(x) - \epsilon k_{TL} r_L(x) \int_0^\infty r_L(y)\,dy - \frac{1}{\Theta} \epsilon r_L(x)$$

II-(5): Liquid Polymer Balance

$$\frac{\partial\{\epsilon p_L(x)\}}{\partial t} = \frac{\epsilon \cdot k_{TL}}{2}\int_0^x r_L(y)\, r_L(x-y)\,dy - h a\, p_L(x) - \frac{1}{\theta}\epsilon\, p_L(x)$$

II-(6): Solid Radical Balance

$$\frac{\partial\{a \cdot r_s(x)\}}{\partial t} + k_{ps} M_s \frac{\partial\{a\, r_s(x)\}}{\partial x} = h a\, r_L(x) - \frac{1}{\theta} a r_s(x) - a k_{TS}\, r_s(x)\int_0^\infty r_s(y)\,dy$$

II-(7): Solid Polymer Balance

$$\frac{\partial\{a \cdot p_s(x)\}}{\partial t} = -\frac{1}{\theta} a\, p_s(x) + h a\, p_L(x) + a k_{TS}\int_0^x r_s(y)\, r_s(x-y)\,dy$$

Where M_o and I_o are the monomer and initiator concentrations in the feed respectively, θ is the mean residence time of material in the reactor; M and M_s are the monomer concentrations in the liquid (mol/cm^3) and solid (mol/cm^2) respectively; ϵ is the fraction of the reactor occupied by the liquid phase; $r_L(x)$ and $p_L(x)$ are the radical and polymer size distributions in the liquid $(mol/cm^3\text{-d.p.})$, $r_s(x)$ and $p_s(x)$ are the radical and polymer size distributions on the precipitated particles $(mol/cm^2\text{-d.p.})$; and $\delta(x)$ is a Dirac Delta function, representing the fact that primary radicals in the liquid are taken to be formed at zero d.p.

The equations II-(1-7) presented here are similar to those previously used (8, 11) to obtain the steady state behavior of continuous precipitation polymerization reactors. Goldstein and Amundson (12) have previously shown that if the relative volumes and interfacial area between two immisible phases are known, the above relationships are sufficient to compute the molecular weight distribution as well as the reactor conversion. Relations involving these quantities given here as a (the total surface area of the precipitated particles per unit reactor volume) and ϵ (the volume of the liquid phase per unit reactor volume) are, therefore, needed to close the set of equations governing the dynamic behavior of such systems. The additional relationships in terms of a and ϵ can be obtained from a knowledge of the size distribution of the stable precipitated particles.

We let f(L) be a size distribution function for the stable particles such that f(L) dL is the number of stable particles lying in a size

range L, L + dL per unit reactor volume where L is a characteristic linear dimension of the particles. (For our purposes L will be the particle radius.)

An equation governing the size distribution of precipitated particles can be written following the method of Hulbert and Katz. (14) Assuming all the stable nuclei are generated at a size infinitesimally small compared to the mean particle size, the equation governing the particle size distribution can be written as follows:

$$\text{II-(8)} \qquad \frac{\partial f(L)}{\partial t} + \frac{\partial \{G \cdot f(L)\}}{\partial L} = \epsilon B \delta(L) - \frac{1}{\theta} f(L)$$

where θ is the mean residence time of the particles in the reactor (min.); B is the nucleation rate per unit liquid volume (#/cm^3-min); G is the particle growth rate (cm/min); and the Dirac delta function $\delta(L)$ represents the assumption that the nuclei are generated at a vanishingly small size.

From f(L), a and ϵ can be computed directly as follows:

$$a = \int_0^\infty 3KL^2 f(L)\, dL$$

$$\epsilon = 1 - \int_0^\infty KL^3 f(L)\, dL$$

Thus, if B and G could be expressed in terms of the reactor variables, the additional relationships needed to compute a and e could be obtained by direct integration of equation II-(8). An expression for the particle growth rate can be formulated independent of the nucleation mechanism. Consider the growth rate of an individual stable precipitated particle. The growth rate $G = \frac{dL}{dt}$ can be expressed in terms of the particle's area and the particle's volumetric growth rate.

$$G = \frac{dL}{dt} = \frac{1}{A} \frac{dV}{dt}$$

There are two principal contributions to the volumetric growth rate of a stable precipitated particle. A precipitated particle grows by capture of radicals and polymer from the liquid and by polymerization of monomer adsorbed on the particle surface. The monomer adsorbed on the surface of the precipitated particles is assumed to have a negligible effect on the total capture surface. For mathematical convenience, the monomer adsorbed on the surface of the precipitated particles is not added to the volume until after it has been polymerized. The volumetric growth rate of a single particle can be written as follows:

$$\frac{dV}{dt} = \begin{array}{l}\text{volume of liquid radicals}\\ \text{captured per unit time}\end{array} + \begin{array}{l}\text{volume of liquid}\\ \text{polymer captured}\\ \text{per unit time}\end{array} + \begin{array}{l}\text{volume of monomer}\\ \text{polymerized on the}\\ \text{surface per unit time}\end{array}$$

or

$$\frac{dV}{dt} = hA\int_0^\infty \left(\frac{\nu_I}{2} + \nu_M x\right) n_L(x)\,dx + hA\int_0^\infty (\nu_I + \nu_M x)\, p_L(x)\,dx + A \cdot k_{ps} M_s \nu_M \int_0^\infty r_s(x)\,dx$$

where the first two terms on the right-hand side represent the total volume of radicals and polymer captured from the liquid per unit time, and the last term represents the volumetric rate at which a particle grows due to polymerization of monomer on its surface. Dividing by A (Assuming h is independent of size) results in a form in which G may be written independent of particle size, as a function of the leading moments of the radical and polymer distributions and $M_s = E(M_L)$.

$$\text{II-(9a)} \quad G = h\int_0^\infty \left(\frac{\nu_I}{2} + \nu_M x\right) n_L(x)\,dx + h\int_0^\infty (\nu_I + \nu_M x)\, p_L(x)\,dx + k_{ps} M_s \nu_M \int_0^\infty r_s(x)\,dx$$

Thus G may be taken out of the brackets in equation II-(8).

$$\left\{ \text{i.e.} \quad \frac{\partial \{G f(L)\}}{\partial L} = G \frac{\partial f(L)}{\partial L} \right\}$$

Finally expressions for B as a function of the reactor variables are needed to close the system's equations.

B, the total number of stable particles formed per unit time per unit liquid volume, can be computed based on the mechanisms of

particle formation discussed previously.

Qualitatively this can be expressed as follows:

II-(10) B = rate at which liquid radicals grow past the critical size + rate at which liquid radicals form polymer above the critical size + rate at which subcritical aggregates coalesce forming particles above the critical size

These contributions may be computed individually.

$B = Bp + B_T + Bc$, where Bp, B_T, and Bc represent the above individual contributions, respectively.

Bp is the rate at which liquid radicals grow past the critical size. Bp can be written as follows:

$$Bp = k_{pL} \cdot M \cdot r_L (X_{cr})$$

B_T is the total rate at which polymer is formed by termination above the critical size. The rate, $b_p(x)$, at which polymer molecules are formed in the liquid at size x is:

$$b_p(x) = \frac{k_{TL}}{2} \int_0^x r_L(y)\, r_L(x-y)\, dy$$

The total number of polymer molecules forming above the critical size per unit time can be computed directly by integratinn:

$$B_T = \mathcal{L} \cdot \int_{x_{cp}}^{\infty} dx \cdot \Delta(x-x_{cp}) b_p(x)$$

where $\Delta(x-x_{cp})$ is a Heavysides unit step at the critical size. Thus, in terms of the radical size distribution $r_L(x)$, one may write B_T as follows:

$$B_T = \mathcal{L}\, \frac{k_{TL}}{2} \int_{x_{cp}}^{\infty} dx\, \Delta(x-x_{cp}) \int_0^x r_L(y)\, r_L(x-y)\, dy$$

The expression for the contribution of coalescence to the nucleation rate can be obtained in terms of the subcritical particle size distribution $\phi(v)$. First, a balance on the subcritical particles in terms of the size distribution $\phi(v)$ must be written. We write the expression for the net rate of accumulation of subcritical clusters at size v per unit reactor volume:

$$\frac{\partial\{\epsilon\phi(v)\}}{\partial t} = \frac{\epsilon\alpha^2}{v_m}\frac{k_{TL}}{2}\int_0^{x(v)} r_L(y)\,r_L(x-y)\,dy\,\left(1-\Delta(V-V_c)\right) - h_a\phi(v) - \frac{1}{\theta}\epsilon\phi(v)$$
$$+ 6\beta_c\left\{\frac{1}{2}\int_0^{v}\phi(z)\phi(v-z)\,dz\left\{1-\Delta(v-v_c)\right\} - \phi(v)\int_0^{v_c}\phi(z)\,dz\right.$$

where, the first term on the right-hand side represents the rate at which clusters are formed at size v when two radicals terminate to form a polymer at a d.p. equivalent to the volume v; the Heavysides Δ (V-Vc) represents the fact that polymer molecules generated at a size above Vc leave the liquid phase instantaneously and should not be counted twice in B; the second term on the right is the rate at which clusters at size v are captured by the existing precipitated particles; the next term is the rate at which subcritical clusters at size v leave the reactor in the effluent stream; the next term represents the rate at which clusters are formed at size v due to coalescence of two clusters below size v; the Heavysides Δ(V-Vc) represents the fact that as clusters are formed above Vc, they immediately form stable particles leaving the solvent rich phase; and the final term is the rate at which clusters at size v are destroyed due to coalescence with any other subcritical cluster.

The rate b_c (v) at which clusters are formed via coalescence at size v per unit liquid volume can be written as:

$$b_c(V) = \frac{\beta_c}{2}\int_0^{v}\phi(z)\,\phi(v-z)\,dz$$

The total number of clusters forming above the critical size per unit time can be computed directly by integration:

$$B_c = \int_{V_c}^{\infty} dV\cdot\Delta(V-V_c)\;b_c(V)$$

Thus, in terms of the subcritical particle size distribution ϕ (v), the contribution of coalescence B_c to the nucleation B can be written as follows:

$$B_c = \frac{\beta_c}{2}\int_{V_c}^{\infty} dV\,\Delta(V-V_c)\int_0^{v}\phi(z)\,\phi(v-z)\,dz$$

The nucleation rate B may now be written in terms of M_L, $r_L^{(x)}$, ϕ(v) as follows:

$$B = \mathcal{L}\,k_{pi}\,M_L\,r_L(x_{cr}) + \mathcal{L}\frac{k_{TL}}{2}\int_{x_{cp}}^{\infty} dx\,\Delta(x-x_{cp})\int_0^{x} r_L(y)\,r_L(x-y)\,dy + \frac{\beta_c}{2}\int_{V_c}^{\infty} dV\,\Delta(V-V_c)\int_0^{v}\phi(z)\,\phi(v-z)\,dz$$

It is now possible to write a closed set of dynamic equations in terms of I, M_L, M_S, r (x), r (x), p_L (x), p_S (x), ϕ (v) and where B, G, a and are expressed as implicit functions of the reactor variables. The equations governing the dynamic behavior of precipitation polymerization in a C.F.S.T.R. is summarized in Table II-1.

Table II-1: Equations Governing Dynamic Behavior of Precipitation Polymerization Reactors

Initiator Balance	$\frac{d\{\epsilon I\}}{dt} = \frac{1}{\Theta} I_0 - \frac{1}{\Theta}\epsilon I - \epsilon k_I I$
Monomer Balance	$\frac{d\{\epsilon M_L + a M_S\}}{dt} = \frac{1}{\Theta} M_0 - \frac{1}{\Theta}\{\epsilon M_L + a M_S\} - \epsilon k_{pL} M_L \int_0^\infty r_L(x)dx - a k_{ps} M_S \int_0^\infty r_s(x)dx$
Equilibrium	$M_S = E[M_L] = \frac{j_1 M_L}{1 + j_2 M_L}$
Liquid Radicals	$\frac{\partial\{\epsilon r_L(x)\}}{\partial t} + k_{pL} M_L \frac{\partial\{\epsilon r_L(x)\}}{\partial x} = \epsilon 2 k_I I \delta(x) - h a r_L(x) - \epsilon k_{TL} r_L(x) \int_0^\infty r_L(y)dy - \frac{1}{\Theta}\epsilon r_L(x) - \epsilon k_{pL} M_L r_L(x)\,\delta(x - x_{cr})$
Liquid Polymer	$\frac{d\{\epsilon p_L(x)\}}{dt} = \epsilon k_{TL} \int_0^x r_L(y) r_L(x-y)dy \{1 - \Delta(x - x_{cp})\} - h a p_L(x) - \frac{1}{\Theta}\epsilon p_L(x)$
Subcritical Clusters	$\frac{d\{\epsilon \cdot \phi(v)\}}{dt} = \epsilon \frac{\chi^2}{v_{mi}} \frac{k_{TL}}{2} \int_0^{x(v)} r_L(y) r_L(x-y)dy \cdot \{1 - \Delta(v - v_c)\} - h a \phi(v) - \frac{1}{\Theta}\epsilon\phi(v) + \epsilon\beta_c \{\frac{1}{2}\int_0^v \phi(z)\phi(v-z)dz(1 - \Delta(v - v_c)) - \phi(v)\int_0^{v_c}\phi(z)dz\}$
Solid Radical	$\frac{\partial\{a r_s(x)\}}{\partial t} + k_{ps} M_S \frac{\partial\{a r_s(x)\}}{\partial x} = h a r_L(x) + \epsilon k_{pL} M_L r_L(x)\delta(x - x_{cr}) - \frac{1}{\Theta} a r_s(x) - a k_{TS} r_s(x) \int_0^\infty r_s(y)dy$
Solid Polymer	$\frac{\partial\{a p_s(x)\}}{\partial t} = -\frac{1}{\Theta} a p_s(x) + h a p_L(x) + a k_{TS} \int_0^x r_s(y) r_s(x-y)dy + \epsilon k_{TL} \int_0^x r_L(y) r_L(x-y)dy \cdot \Delta(x - x_{cp})$
Precipitated Particles	$\frac{\partial f(L)}{\partial t} + G \cdot \frac{\partial f(L)}{\partial L} = \epsilon B \delta(L) - \frac{1}{\Theta} f(L)$
Area Concentration	$a = 3K \int_0^\infty L^2 f(L)dL$
Liquid Fraction	$\epsilon = 1 - K \int_0^\infty L^3 f(L)dL$
Nucleation Rate	$B = \mathcal{L} k_{pL} M_L r_L(x)\delta(x - x_{cr}) + \mathcal{L}\frac{k_{TL}}{2}\int_{x_{cp}}^\infty dx\, \Delta(x - x_{cp}) \int_0^x r_L(y) r_L(x-y)dy + \frac{\beta_c}{2}\int_{v_c}^\infty dv\, \Delta(v - v_c)\int_0^v \phi(z)\phi(v-z)dz$
Growth Rate	$G = h\int_0^\infty (\frac{v_I}{2} + v_M x) r_L(x)dx + h\int_0^\infty (v_I + v_M x) p_L(x)dx + k_{ps} M_S v_M \int_0^\infty r_s(x)dx$
Critical Size	$\frac{v_I}{2} + x_{cr} v_M = v_I + x_{cp} v_M = \mathcal{L} K L_c^3 = \mathcal{L} v_c$

STEADY STATE ANALYSIS

The steady state behavior of precipitation polymerization reactors has been obtained from solution of the equations on page (14) with the time derivatives set to zero (8, 11). Criteria for the uniqueness of such steady state solutions have previously been discussed (10). Over a wide range of operating conditions, there will be a unique soluttion to the governing equations. Before presenting a brief outline of the solution for the steady state, it is convenient to first rewrite the steady state equations in dimensionless form.

One may scale the physical variable in terms of the internal transport and kinetic constants and the reactor inlet conditions. The following set of dimensionless variables are defined in terms of the physical variables replaced.

Replace physical variable	by	dimensionless variable
x		$\frac{3k\mathcal{L}}{\nu_m}\left(\frac{k_{pL} m_o \nu_m}{9hk\mathcal{L}}\right)^{3/2} \cdot x$
$r_L(x)$		$\frac{2k_I I_o}{k_{pL} M_o} r_L(x)$
$p_L(x)$		$\frac{2k_I I_o}{k_{pL} M_o} p_L(x)$
$r_s(x)$		$\frac{1}{3}\left(\frac{k_{pL} M_o \nu_M}{9hk\mathcal{L}}\right)^{\frac{1}{2}}\left(\frac{2k_I I_o}{k_{pL} M_o}\right) r_s(x)$
$p_s(x)$		$\frac{1}{3}\left(\frac{k_{pL} M_o \nu_M}{9hk\mathcal{L}}\right)^{1/2}\left(\frac{2k_I I_o}{k_{pL} M_o}\right) p_s(x)$
L		$\left(\frac{k_{pL} M_o \nu_m}{9hkI}\right)^{1/2} L$

Replace physical variable	by	dimensionless variable
V		$\left(\frac{k_{pL} M_o v_M}{2 k_z I_o \mathcal{L}^2}\right)^{1/2} \cdot V$
f		$\frac{1}{K}\left(\frac{9hK\mathcal{L}}{k_{pL} M_o V_M}\right)^{1/2} \cdot f$
ϕ		$\frac{2 k_z I_o \mathcal{L}^2}{k_{pL} M_o V_M} \cdot \phi$
a		$3\left(\frac{9hK\mathcal{L}}{k_{pL} M_o V_M}\right) \cdot a$
ϵ		$\epsilon_o \cdot \epsilon$
I		$I_o \cdot I$
M_L		$M_o \cdot M_L$
M_S		$E[M_D] \cdot M_S$

Replacement of the physical variables by the dimensionless variables in the equations governing the steady state behavior of the system results in the following dimensionless parameter constants and the appropriate forms for a dimensionless residence time and critical size.

The dimensionless values for θ, L_C, Xcr, X_{cp} and V_C are:

$$\Theta = \frac{K\mathcal{L}\, 2k_z I_o}{M_o V_M}\left(\frac{k_{pL} M_o V_M}{9hK\mathcal{L}}\right)^{3/2} \cdot \Theta$$

$$\left[L_c = \left\{3\left(x_{cr} + \frac{V_o}{2}\right)\right\}^{1/3} = \left\{3\left(x_{cp} + V_o\right)\right\}^{1/3} = \left(\frac{3V_c}{2\sqrt{M_z}}\right)^{1/3}\right] = \left(\frac{9hK\mathcal{L}}{k_{pL} M_o V_M}\right)^{1/2} \cdot L_C$$

$$V_o = \frac{V_I}{3\mu\mathcal{L}} \left(\frac{9h\mu\mathcal{L}}{k_{pL} M_o V_M}\right)^{3/2}$$

$$q = \frac{k_{pL} M_o V_M}{3h\,(M_o V_M)^{1/2}} \left(\frac{2k_I I_o}{9h\mu\mathcal{L}}\right)^{1/2}$$

$$\mu = 3 \cdot \left(\frac{9hK\mathcal{L}}{k_{pL} M_o V_M}\right)^{1/2} \frac{E[M_o]}{M_o}$$

$$\beta_c = \frac{\beta_c \cdot \mathcal{L}}{k_{pL} M_o V_M}$$

$$K = \frac{M_o V_M}{2K\mathcal{L} I_o} \left(\frac{9hK\mathcal{L}}{k_{pL} M_o V_M}\right)^{3/2}$$

$$k_T = \frac{k_{TL}}{2} \left(2k_I I_o\right)\left(\frac{k_{pL} M_o V_M}{9hK\mathcal{L}}\right)$$

$$l_T = \frac{k_{TS}}{k_{TL}} \cdot \frac{E[M_o]}{M_o}$$

$$l_p = \frac{k_{ps}\, E[M_o]}{k_{pL}\, M_o}$$

$$j = j_2 M_o$$

$$M_I = M_o V_M$$

The equations governing the steady state behavior of precipitation polymerization reactors may now be written in dimensionless form. The equations governing the steady state behavior of precipitation polymerization reactors are listed in Table II-2.

The equations governing the steady state behavior can be reduced significantly.

It is possible to compute f(L) for the steady state by direct integration.

II - 11 $$f(L) = \frac{\epsilon B}{G} e^{-\frac{L}{m_1 \Theta G}}$$

Expressions for a and can be obtained directly by computing moments.

$$a = \epsilon \cdot 2 (m_1 \Theta)^3 B G^2$$

$$1 - \epsilon = \epsilon \cdot 6 (m_1 \Theta)^4 B G^3$$

Rearrangement of the above relations yields:

II - 12a $$a = \frac{2 (m_1 \Theta)^3 B G^2}{1 + 6 (m_1 \Theta)^4 B G^3}$$

II - 12b $$\epsilon = \frac{1}{1 + 6 (m_1 \Theta)^4 B G^3}$$

from which an expression for the ratio a/ϵ can be obtained;

II - 12c $$\frac{a}{\epsilon} = 2 (m_1 \Theta)^3 B G^2$$

It is rare that one can develop explicit forms for both particle nucleation and growth rates. Here, however, one can obtain explicit expressions for B and G in terms of the reactor variables.

Consider first the equations for r_L (x), p_L (x), r_S (x) and ϕ (v).

Table II-2: Equations Governing Steady State Behavior of Precipitation Polymerization Reactors

Initiator Balance	$0 = 1 - (1+K\Theta)\epsilon \cdot I$
Monomer Balance	$0 = 1 - \epsilon \cdot M_L - U \cdot a \cdot M_S$
Equilibrium	$M_S = J[M_L] = \left(\frac{1+j}{1+jM_L}\right) \cdot M_L$
Liquid Radicals	$M_L \frac{\partial r_L(x)}{\partial x} = I\,\delta(x) - M_L r_L(x)\,\delta(x-x_{cr}) - \left(\frac{a}{\epsilon}\right) r_L(x) - k_T r_L(x) \int_0^\infty r_L(y)dy - \frac{\beta^2}{3\Theta} r_L(x)$
Liquid Polymer	$0 = -\frac{\beta^2}{3\Theta} p_L(x) + \frac{k_T}{2} \int_0^x r_L(y)\, r_L(x-y)dy \left\{1 - \Delta(x-x_{cp})\right\} - \left(\frac{a}{\epsilon}\right) p_L(x)$
Subcritical Clusters	$0 = \frac{k_T}{2\beta\sqrt{M_2}} \int_0^{x(v)} r_L(y)\, r_L(x-y)dy \left(1 - \Delta(x-x_{cp})\right) - \frac{\beta\sqrt{M_2}}{3\Theta} \phi(v) - \left(\frac{a}{\epsilon}\right)\phi(v) + \beta\left\{\frac{(\phi * \phi)(v)}{2}\left(1 - \Delta(v-v_c)\right) - \phi(v)\int_0^{v_c} \phi(z)dz\right\}$
Solid Radical	$\rho_p M_S \frac{\partial r_S(x)}{\partial x} = \frac{M_L}{a\epsilon} r_L(x)\,\delta(x-x_{cr}) + r_L(x) - \frac{k_T k_T}{4} r_S(x) \int_0^\infty r_S(y)dy - \frac{\beta^2}{3\Theta} r_S(x)$
Solid Polymer	$0 = -\frac{\beta^2}{3\Theta} p_S(x) + \frac{k_T k_T}{4} \int_0^x r_S(y)\, r_S(x-y)dy + \frac{k_T}{2} \int_0^x r_L(y)\, r_L(x-y)dy\, \Delta(x-x_{cp}) + p_L(x)$
Precipitated Particles	$G \frac{\partial f(L)}{\partial L} = \epsilon B\,\delta(L) - \frac{1}{m_2 \Theta} f(L)$
Area Concentration	$a = \int_0^\infty L^2 f(L)dL$
Liquid Fraction	$1 - \epsilon = \int_0^\infty L^3 f(L)dL$
Nucleation Rate	$B = M_L r_L(x_{cr}) + \frac{k_T}{2} \int_{x_{cp}}^\infty dx\, \Delta(x-x_{cp}) \int_0^x r_L(y)\, r_L(x-y)dy + \frac{\beta_c}{2} \int_{v_c}^\infty dV\, \Delta(v-v_c) \int_0^v \phi(z)\phi(v-z)dz$
Growth Rate	$G = \int_0^\infty \left(\frac{v_0}{2} + x\right) r_L(x)dx + \frac{1}{\beta^2 M_2} \int_0^{v_c} v \cdot \phi(v)dv + \rho_p M_S \int_0^\infty r_S(x)dx$
Critical Size	$x_{cr} + \frac{v_0}{2} = x_{cp} + v_0 = \frac{L_c^3}{3} = \frac{v_c}{\rho_0 M_2}$

Assume that the outflow rate is negligible compared to internal transport and chemical reaction rates. The solution for the distribution $r_L(x)$ is:

II-(13a) $$r_L(x) = \frac{I}{M_L} e^{-\frac{a/\epsilon + k_T \lambda_{0L}}{M_L} \cdot X} \quad ; \; X \leq X_{cr}$$
$$r_L(X) = 0 \quad ; \; X > X_{cr}$$

II-(14a) $$\lambda_{nL} = \int_0^\infty x^n r_L(x) dx$$

Computing the zeroth moment $\lambda_{0L} = \int_0^\infty r_{L0} dx$ results in the following expression:

II-(14b) $$k_T \lambda_{0L}^2 + \frac{a}{\epsilon} \lambda_{0L} - I\{1 - e^{-T}\}$$

where

II-(15) $$T = \left(\frac{a/\epsilon + k_T \lambda_{0L}}{M_L} \right) X_{cr}$$

Note that e^{-T} represents the fraction of radicals that grow by monomer addition past the critical size. Even in the case where coalescence may be negligible, the number of radicals that reach the critical size is negligible compared to the total number of radicals generated. (In a typical working range e^{-T} is of the order 10^{-10} and therefore may be neglected compared to 1 in the expression governing λ_{0L} .) With $e^{-T} \ll 1$, λ_{0L} may be expressed independent of M_L

II-(14c) $$\lambda_{0L} = \frac{a/\epsilon}{2k_T} \left(-1 + \sqrt{1 + 4 k_T I / (a/\epsilon)^2} \right)$$

It is convenient to define another dimensionless ω which carries the physical significance of being a measure of the termination to capture rate of radicals in the liquid phase.

II-(16) $$\omega = \frac{4 k_T I}{(a/\epsilon)^2}$$

Thus, it is possible to rewrite $r_L(X) = r_L(M_L, I, a/\epsilon)$.

II-)13b) $$r_L(X) = \frac{I}{M_L} e^{-\frac{a/\epsilon}{M_L}(1+\sqrt{1+\omega})\frac{X}{2}} = \frac{I}{M_L} e^{-T\frac{X}{X_{cr}}} \quad ; \; X \leq X_{cr}$$

$$r_L(X) = 0 \quad ; \; X > X_{cr}$$

Similarly, the equation governing the subcritical particle size distribution may be solved, leaving ϕ (v) as an explicit function of M_L, I and a/ϵ. Here, the outflow term is also neglected compared to the internal transport (capture) rate. The solution of this integral equation in ϕ (v) has previously been obtained (11). The solution is:

$$\phi(v) = k_\phi \frac{I}{M_L} e^{-\tau \frac{v}{v_c}} \int_0^v \frac{I_1(\tau z)}{z} dz \quad ; \quad v \leq v_c$$

$$\phi(v) = 0 \quad ; \quad v > v_c$$

where

$$k_\phi = \sqrt{k_T / (\rho_c \beta^2 m_L)}$$

$$\tau = \sqrt{\omega^2 / \left(\omega^2 + 4 k_\phi^2 \left(1 + \sqrt{1+\omega}\right)^2\right)} \cdot \frac{T}{v_c}$$

This expression gives ϕ (v) explicitly as a function of M_L, I and a/ϵ. (Here the fraction of subcritical clusters growing past the critical size is assumed to be negligible compared to the fraction of clusters which are captured by existing stable particles.) At this point one need only consider the zeroth moment of the solid radical balance. Integrating the steady state equation for r_s (x) yields:

II-(18a) $$0 = \lambda_{0L} - \frac{l_T k_T}{u} \lambda_{0s}^2$$

where

$$\lambda_{0s} = \int_0^\infty r_s(x) dx$$

The expression for λ_{0s} may be solved explicitly as a function of I and a/ϵ $\{$ for $e^{-T} \ll 1\}$

II-(18b) $$\lambda_{0s} = \sqrt{\frac{u}{l_T k_T} \frac{a/\epsilon}{2k_T} \left(-1 + \sqrt{1+\omega}\right)}$$

One may also solve for the liquid polymer size distribution by direct integration:

$$p_L(x) = \frac{k_T}{2a/\epsilon} \int_0^x r_L(y)\, r_L(x-y)\, dy \left\{1 - \Delta(x - x_{cp})\right\}$$

From the equation II-(13b) for r_L (x), p_L (x) becomes:

II-(19) $$p_L(x) = \frac{k_T}{2a/\epsilon} \left(\frac{I}{M_L}\right)^2 x\, e^{-T \frac{x}{x_{cr}}} \quad ; \quad x \leq x_{cp}$$

$$p_L(x) = 0 \quad ; \quad x > x_{cp}$$

It is now possible to reduce the expressions for B and G to explicit functions of M_L, I and a/ϵ.

The particle growth rate G will be divided in terms of the two principal contributions to particle growth. Let G_c be the portion of the growth rate due to capture of radicals and polymers from the liquid phase and G_p be the portion of the growth rate due to polymerization of monomer adsorbed on the particles' surfaces,

II-(9b) $$G = G_c + G_p$$

where

II-(20a) $$G_c = \int \left(\frac{V_0}{2}+x\right) r_L(x)\,dx + \int (V_0+x)\, p_L(x)\,dx$$

II-(21a) $$G_p = \ell_p M_s \int r_s(x)\,dx$$

G_c can be computed by taking the leading moments of $r_L(x)$ and $p_L(x)$. Integration and simplification yields:

II-(20b) $$G_c \approx \frac{V_0}{4k_T}\frac{(a/\epsilon)\omega(1+\omega+\sqrt{1+\omega})}{(1+\sqrt{1+\omega})^2} + \frac{M_L}{k_T}\left\{\frac{1+\frac{\omega}{4}+\sqrt{1+\omega}}{(1+\sqrt{1+\omega})^3}\right\}$$

G_p can be simplified by rewriting M_s and λ_{os} in terms of M_L, I and a/ϵ as follows:

II-(21b) $$G_p \approx \ell_p \left\{\frac{(1+j)M_L}{1+j\cdot M_L}\right\}\sqrt{\frac{u}{\ell_T k_T}\left(\frac{a/\epsilon}{2k_T}\right)\left(-1+\sqrt{1+\omega}\right)}$$

Therefore, the particle growth rate is expressible explicitly as a function of ML, I and a/ϵ, and the dimensionless parameter constants.

$$G = G_c + G_p = G\{M_L, I, a/\epsilon\}$$

II-(22) $$G \approx \frac{V_0}{4k_T}\frac{(a/\epsilon)\omega(1+\omega+\sqrt{1+\omega})}{(1+\sqrt{1+\omega})^2} + \frac{M_L\,\omega\left\{1+\frac{\omega}{4}+\sqrt{1+\omega}\right\}}{k_T\left\{1+\sqrt{1+\omega}\right\}^3} + \ell_p\frac{(1+j)M_L}{(1+j\cdot M_L)}\sqrt{\frac{u}{\ell_T k_T}\frac{a/\epsilon}{2k_T}\left(-1+\sqrt{1+\omega}\right)}$$

It is also possible to write B as an explicit function of M_L, I and a/ϵ. At this point it is first convenient to combine the contributions of liquid radical growth and termination to nucleation, B_p and B_T as B_g;

$B_g = B_p + B_T$

i.e. $$B_g = M_L r_L(x_{cr}) + \frac{k_T}{2}\int_{x_{cp}}^{\infty} dx\, A(x-x_{cp}) \int_0^x r_L(y)\, r_L(x-y)\, dy$$

B_g may be computed by direct integration using equation II-(13b) as follows:

$$B_g \approx I \cdot \left\{ 1 + \frac{W}{2} \frac{(T-1)}{(1+\sqrt{1+W})^2} \right\} \cdot e^{-T}$$

where;

$$e^{-T} << 1 \quad \text{and} \quad x_{cp} \approx x_{cr}$$

and W and T are explicit functions of M_L, I and a/ϵ. (See equations II-(15 & 16)

The contribution of coalescence to nucleation may be obtained by evaluation of the collision integral for B_c.

II-(23) $$B_c = \frac{\beta_c}{2}\int_{V_c}^{\infty} dV\, A(V-V_c) \int_0^V \phi(z)\,\phi(V-z)\, dz = \frac{\beta_c}{2}\int_{V_c}^{2V_c} dV \int_{V-V_c}^{V_c} \phi(z)\,\phi(V-z)\, dz$$

where

$$\phi(V) = \phi\left[V, (M_L, I, a/\epsilon)\right]$$ as given in equation II-(17)

Here, again, we have an expression for the nucleation rate which depends on M_L, I and a/ϵ and the dimensionless parameter constants. Due to analytic complexity this expression cannot be reduced further. Computation for B_c (M_L, $I, a/\epsilon$) must proceed by numerical integration. B can then be computed as $B(M_L, I, a/\epsilon) = B_g + B_c$

Applying the expressions for λ_{oL} and λ_{oS} as functions of I and a/ϵ to the monomer consumption balance and using the initiator balance to express $\epsilon = \epsilon(I) = \frac{1}{1+K\Theta}$ one may solve the equation M_L explicitly as functions of I, and a/ϵ.

II-(24) $$M_L = \left(\frac{1 + \lambda_{oL} + (a/\epsilon)(1+j)(u+l_p\lambda_{oS})}{2j(1+\lambda_{oL})} \right) \left(-1 + \sqrt{1 + \frac{4j(1+\lambda_{oL}(K\Theta+1)I)}{(1+\lambda_{oL}+(a/\epsilon)(1+j)(u+l_p\lambda_{oS}))}} \right)$$

Rewriting equations II-(12b) and II-(12c), with ϵ replaced by $\epsilon(I)$, one is left with two equations whose solution yields the steady state behavior of continuous precipitation polymerization reactors.

(12c) $$\frac{a}{\epsilon} = 2(m_I\theta)^3 B G^2$$

(12b) $$I = \left(\frac{1}{1+k\theta}\right)\left(1 + 6(m_I\theta)^4 B G^3\right)$$

where

$M_L = M_L(I, a/\epsilon)$ equation II-(24)

$B = B\{M_L(I, a/\epsilon), I, a/\epsilon\}$ equation II-(10c)

$G = G\{M_L(I, a/\epsilon), I, a/\epsilon\}$ equation II-(9c)

Solution of the above equation cannot be obtained by direct iteration or by Newton-Raphson iteration. (The above relations do not result in a contraction mapping.) Solutions for the steady state reactor performance have been obtained by a complex numerical interpolation. In figures II-(1, 2) results are presented comparing the solutions obtained for a system in which coalescence is the predominate mechanism to that obtained by neglecting coalescence (i.e. taking $\beta_c = 0$). Solution of the coalescence model required repeated computation of a (computer) time-costly numerical integration; thus, only the effects of varying initiator and monomer concentration in the feed have been considered. Although the growth model cannot quantitatively model the coalescence model, some of the basic properties of the models do follow one another qualitatively. These properties shall be amplified in the discussion of the dynamic behavior of the system.

Finally, it should be noted that these equations have unique solutions over the residence time range studied. Uniqueness criteria for the steady state have been presented in the previous section. From the dependence of B and G on M_L, I and a/ϵ, it should be clear that the unique solutions are obtained in the physical working range of such systems.

Figure II-1: Surface concentration of solids versus residence time for growth and coalescence models of various feed conditions. Stability limits for growth model are included.
G, C-1: Mo = 2×10^{-3}, Io = 5×10^{-6}
G, C-2: Mo = 1.5×10^{-3}, Io = 5×10^{-6}
G, C-3: Mo = 1.5×10^{-3}, Io = 2×10^{-6}
} mol/cm³

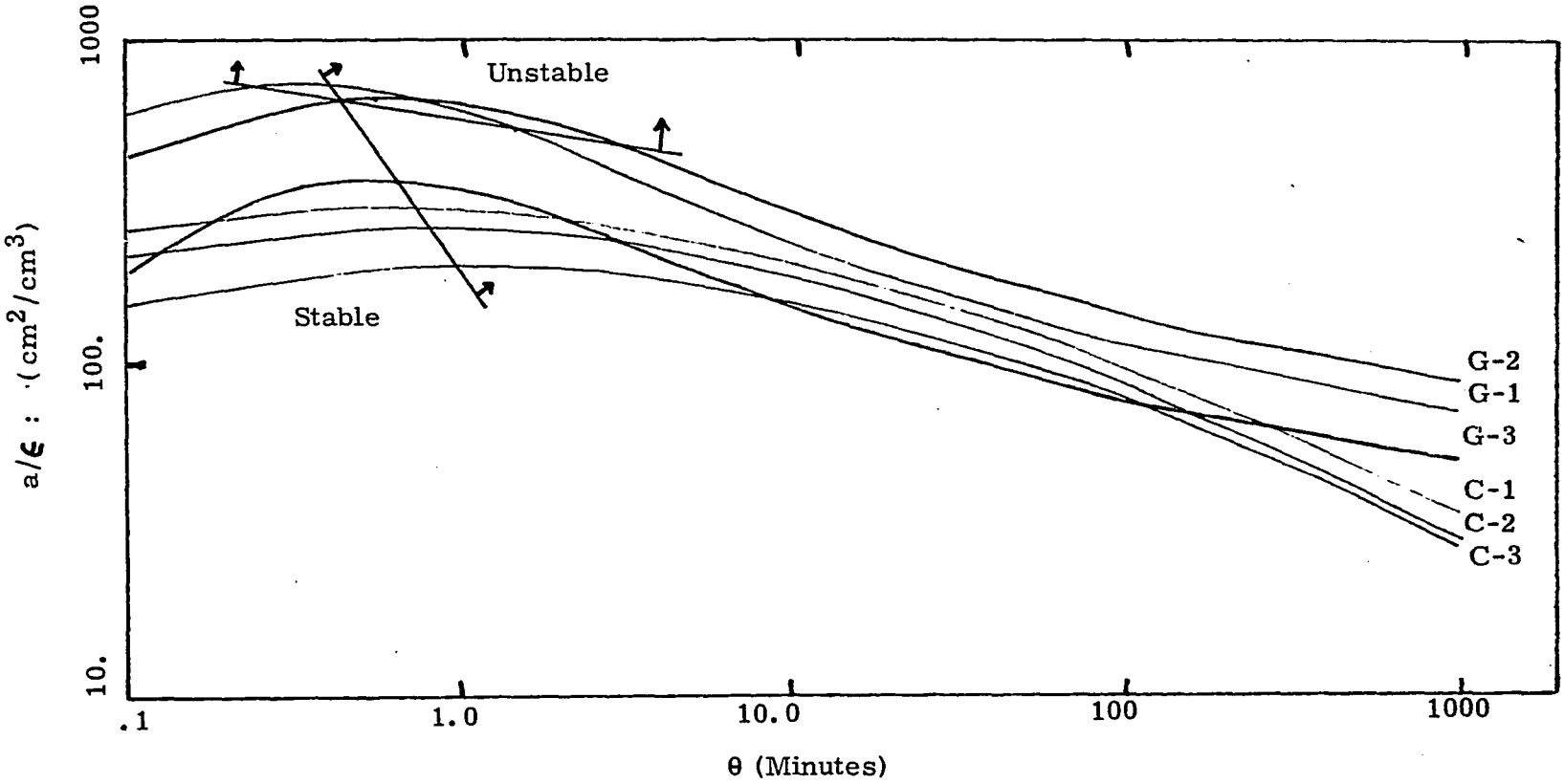

Figure II-2: Comparison of Nucleation rate versus growth rate for the aqueous polymerization of a precipitating polymer using growth and coalescence models.

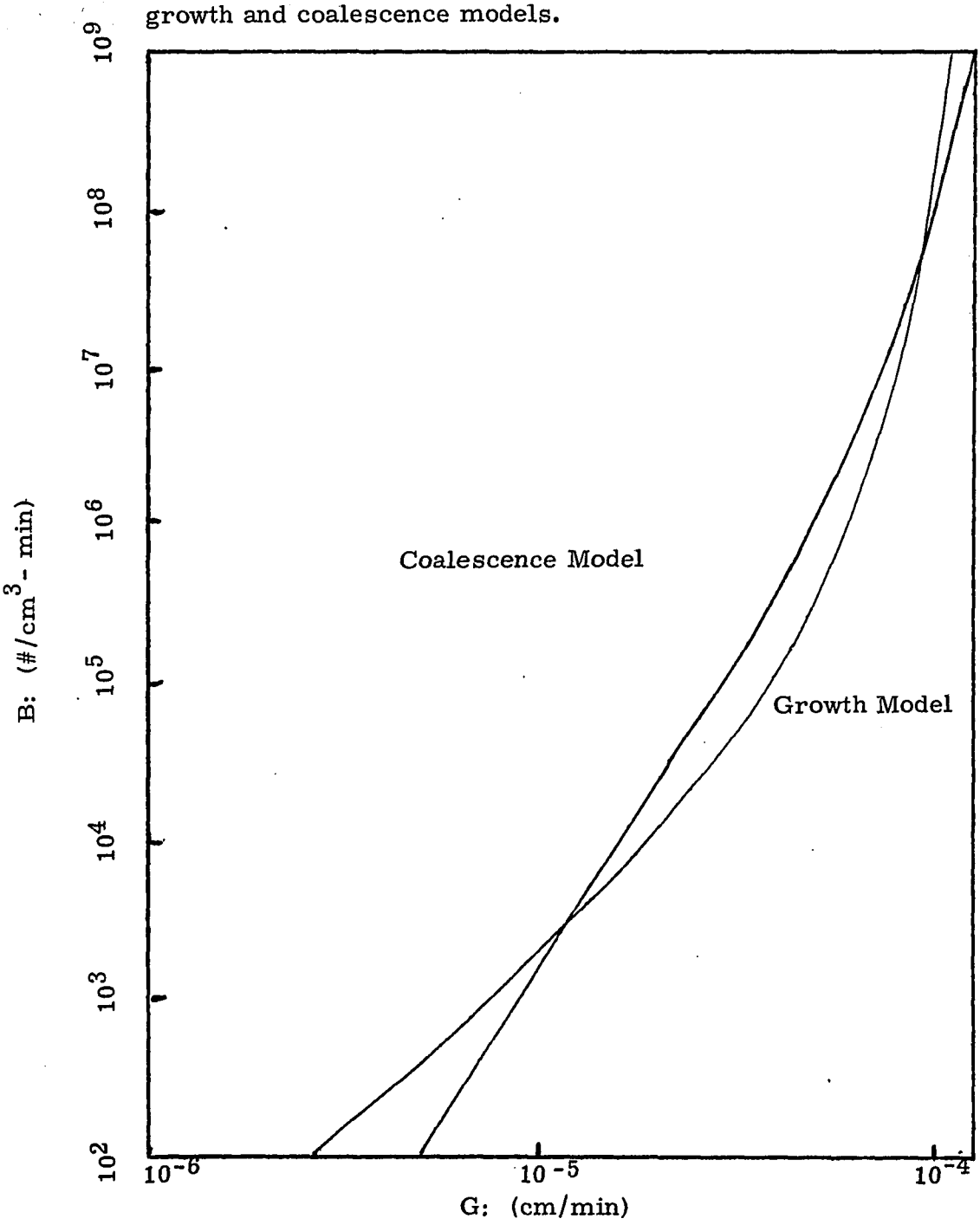

DYNAMIC ANALYSIS

The equations governing the dynamic behavior of continuous precipitation polymerization reactors were given on page (14). These equations are highly non-linear, and in their present form are virtually untractable. It is possible to make several sound physical approximations that will reduce the complexity of the governing equations and permit a linearized stability analysis to be carried out from which physically identifiable stability criteria can be obtained.

In the continuous production of the precipitating polymers, variations in the monomer, initiator, and area concentrations in the liquid occur on a time scale which is of the order of magnitude of the mean residence time of the reactor. With respect to a small instant of time (that is, compared to the mean residence time) the values of M_L, M_S, I, a, and ϵ will not change very drastically. In this short period of time where M_L, M_S, I, a and ϵ are nearly constant, the radical and subcritical polymer balances can be viewed to be in a quasi-steady state. That is, in this time period, the size distributions of these species will reach what may be referred to as quasi-steady values due to the fact that the time scale for internal transport and chemical reaction are infinitesimally small compared to the time scale for variations in M_L, M_S, I, a and ϵ . We neglect the accumulation and outflow rates of $r_L(x)$, $p_L(x)$, $r_S(x)$, and $\phi(v)$ in their governing equations and consider that their time variations occur implicitly through the time dependence of M_L, M_S, I, a and ϵ .

Based on these quasi-steady approximations, we compute the time dependence of the nucleation rates implicitly through their dependence on

M_L, I, and a/ϵ. That is, the liquid and solid radical balances and the liquid polymer and polymer cluster distributions can be solved by consecutive integration resulting in expressions in a form equivalent to those obtained in the steady state analysis. Thus, one may write expressions for B and G where the time variations in

II-(10d) $$B = \mathcal{L}\{k_{pL} M_L r_L(x_{cr}) + \mathcal{L}\frac{k_{TL}}{2}\int_{x_{cp}}^{\infty} dx\, A(x-x_{cp})\int_0^x r_L(y) r_L(x-y)\,dy + \frac{k_c}{2}\int_{v_c}^{\infty} dv\, A(v-v_c)\int_0^v \phi(z)\phi(v-z)\,dz$$

II-(9d) $$G = h\int\left(\frac{v_r}{2}+v_m x\right) r_L(x)\,dx + h\int(v_c+v_m x)\, p_L(x)\,dx + k_{ps} M_S V_m \int r_S(x)\,dx$$

can be expressed implicitly through the variations of M_L, I, and a/ϵ. These expressions are exactly equivalent in terms of the functional dependence on M_L, I, and a/ϵ of particle nucleation and growth to those developed in the steady state solution.

Further, it should be noted that virtually all monomer polymerized in the liquid phase leaves the system as part of the precipitated particles. This is inherent in the assumption that the capture rate is much larger than the outflow rate. The monomer balance may then be written as a resource balance; where ($\epsilon \cdot M_L + a \cdot M_S$) represents the total unreacted monomer in the system and ($1-\epsilon$) ρ represents the total mass of the polymerized monomer. (ρ is the polymer product density.) At this point one may rewrite the governing equations in the following form:

II-(25)	Initiator balance	$\frac{d(\epsilon I)}{dt} = \frac{1}{\theta} I_0 - \frac{1}{\theta}\epsilon I - k_I \epsilon I$
II-(26)	Monomer equilibrium	$M_S = E[M_1] = \frac{j_1 \cdot M_L}{1 + j_2 \cdot M_L}$
II-(27)	and resource balance	$\frac{d\{\epsilon M_L + a M_S + (1-\epsilon)\rho\}}{dt} = \frac{1}{\theta} M_0 - \frac{1}{\theta}\{\epsilon M_L + a M_S + (1-\epsilon)\rho\}$

II-(28a) Particle balance $$\frac{\partial f(L)}{\partial t} + G\frac{\partial f(L)}{\partial L} = -\frac{1}{\theta} f(L) \quad ; \; L>0$$

II-(28b) $$G \cdot f(L) = \epsilon \cdot B \quad ; \; L=0$$

where

II-(29) $$a = 3k\int f(L) L^2 dL$$

II-(30) $$\epsilon = 1 - k\int f(L) L^3 dL$$

and

II-(10d) $$B = B(M_L, I, a/\epsilon)$$

II-(9d) $$G = G(M_L, I, a/\epsilon)$$

The $\epsilon \cdot B \cdot \delta L$ in the particle balance has been replaced by the appropriate boundary conditions.

The nucleation and growth rates used here are continuous functions of M_L, I and a/ϵ based on the quasi-steady state kinetic analysis. Therefore, they can be differentiated explicitly with respect to M_L, I, and a/ϵ, thereby permitting linearization to be carried out explicitly.

The dynamic behavior of precipitation polymerization reactors can now be studied by performing a linearized analysis on the system's equations II-(10)

Linearization of the system's equations results in the identification of a linear operator governing the dynamic behavior of the system. Solution of the associated eigen value problem results in the characteristic equation of the system. The characteristic equation is I-(16):

II-(31) $$P(s) = s^4 + (4+g^*)s^3 + (6+4g^*)s^2 + (4+6g^*-m)s + (1+b^*+3g^*-m)$$

where

$$b^* = \alpha \cdot \left\{ \left[\left(1 + \frac{\sigma_L b_M}{1+\sigma_S \hat{M}_S}\right) - b_I \right] \left[1+\gamma - \frac{\sigma_S}{1+\sigma_S \hat{M}_S} g_M \right] - \beta \left[1 - g_I \left(\frac{\sigma_L - \sigma_S}{1+\sigma_S \hat{M}_S} \right) g_M \right] \right\}$$
$$+ \left[\left(\frac{\sigma_L}{1+\sigma_S \hat{M}_S} \right) g_M - g_I - \gamma \right] \left[\left(\frac{\sigma_S}{1+\sigma_S \hat{M}_S} \right) b_M \right]$$

$$g^* = \alpha \left\{ \left(\frac{\sigma_L + \frac{\sigma_S}{\alpha}}{1+\sigma_S \hat{M}_S} \right) g_M - g_I - \left(\frac{\alpha+1}{\alpha} \right) \gamma \right\}$$

$$m = \beta - \gamma - \left(\frac{\sigma_S}{1+\sigma_S \hat{M}_S} \right) (b_M - g_M)$$

are stability sensitivity parameters evaluated at the steady state under study. The terms on the right-hand side are taken at the steady state under study are defined as follows:

$$b_m = \frac{\partial \ln B}{\partial \ln M_L}, \quad b_I = \frac{\partial \ln B}{\partial \ln I}, \quad \beta = \frac{\partial \ln B}{\partial \ln q/\epsilon}$$

$$g_m = \frac{\partial \ln G}{\partial \ln M_L}, \quad g_I = \frac{\partial \ln G}{\partial \ln I}, \quad \gamma = \frac{\partial \ln G}{\partial \ln q/\epsilon}$$

$$\sigma_S = 4 \frac{a}{\epsilon} \frac{M_S}{M_L}, \quad \sigma_L = \left(\frac{\frac{1}{m_I} - M_L}{M_L} \right)$$

σ_L is a measure of the ratio of polymerized to unpolymerized monomer. σ_S is a rato of the unreacted monomer adsorbed on the surface of the precipitated particles to the unreacted monomer residing in the liquid. (Note the density of the polymer product is taken equal to the density of monomer for mathematical simplicity.)

Note that the nucleation and growth sensitivities to monomer are weighted by σ_L which for aqueous polymerizations will typically be around 4 to 1. Thus, even in the range where nucleation and growth sensitivities to initiator are of the same order of magnitude as the monomer sensitivities, they are a small contribution to the stability parameters b* and g*.

In the numerical cases tested, the monomer adsorbed on the surface of the precipitated particles was a negligible fraction of the unreacted monomer in the system. The term in b* containing σ_S was small for such cases. Further, if the nucleation rate is area independent, the term will also be negligible compared to the monomer sensitivity. Also note that as γ approaches -1 the first term in b* will be small. If the adsorbed monomer were not small, the computation of the capture surface based on the size distribution of the precipitated particles would not be exact. If σ_S is not small ($\sigma_S \ll 1$) the expressions for the growth rate and computation of the total surface must be rederived. Even in this form, the effect of a large σ_S on stability can be accounted

for physically in a qualitative manner.

Application of the Routh-Hurwitz criterion to the characteristic equation results in the following stability criteria for a steady state operating point of a continuous precipitation polymerization reactor (10).

II-33 $$-\left\{3g^*+1-m\right\} < b^* < \left\{\frac{2g^{*3}+(87-3m)g^{*2}+(112-2m)g^*+64-m^2}{(g^*+4)^2}\right\}$$

$$g^* > -2+\sqrt{-\left(\frac{m+4}{4}\right)} \quad ; \quad m \leq -5$$

$$g^* > -\frac{2}{3}\left\{2+\left(\sqrt{-\left(\frac{m+4}{4}\right)}\right)^2\right\} ; \quad m \geq -5$$

These results may be presented graphically in the (b*, g*) plane with m as a parameter. (See Figure I-6, pp 27) Note that for g* much greater than $|m|$ and 1, the ratio of b*/g* at the upper stability limit approaches 21. Further the results for the case where m = 0, which will occur in the range in which B and G are independent of area, are exactly equivalent to the results obtained by Sherwin (3) for the isothermal continuous crystallizer.

Thus, with a knowledge of the nucleation and growth sensitivites at a steady state in question, one can test the linear stability of the system by computation of b*, g* and m and application of the above stability criteria.

GROWTH SENSITIVITIES IN PRECIPITATION POLYMERIZATION

The expression for the growth rate of precipitated particles G has been formulated independent of the nucleation kinetics. It is possible to obtain general expressions for the growth sensitivities g_m, g_I, and in terms of the steady state operating condition under study. As one is dealing here with logarithmic derivatives, it is possible to use the dimensionless expression for G to obtain the growth sensitivities. With $\omega = \frac{4k_T I}{\sigma(1-\epsilon)^2}$

$$G \approx \frac{V_0(\frac{a}{\bar{a}})\omega(1+\omega+\sqrt{1+\omega})}{2k_T(1+\sqrt{1+\omega})^2} + \frac{M_{1L}\omega\cdot(1+\omega+\sqrt{1+\omega})}{k_T(1+\sqrt{1+\omega})^3} + \frac{\ell_p(1+j)M_L}{(1+j\cdot M_L)}\cdot\sqrt{\frac{u}{\ell_T k_T}\frac{(a/\epsilon)}{2k_T}(-1+\sqrt{1+\omega})}$$

the growth sensitivities can be obtained by direct differentiation of the expression for G. The growth sensitivities computed in terms of the steady state operating conditions are:

$$\frac{\partial \ln G}{\partial \ln M_L} = g_m = \left\{ \frac{\lambda_{1L} + M_{1L} + \frac{\partial \ln M_S}{\partial \ln M_L}\cdot \ell_p M_S \lambda_{0S}}{V_0\left(\frac{\lambda_{0L}}{2} + M_{0L}\right) + \lambda_{1L} + M_{1L} + \ell_p M_S \lambda_{0S}} \right\}$$

$$\frac{\partial \ln G}{\partial \ln I} = g_I = \left\{ \frac{V_0\left(\frac{\lambda_{0L}}{4}\cdot\frac{\omega}{\sqrt{1+\omega}(-1+\sqrt{1+\omega})} + M_{0L}\left(2 - \frac{\omega}{\sqrt{1+\omega}(1+\sqrt{1+\omega})}\right)\right) + \frac{\lambda_{1L}}{\sqrt{1+\omega}} + M_{1L}\left(2 - \frac{3\omega}{2\sqrt{1+\omega}(1+\sqrt{1+\omega})}\right) + \frac{\ell_p M_S \lambda_{0S}\,\omega}{4\sqrt{1+\omega}(-1+\sqrt{1+\omega})}}{V_0\left(\frac{\lambda_{0L}}{2} + M_{0L}\right) + \lambda_{1L} + M_{1L} + \ell_p M_S \lambda_{0S}} \right\}$$

$$\frac{\partial \ln G}{\partial \ln a/\epsilon} = \gamma = -\left\{ \frac{V_0\left(+ M_{0L}\left(3 - \frac{2\omega}{\sqrt{1+\omega}(1+\sqrt{1+\omega})}\right) + \frac{2\lambda_{1L}}{\sqrt{1+\omega}} + M_{1L}\left(4 - \frac{3\omega}{\sqrt{1+\omega}(1+\sqrt{1+\omega})}\right) + \frac{\ell_p M_S \lambda_{0S}}{2\sqrt{1+\omega}}\right.}{V_0\left(\frac{\lambda_{0L}}{2} + M_{0L}\right) + \lambda_{1L} + M_{1L} + \ell_p M_S \lambda_{0S}} \right\}$$

where general expressions for $\lambda_{0L}, \lambda_{1L}, M_{0L}, M_{1L}, \lambda_{0S}$ are summarized in the first column of Table II-3. With these expressions for g_m, g_I, and γ the value of g* for a given steady state operating condition can be computed directly.

Table II-3: Expressions for leading moments of radical and polymer size distributions and monomer equilibrium

Quantity	Generalized Form	Asymptotic Forms	
		$\omega \gg 1$	$\omega \ll 1$
λ_{0L}	$\frac{a/\epsilon}{2k_T}\left(-1+\sqrt{1+\omega}\right)$	$\sqrt{k_T I}$	$\frac{I}{a/\epsilon}$
λ_{1L}	$\frac{M_L}{k_T}\frac{\omega}{(1+\sqrt{1+\omega})^2}$	$\frac{M_L}{k_T}$	$\frac{M_L I}{(a/\epsilon)^2}$
μ_{0L}	$\frac{a/\epsilon}{8k_T}\frac{\omega^2}{(1+\sqrt{1+\omega})^2}$	$\frac{I}{2\,a/\epsilon}$	$\frac{k_T I}{2(a/\epsilon)^3}$
μ_{1L}	$\frac{M_L}{2k_T}\frac{\omega^2}{(1+\sqrt{1+\omega})^3}$	$\frac{M_L\sqrt{I}}{a/\epsilon}$	$\frac{8k_T I^2 M_L}{(a/\epsilon)^4}$
λ_{0S}	$\sqrt{\frac{u}{l_T k_T}\frac{a/\epsilon}{2k_T}\left(-1+\sqrt{1+\omega}\right)}$	$\sqrt{\frac{u}{l_T k_T}\sqrt{k_T I}}$	$\sqrt{\frac{u}{l_T k_T}\frac{I}{a/\epsilon}}$
M_S	$\left(\frac{(1+j)\,M_L}{1+j\cdot M_L}\right)$	$j \gg 1$, $M_S \sim 1$ $j \ll 1$, $M_S \sim M_L$	

NUCLEATION SENSITIVITIES IN PRECIPITATION POLYMERIZATION

In this section it will be shown how expressions for the nucleation sensitivities can be obtained analytically. The nucleation sensitivities b_m, b_I, and β are computed as the weighted sum of the contributions of each nucleation mechanism. That is, for each generalized formulation, we have B in the form $B = B_g + B_c$, and therefore

$$\frac{\partial \ln B}{\partial \ln Y} = \frac{B_g}{B} \frac{\partial \ln B_g}{\partial \ln Y} + \frac{B_c}{B} \frac{\partial \ln B_c}{\partial \ln Y}$$

(Y represents M_L, I, or a/ϵ.) In the first formulation, radical growth and termination past the critical size are included in B_g and pure polymer coalescence is the B_c contribution. For the averaged coalescence model, B_g and B_c refer to the averaged growth and coalescence of the subcritical clusters past the critical size, respectively. (See Appendix II-A) With the nucleation and growth sensitivities at hand b* and m may then also be computed. Along with the value of g* computed, one may then test the stability of a given steady state operating point.

Consider the contribution of radical growth and termination to nucleation. In the quasi-steady state hypothesized, the nucleation rate has the same form as that obtained in the steady state analysis. The dimensionless steady state equation for B_g can be differentiated directly to obtain $\frac{\partial \ln B}{\partial \ln Y}$. The dimensionless form for B_g is:

$$B_g \approx I \cdot \left\{ 1 + \frac{\omega (T-1)}{2 (1+\sqrt{1+\omega})} \right\} e^{-T} \quad ; e^{-T} \ll 1$$

The particle nucleation sensitivities obtained by direct differentiation are:

$$\frac{\partial \ln B_g}{\partial \ln M_L} \approx T \cdot \left(\frac{1 + \frac{\omega (T-2)}{2 (1+\sqrt{1+\omega})^2}}{1 + \frac{\omega (T-1)}{2 (1+\sqrt{1+\omega})^2}} \right)$$

$$\frac{\partial \ln B_g}{\partial \ln I} \approx 1 + \left\{ \frac{\frac{\omega}{\sqrt{1+\omega}} \left(\frac{T-1}{2} \right) \frac{1}{(1+\sqrt{1+\omega})^2} - T \cdot \left(1 + \frac{\omega (T-2)}{2 (1+\sqrt{1+\omega})^2} \right) \left(\frac{\omega}{\sqrt{1+\omega} (1+\sqrt{1+\omega})} \right)}{1 + \frac{\omega (T-1)}{2 (1+\sqrt{1+\omega})^2}} \right\}$$

$$\frac{\partial \ln B_q}{\partial \ln q/\epsilon} \approx \left\{ \frac{-\frac{\omega}{\sqrt{1+\omega}}\left(\frac{T-1}{4}\right)\frac{1}{(1+\sqrt{1+\omega})^2} - \frac{T}{\sqrt{1+\omega}}\left(1+\frac{\omega}{2}\frac{(T-2)}{(1+\sqrt{1+\omega})^2}\right)}{1+\frac{\omega(T-1)}{2(1+\sqrt{1+\omega})^2}} \right\}$$

Now consider the term representing the contribution of pure polymer coalescence in particle formation. The solution of the sub-critical cluster balance in the quasi-steady state is exactly equivalent in functional dependence on M_L, I and a/ϵ as the dimensionless solution in the steady state analysis. The dimensionless form of the steady state solution is again used to obtain the logarithmic derivatives in terms of the steady state operating condition under study.

The nucleation rate due to coalescence of the sub-critical aggregates is computed as follows;

$$B_c = \frac{\beta_c}{2}\int_{V_c}^{2V_c} dV \cdot \int_{V-V_c}^{V_c} \phi(z)\,\phi(V-z)\,dz$$

where:

$$\phi(V) = P_c\, e^{-T\frac{V}{V_c}\int_0^V \frac{I_1(\tau z)}{z}\,dz}$$

$$P_c = k_\phi \frac{I}{M_L}$$

$$k_\phi = \sqrt{k_T/(\beta_c \beta^2 m_s)}$$

$$\tau_c = \sqrt{1/(1+\lambda_\phi^2)} \cdot \frac{T}{V_c}$$

$$\lambda_\phi = 2k_\phi(1+\sqrt{1+\omega})/\omega$$

The values of $\frac{\partial \ln \beta_c}{\partial \ln Y}$ may then be computed from the complex collision integral as follows:

$$\frac{\partial \ln B_c}{\partial \ln Y} = \frac{\int_{V_c}^{2V_c} dV \cdot \int_{V-V_c}^{V_c} dz \cdot \left\{ Y \cdot \frac{\partial \phi(z)}{\partial Y}\cdot \phi(V-z) + Y \cdot \phi(z)\frac{\partial \phi(V-z)}{\partial Y}\right\}}{\int_{V_c}^{2V_c} dV \int_{V-V_c}^{V_c} dz \cdot \phi(z)\,\phi(V-z)}$$

Taking the partial derivatives of $\phi(z)$ and $\phi(V-z)$ with respect to Y and regrouping terms leaves the following expression for $\frac{\partial \ln B_c}{\partial \ln Y}$:

$$\frac{\partial \ln B_c}{\partial \ln Y} = 2\cdot\left\{\frac{\partial \ln P_c}{\partial \ln Y} + \left(\langle S(V)\rangle - 1\right)\frac{\partial \ln \tau_c}{\partial \ln Y}\right\} - T\cdot\frac{\partial \ln T}{\partial \ln Y}$$

where

$$\left\langle \frac{V}{V_c}\right\rangle = \frac{\int_{V_c}^{2V_c} dV\cdot\left(\frac{V}{V_c}\right)\int_{V-V_c}^{V_c}\phi(z)\,\phi(V-z)\,dz}{\int_{V_c}^{2V_c} dV\cdot\int_{V-V_c}^{V_c}\phi(z)\,\phi(V-z)\,dz}$$

$$S(V) = \left\{\int_0^V I_0(\tau z)\,\tau\,dz \Big/ \int_0^V \frac{I_1(\tau z)}{z}\,dz\right\}$$

$$\langle S(V)\rangle = \frac{\int_{V_c}^{2V_c} dV\cdot\int_{V-V_c}^{V_c} S(z)\,\phi(z)\,\phi(V-z)\,dz}{\int_{V_c}^{2V_c} dV\int_{V-V_c}^{V_c}\phi(z)\,\phi(V-z)\,dz}$$

$\langle \frac{v}{v_c} \rangle$ has the physical significance of being a weighted average of the particle size at which stable nuclei are produced via coalescence. It varies between 1 and 2 and in most cases is only slightly above 1. The weighting function S (v) which arose in the complex differentiation varies from 2 when $\tau_z \sim 0$ to approximately τ_v for $\tau \gg 1$. The resulting $\langle S(v) \rangle$ for subsequent qualitative discussion of system stability, is approximated as $(\frac{\tau V_c}{2})$.

P_c, τ_c, T are continuous differentiable functions of M_L, I, and a/ϵ. Therefore, it is possible to compute $\frac{\partial \ln P_c}{\partial \ln \gamma}$, $\frac{\partial \ln \tau_c}{\partial \ln \gamma}$ and $\frac{\partial \ln T}{\partial \ln \gamma}$ analytically, and evaluate them for a given steady state operating point under question. It is then possible to obtain $\frac{\partial \ln B_c}{\partial \ln M_L}$, $\frac{\partial \ln B_c}{\partial \ln I}$ and $\frac{\partial \ln B_c}{\partial \ln a/\epsilon}$ from the values of each $\frac{\partial \ln P_c}{\partial \ln \gamma}$, $\frac{\partial \ln \tau_c}{\partial \ln \gamma}$, $\frac{\partial \ln T}{\partial \ln \gamma}$ and the values of the collision integrals $\langle \frac{v}{v_c} \rangle$ and $\langle S(v) \rangle$. Explicit expressions for these partial derivatives in terms of the steady state operating condition under study are:

$$\frac{\partial \ln B_c}{\partial \ln M_L} = T \cdot \langle \frac{v}{v_c} \rangle - 2 \cdot \langle S(v) \rangle$$

$$\frac{\partial \ln B}{\partial \ln I} = \frac{2 \cdot (1 + \lambda_\omega/2)}{1 + \lambda_\phi^2} - \frac{\lambda_\omega}{2} \cdot T \cdot \langle \frac{v}{v_c} \rangle + \frac{2 \cdot \langle S(v) \rangle \cdot (\lambda_\phi^2 + \frac{\lambda_\omega}{2})}{(1 + \lambda_\phi^2)}$$

$$\frac{\partial \ln B}{\partial \ln a/\epsilon} = -2 \cdot \frac{(1 - \lambda_\phi^2 - \lambda_\omega)}{(1 + \lambda_\omega^2)} - (1 - \lambda_\omega) \cdot T \cdot \langle \frac{v}{v_c} \rangle + \frac{2 \cdot \langle S(v) \rangle \cdot (1 - \lambda_\phi^2 - \lambda_\omega)}{(1 + \lambda_\phi^2)}$$

where

$$\lambda_\omega = \frac{\omega}{\sqrt{1+\omega}\,(1 + \tau + \sqrt{1+\omega})}$$

$$\lambda_\phi = \frac{2 k_\phi (1 + \sqrt{1+\omega})}{\sqrt{1+\omega}}$$

With expressions for the nucleation and growth sensitivities at hand, the stability of a given steady state operating condition can be tested based on a given nucleation model by evaluation of b*, g* and m and application of the stability criteria obtained previously.

Limiting Relationships For Nucleation and Growth Sensitivities

It is possible to simplify the forms for the nucleation and growth sensitivities based on the relative value of the termination to capture rate of liquid phase radicals.

This corresponds to the order of magnitude of $\omega = \frac{4 k_T I}{(q l \epsilon)^2}$

From a study of these limiting cases, the range of values for the nucleation and growth sensitivities may be narrowed. The resulting limiting cases shall be useful in simplifying the discussion of reactor stability as they shed light on the physics underlying the competitive processes which are occurring simultaneously in such systems.

The range of values over which the growth sensitivities may vary can be narrowed by considering the expressions for the growth sensitivities for the limiting cases where all polymerization is occurring either in the liquid or in the solid. Asymptotic forms for the growth sensitivities gm, g_I, and γ may be obtained when either phase is the predominate locus of polymerization, corresponding to the kinetic regimes in which the radical capture rate is either negligible or large compared to the termination rate of radical in the liquid phase. Quantitatively this corresponds to the ranges in which $\omega \gg 1$ and $\omega \ll 1$ respectively. Asymptotic forms for the growth sensitivities obtained from equations II-(34a, 34b, 34c) are tabulated in Table II-4.

Independent of the value of ω, $g_m \sim 1$ when the liquid in the predominate locus of polymerization. This is due to fact that λ_{1L} and μ_{1L} are both linear in M_L. When the solid is the primary locus of polymerization, $g_m \sim \frac{\partial \ln M_S}{\partial \ln M_L} = \frac{1}{1+j \cdot M_L}$, independent of ω. Thus for this case, gm, may vary from 1, when the adsorption equilibrium is virtually linear in M_L, to O, corresponding to M_S at its saturation value, where G is independent of M_L. When the liquid is the primary locus of polymerization, the terms involving μ_{1L} and λ_{1L} will predominate in g_I and γ when $\omega \gg 1$ and $\omega \ll 1$ respectively. That is, most of the polymerized monomer will be associated with terminated polymer molecules (μ_{1L}) when termination is large compared

to capture of radicals ($\omega \gg 1$). Most of the polymerized monomer will be associated with growing radicals (λ_{1b}) when termination is small compared to capture of radicals ($\omega \ll 1$). Thus the value of g_I and γ for $\omega \gg 1$ and $\omega \ll 1$ correspond to the exponents of I , a/ϵ in μ_n and λ_{1b} respectively (See Table 2). When the solid is the primary locus of polymerization, the term representing the polymerization rate in solid = $k_p \cdot M_s \cdot \lambda_{0s}$ predominate in the expressions for g_I and γ . Since $\lambda_{0s} \propto \sqrt{\lambda_{0a}}$, the values of g_I and γ are simply the exponential dependence on λ_{0s} of I and a/ϵ in the limiting ranges $\omega \gg 1$ and $\omega \ll 1$ (See Table 1).

Limiting forms for the nucleation sensitivites may also be obtained for each model in the regions in which $\omega \gg 1$ and $\omega \ll 1$. With the approximation that $\langle S(v) \rangle \approx \frac{\pi v_s}{2} \left\langle \frac{v}{v_c} \right\rangle$ for the pure coalescence model the resulting forms for the nucleation sensitivities are summarized in Table II - 5.

Table II-4: Limiting values of growth sensitivity of reactor variables

GROWTH SENSITIVITY	LOCUS OF POLYMERIZATION			
	ALL IN LIQUID		ALL IN SOLID	
	$\omega \gg 1$	$\omega \ll 1$	$\omega \gg 1$	$\omega \ll 1$
$\frac{\partial \ln G}{\partial \ln M_L} = g_m$	1	1	$\frac{1}{1+j M_L}$	$\frac{1}{1+j M_L}$
$\frac{\partial \ln G}{\partial \ln I} = g_I$	.5	1	.25	.5
$\frac{\partial \ln G}{\partial \ln q/\epsilon} = \gamma$	-1	-2	0	-.5

Table II-5: Limiting Values of Nucleation Sensitivity To Reactor Variables

NUCLEATION SENSITIVITY	$\omega \gg 1$	$\omega \ll 1, \omega \cdot T \ll 1$
$\frac{\partial \ln B_g}{\partial \ln M_L}$	$T-1$	T
$\frac{\partial \ln B_g}{\partial \ln I}$	$-\frac{T}{2}-\frac{3}{2}$	1
$\frac{\partial \ln B_g}{\partial \ln a_{l\epsilon}}$	0	$-T$
$\frac{\partial \ln B_c}{\partial \ln M_L}$	$\frac{\lambda_\phi^2}{2} T$	T
$\frac{\partial \ln B_c}{\partial \ln I}$	$\frac{1}{2}+\frac{\lambda_\phi^2}{2} T$	$\frac{T}{\lambda_\phi}$
$\frac{\partial \ln B_c}{\partial \ln a_{l\epsilon}}$	$-\lambda_\phi^2 (T-1)$	$-2T$

DISCUSSION

The models considered in this paper can be used to determine quantitatively whether continuous precipitation polymerization reactors will be linearly unstable for a given steady state operating condition. Data tested for continuous production of polyacrylonitrile in an aqueous medium indicate cyclic variation in product quality (mean particle size, M.W.D.) will occur. Large fluctuations in M.W.D. are possible, as the locus of polymerization varies over a cycle if the propagation and termination rates for each phase differ significantly. These fluctuations may be enhanced, as diffusional effects, neglected in our treatment, increase the dependence of molecular weight on particle size. The mechanism of this cyclic instability can best be viewed in terms of the complex interaction between the nucleation and the growth of the precipitated particles.

Due to the high sensitivity of the instantaneous nucleation rate to reactor variables, a small perturbation from the steady state operating condition can drastically affect the number of stable nuclei which are being produced. Since it takes on the order of the several mean residence times for these new nuclei to grow to the mean size, there will be a considerable lag in time from which the particles were produced to the time at which they have an appreciable effect on the material balances. The effect of this complex interaction between nucleation and growth can be viewed more easily by considering a specific mechanism for particle formation.

Consider the simple case in which coalescence is assummed negligible. (Note that in the averaged coalescence model, setting $\beta_c = 0$ (no coalescence of subcrits) infers that termination in the liquid is negligible. (In the averaged coalescence model termination inherently occurs subsequent to coalescence.)

In this discussion, we need not be limited to this case and we first consider the growth model. In the growth model, the nucleation rate is characterized by the value of T, the ratio of the death to growth rates of liquid phase radicals past the critical size. This exponential character or nucleation sensitivity is, for the sake of discussion, the essential functional dependence of the nucleation rate on M_L, I and a/ϵ, the reactor variables. That is, one may approximate $B \propto e^{-T}$

where $$T = \frac{a/\epsilon}{M_L}\left(1+\sqrt{1+\frac{4k_T I}{(a/\epsilon)^2}}\right)\frac{L_c^3}{3}$$

Independent of the predominant death mechanism for the liquid radicals, (i.e. the order of magnitude of $\omega = \frac{4k_T I}{(a/\epsilon)^2}$) the nucleation sensitivity to monomer concentration in the liquid is

$$\frac{\partial \ln B}{\partial \ln M_L} \sim T.$$

The nature of the potential cyclic instability can be viewed in terms of a perturbation in monomer concentration. The effects of initiator and area dependence can be superimposed to give a composite description.

Consider the continuous production of a precipitating polymer in aqueous solution in a C. F. S. T. R. at a steady state operating point. A small positive perturbation in monomer concentration can cause a large increase in the number of potential nuclei reaching the critical size. (This can be best seen by a simple sample calculation. Say T = 27 for the growth model at the steady state in question. A 10% fluctuation in the instantaneous value of $M_L \propto 1/T$ will cause a large variation in $B \propto e^{-T}$. That is, the instantaneous nucleation rate can increase by an order of magnitude.) Physically, this can be explained in terms of the increase in the propagation rate of growing liquid radicals due to the higher monomer concentration. With this small increase in polymerization rate in the liquid, a great increase in probability of a radical surviving to produce a nuclei occurs. Thus, a small perturbation in monomer concentration causes a drastic effect on the

instantaneous nucleation rate due to this highly nonlinear dependence of $\mathcal{B}$ on M_L. For a time, the surplus of stable nuclei produced above the steady state level will have little noticeable effect. That is, initially they contain negligible mass, and have no effect on the material balances. The growth of these particles to mean size will take several residence times to occur. Thus, the production of a higher area concentration of solids in the system lags in time from the point at which the precipitated particles were formed.

Consider the range in this potentially cyclic system where the area concentration of solids is reaching a maximun. As the system approaches the extremum point, the monomer concentration in the liquid will now be at its lowest point. The increase in the area concentration of solids will coincide with an increase in monomer consumption as the locus of polymerization shifts towards the surface of the precipitated particles. This increase in monomer consumption is due to the fact that the termination rate of radicals adsorbed by the solid particles should be much lower than that occurring in the liquid. This results in a longer mean lifetime of the radicals for growth. Thus, with a larger polymerizing surface, the overall rate of monomer consumption will increase. This lowering of M_L is further enhanced by the fact that a larger surface will adsorb more monomer than at steady state conditions. The effect of this low monomer concentration in the liquid (relative to the steady state) will be to drastically reduce the instantaneous nucleation rate of new precipitated particles. Further, since the nucleation dependence on area of solids $\beta \leq 0$, the larger area relative to the steady state operating condition will also tend to decrease the nucleation rate. This is due to the increased capture rate of potential nuclei relative to the steady state rate. The lower level of the critical asymptotic stability limits for $\omega \ll 1$ as compared to the area independent range of $\omega \gg 1$, is

thus qualitatively, as well as quantitatively clear. That is, a large negative β clearly has an unstablilizing effect on reactor dynamics.

At the other extreme of a potential limit cycle, the monomer concentration in the liquid will be at its relative maximum and the area concentration will be at its minimum. Both of these factors will tend to maximize the instantaneous nucleation rate. Thus, it can be seen how the lag between the time at which stable precipitated particles are formed to the time at which they grow and consume the surplus monomer which produced them, provides the fundamental mechanism for cyclic behavior in the production of precipitating polymers in the continuous flow stirred tank reactors. The effects of initiator and area concentration follow directly from the previous analysis. If one is dealing with a system in which the kinetic regime $\omega \gg 1$, fluctuations of initiator concentration effects nucleation due to changes in the termination or rather the death rate of growing radicals: for $w \gg 1$ (i.e., in a system in which termination is large compared to capture,) $T \sim \frac{\sqrt{k_t I}}{M_L} \chi_{cr}$. However, note the initiator sensitivity in equation II-(32a) for b* is not weighted as heavily as the monomer sensitivity. It is not through the value of b_I in b* that the effect of initiator concentration is weighted, but rather covertly through its effect on locus of polymerization (related in γ). When $\omega \ll 1$, $T \sim \frac{a/\epsilon}{M_L} \cdot \chi_{cr}$ as capture is the only death mechanism for liquid phase radicals. Here the negative nucleation sensitivity to area has a strong unstabilizing effect which has been discussed qualitatively above, and quantitatively through its effect on the critical stability limits.

For two monomer levels M_o in the feed, log a/ϵ is plotted vs. log θ in Figure II-(1). The critical stability limits are plotted for each feed condition. Note that at the higher level of M_o, the system tends to be unstable at a lower residence time. (This effect is also occurring at lower coversions.) Optimum reactor conditions will, therefore, be a delicate balance between reactor yield and product quality.

For two initiator levels in the feed, ln a/ϵ is plotted vs ln θ in Figure II-(1). The critical stability limits are plotted for each feed condition. Note, that at the lower level of I_o the system tends to be unstable at a shorter residence time. (This also occurs at lower conversions.) Here again, one is reminded that optimum reactor conditions will be a compromise between reactor yield and product quality. That is, although high initiator levels in the feed has a stabilizing effect on the system's dynamic behavior, it has an adverse effect on achieving high molecular weight. (11)

The increase in stability at lower monomer concentrations and high initiator concentrations is due primarily to the manner in which their variation shifts the locus of polymerization. This effect may be viewed in the following manner. The nucleation sensitivity to monomer, quantitatively, is weighted with the growth sensitivity to area. Consider the nucleation sensitivity in the range $w \gg 1$, i.e., the range in which the probability of radical termination in the liquid is large compared to the probability of capture by solid particles. The overall nucleation sensitivity $b^* \approx \left(\frac{1-\epsilon}{\epsilon} \frac{\partial \ln B}{\partial \ln M_L}(1+\gamma)\right)$. The larger the percentage of polymerization which occurs in the liquid phase, the closer γ will be to -1. Thus, factors that tend to decrease γ can have a stabilizing effect due to the lowering of b*, independent of the change value of $\frac{\partial \ln B}{\partial \ln M_L}$.

The critical stability limits plotted previously in the (log a/ϵ log θ) plane all do occur slightly to the right of the peak in a/ϵ. In this range, a positive perturbation in monomer will produce an overall increase in solid polymerization because the accompanying increase in a/ϵ occurs with simultaneous increase in particle number.

This has the predicted destabilizing effect provided one is operating in the range where a/ϵ decreases as the fraction of polymerization occurring in the liquid increases. The accompanied decrease in $(1+\gamma)$ clearly has a stabilizing effect.

Increasing I_o in the feed decreases the number of particles being formed at steady state due to the increase in termination rate at higher I_o. Here again, if one is operating in the range where a decrease in N results in a decrease in a/ϵ, the accompanied decrease in $(1 + \gamma)$ will clearly have a stabilizing effect. In the coalescence model, in contrast, increasing I_o increases the nucleation rate independent of the magnitude ω.

In the range $\omega << 1$, $B \sim I \cdot e^{-\frac{a/\epsilon}{M_L} X_{cr}}$. Although increasing I_o in this range increases the nucleation rate, the strong exponential area dependence (larger negative value of β) predominates in b* over the linear initiator term. Thus, based on the growth model, a variation in I can either increase or decrease nucleation.

The mechanism of the potential cyclic instability in situations in which coalescence cannot be neglected in the particle formation mechanism can also be accounted for in terms of the sensitivity of nucleation via coalescence to the reactor variables M_L, I and a/ϵ and the complex interaction between the nucleation and growth of the precipitated particles.

Consider the effect of a small positive perturbation δM_o on the performance of a given steady state operating condition. In the pure coalescence model, the δM_o results instantaneously in an increase in M_L resulting in an instantaneous increase in the mean size at which the subcritical particles are being generated. Thus, although the δM_L does not affect the number of subcrits generated, the terminated polymer molecules that are forming will be at a larger molecular volume relative to their steady state size. Therefore, relative to the steady state in question, more clusters will be reaching the critical nuclei size in an instant of time. Initially, these surplus nuclei contain a negligible fraction of the total system mass and no appreciable surface. There is, as in the discussion of the growth model, a lag in time from which the particles are formed to the time at which they contribute to a change

in the material balances (increasing a/ϵ and decreasing M_L).

As the surface concentration a/ϵ increases (i.e. as the total area which subcritical size clusters in the liquid contact increases), the instantaneous nucleation rate decreases. That is, the increase in capture rate of subcrits due to the larger capture surface relative to the steady state drastically reduces the survival probability of a growing cluster and can virtually halt instantaneous nucleation. This effect will be at its maximum as a/ϵ approaches its cycle maximum. This effect is further enhanced by the fact that as a/ϵ increases relative to the steady state level, the locus of polymerization shifts towards the solid phase. With a lower termination rate associated with the solid phase, total monomer consumption in the solid phase increases, lowering the value of M_L well below the steady state level. Thus for a time, there will be little instantaneous nucleation as the particles previously present grow at the expense of new particle formation. As the existing large particles are swept out of the system in the reactor effluent, the magnitude of a/ϵ will gradually be reduced below the steady state level as there would have been effectively no new particles nucleating and growing during the period of high a/ϵ . For the averaged coalescence model, the mechanism of the cyclic instability to a perturbation δM_0 is virtually equivalent to that for the pure coalescence model. The only difference lies in the place at which each model accounts for the contribution of a higher instantaneous value of M_L. That is, in the pure coalescence model the δM_L results in an increase in size of the subcrits as they are formed due to an increase in propagation rate of growing radicals prior to termination. The averaged coalescence model picks up this contribution in the averaged growth term for the subcritical clusters.

The mechanism of instability based on the coalescence models to a perturbation in I_o can be viewed in a similar fashion. In the pure coalescence model, a positive δI_o would instantantaneously increase the number of terminated polymer molecules generated due to an increase

in termination rate at high I. Although more subcrits are being generated, the mean size at which they are generated will be smaller. The overall effect of the δI_0 will be to increase the amount of polymerized monomer per unit liquid volume and through this high concentration of polymerized mass an increase in the probability that clusters will grow past the critical size occurs. A positive δI_0 increases the instantaneous nucleation rate for the pure coalescence model. In the averaged coalescence model, a positive δI_0 increases the number of subcrits generated (their generation rate is simply twice the initiator decomposition rate) and has little effect on the averaged growth rate of the subcritical clusters. (See expression for G_A.) A positive δI_0 also produces more polymerized mass in the liquid and, hence, more clusters reaching the critical size. Thus in both coalescence models a positive δI_0 increases the instantaneous nucleation rate in contrast to the growth mechanism in the range $\omega \gg 1$.

Again there will be a lag from the time at which the new nuclei are produced to the time at which they grow to significant size. The effect of the surplus nuclei is to again create a larger a/ϵ relative to the steady state, although there is a time lag from the point at which the particles are produced to the time at which they produce a considerable surface. As a/ϵ becomes large compared to the steady state value, instantaneous nucleation can virtually be suppressed due to the higher capture probability of subcritical clusters and due to the lowering of relative to the steady state that accompanies the shift of polymerization to the solid phase at the higher a/ϵ .

The values of the physical constants used in the quantitative treatment are only first level approximations. They may in reality be off by several orders of magnitude. Rather than attempting to draw conclusions from specific results presented, a general discussion of the applicability of the nucleation models used is in order.

There is evidence that the nucleation process is thermodynamically controlled (4, 5). The need for subcritical particles to reach a "colloidally" stable nuclei size in the nucleation models presented implicitly contains this phenomena. Again the reader is reminded that stability here refers not to reactor stability, but to the fact that particles above the critical nuclei size will not coalesce with one another although a particle above the critical size may capture subcritical particles from the liquid. This is equivalent to considering that although phase transformation of a growing liquid radical may be occurring at a degree of polymerization relatively small compared to the total number of monomer units contained in a particle at the critical nuclei size, one should continue to view the subcritical particles, independent of the nucleation model, as pertaining to the liquid phase. Although the morphology of a growing liquid radical may change from a random coil to a more compacted sphere, this distinction can be neglected with respect to the particle growth and nucleation kinetics. In this analysis kinetic parameters such ad k_{pL}, k_{TL}, h, β , etc. were assumed to be size independent. There may be in reality an acceleration of the growth rate of the growing liquid radicals due to the steric hindrance to termination that will occur as the morphology of the growing radical changes as it reaches its thermodynamically determined solubility limit. Use of size independent rate constants should not bear on the qualitative interpretation of the results presented. The actual stable "colloidal" nuclei size may be much larger than the apparent value used in the numerical calculation. A lower critical size can compensate numerically for the potential autoaccelerative effect without losing the models' characteristic sensitivity of nucleation to reactor variables. The reader, at this point, should be reminded that this development has proceeded from the need to establish a model for the nucleation mechanism from which the nucleation sensitivity to reactor variables can be obtained and not from the point of view of being a model for the actual reaction kinetics.

It has been shown that in the asymptotic range of steady state operating conditions, the critical stability limits, above which limit cycles may occur, is a direct measure of the death to growth rate of subcrits past the critical size, independent of the nucleation model used. That is, in the growth model the critical stability limit is T the death to growth rates of radicals alone past the critical size and for the coalescence models $k\phi^2 \cdot \frac{T}{\omega}$, where $\frac{k^2\rho}{\omega}$ adds a weighting of death via capture to growth via coalescence.

In a system in which coalescence on the colloidal scale is occurring along with liquid radical growth and termination, values of T are much larger than the values obtained by fitting the growth model to a given steady state operating condition. That is, when coalescence is appreciable, pure radical growth and termination are a negligible contribution to B. We have used a change in scale of the critical size to permit a coalescence process to be modelled as a pure birth, growth, death process to achieve steady state results without the numerical difficulties encountered in the evaluation of the coalescence collision integrals. While the growth model cannot quantitatively model the coalescence processes (See comparison of log B vs log G in Figure II-2), one needs to regard the numerical calculation from the qualitative insight gained rather than from the quantitative aspect of the results. There may, indeed, be systems where simple radical growth and termination are the predominant nucleation mechanism although these numerical calculations for acrylonitrile based on the growth model are highly questionable.

In the discussion of the reactor stability, one did not need the precise physical mechanism to account for system instabilities. Rather, independent of the actual complexity of the physical mechanism governing nucleation, it was only necessary to consider the sensitivity of the subcritical particle population to reactor variable fluctuations. Thus, although microscopically each mechanism contains fundamentally different processes, their macroscopic behavior yields similar results.

The pure polymer coalescence model should be a reasonable physical approximation to the nucleation kinetics in systems in which the termination rate of radicals in the liquid is large compared to their capture rate and $k_{Tl} > \beta_c$. This corresponds to the range in which $\omega \gg 1$ and $k_\phi \gg 1$. Even though there might be a finite probability of a radical coalescing with a subcritical polymer aggregate, the contribution of further growth of the coagulated radical will not be a considerable contribution to nucleation provided coalescence is occurring on the same order of magnitude as termination.

The averaged coalescence model should apply to systems in the range in which capture probability of radicals is much larger than chance of mutual termination. This corresponds to systems operating in the range in which $\omega \ll 1$. It has been shown that even when $\omega \gg 1$, the averaged coalescence model can be used provided # radicals/particle is o(1) or greater.

These models account for the fact that as one adds seeds to a batch precipitation polymerization or even emulsion polymerization in progress, one can virtually instantaneously halt further particle formation. If one is operating a system in the range $\omega \ll 1$, then addition of seeds may significantly increase the total surface in the system. But the nucleation sensitivity to area in such cases is proportional to a/ϵ (i.e. $T \approx \frac{a/\epsilon}{M_\nu} x_{cr}$). Thus a small increase in a/ϵ can drastically reduce $B \propto e^{-T}$. Similarly, further addition of initiator only increases the death rate of liquid radicals and, therefore, decreases the probability of subcritical particles reaching the critical size.

The growth model should physically pertain to systems in which coalescence is a minor contribution to nucleation. This would occur in systems in which the polymerization rate of radicals in the liquid is large enough to reach the critical nuclei size prior to physical capture by existing stable particles or prior to mutual coagulation. Variation in ionic strength of the solvent and presence of surface active agents

should clearly play a determining role in these cases as well as the specific systems' monomer-polymer-solvent compatibility.

The effect of the reaction medium in determining the critical nuclei size is beyond the scope of this paper. However, it should be pointed out that due to the strong dependence of the critical stability limits on the initial size, it should be possible to improve stability by variation of ionic strength in the solvent rich phase or by addition of surface active agents. Another method of reduction of the nucleation sensitivity to reactor variable fluctuations would be to seed the system with stable nuclei.

APPENDIX I-A

Development of an Area Dependent Nucleation and Growth Model:

A strong negative dependence of surface on nucleation is inherent in the crystallization mechanism recently proposed by Glassner (12) as are the nucleation models for precipitation polymerization (21, 22, 49). Here Glassner's mechanism is supplied to continuous crystallization. A complex ion or molecule or macromolecular particle serves as a center of condensation for the molecular entities of the crystallizing material. Most of the crystallites, 40-200 A^{o} in diameter are captured by large crystals which are present. A small fraction of the small crystals are able to grow by condensation until they reach a size where their surface then serves as a receptor for other tiny crystallites. Although exact equations for describing such a process involve complex collision integrals that are mathematically virtually untractable, much insight can be obtained by modelling such a coalescence process as a pure birth, growth, death process.

Let B^{o} be the feed rate of the complex ion (22), seed nuclei or macromolecular particle which is serving as a nucleator. Alternatively it might be the total rate of cluster formation, at or near a surface in a secondary nucleation mechanism. Removal of preordered structures from the adsorption layer near a crystal surface (16, 47) as well as growth by incorporation of ion clusters (14) have been discussed. In either case, we take the formation rate to occur in a narrow size range permitting the source term to be written as a delta function at the nuclei size r_o. The tiny growing crystallites are captured by the existing suspension at a rate proportional to the total surface of the suspension per unit liquid volume a/ξ, with a mass transfer coefficient h_c. (For analytic simplicity we take h_c to be size independent.) When a crystallite grows past the critical nuclei size a stable crystal is said to have been nucleated. Here stability refers to the fact that above a critical size, crystals will not be captured by

the large existing large crystals. That is, we are not referring to the thermodynamic stability with respect to dissolution, but rather to stability with respect to coalescence in terms of the probability of death by capture.

We now set down an equation governing the size distribution $\psi(r)$ for the small crystallites.

$$\frac{\partial\{\epsilon\cdot\psi(r)\}}{\partial t} + G_L \frac{\partial\{\epsilon\cdot\psi(r)\}}{\partial r} = B^\circ \delta(r-r_o) - h_c a \psi(r) - \frac{1}{\Theta}\psi(r) - G_L a \psi(r)\delta(r-r_c)$$

Where r_c is the critical nuclei size, r_o is the size of the feed nucleators, Θ is the mean residence time and ϵ is the liquid volume fraction. The last term on the right hand side represents the disappearance from the liquid by the growth of a subcritical nucleus past the critical nuclei size.

If the time scale for crystallite growth and capture is small compared to the mean residence time, one may neglect the time derivative and the takeoff rate and obtain the following quasi-steady state equation for the size distribution:

$$\text{I - (A-1)} \quad \psi(r) = \frac{B^\circ}{\epsilon\cdot G_L} e^{-\frac{h_c a \epsilon (r-r_o)}{G_L}} \quad ; \; r_o < r < r_c$$

The nucleation rate can then be expressed implicity as a function supersaturation* and area concentration as follows:

$$\text{I - (A-2)} \quad B = \text{Growth rate past } r_c = G_L \psi(r_c) = \frac{B^\circ}{\epsilon} e^{-\frac{h_c a \epsilon (r_c - r_o)}{G_L}}$$

($\epsilon \approx \frac{\rho - c_1}{\rho - c}$ as a quasi-steady state approximation.)

The growth rate of the stable crystals may also be expressed as a function of supersaturation and area concentration. Growth of the non-coagulating crystals is taken to be the sum of the contributions of cluster capture and solute mass transfer. That is: Growth rate = cluster capture + solute mass transfer

$$\text{I-(A-3)} \quad G = h_c \int_{r_o}^{r_c} k r^3 \psi(r) dr + G_m$$

where G_m, the contribution of solute mass transfer and surface integration

to growth, is taken here to be a function of supersaturation only.

With r_o small and r_c large compared to the mean crystallite size, A-(A-3) can be written as

I - (A-3a) $$G = k_c \left(\frac{\rho - c}{\rho - c_f}\right) \frac{B^\circ \cdot G_L}{(k_c a/\epsilon)^4} + G_m$$

We now have quasi-steady state kinetic type expressions for $B(c, a/\epsilon)$ and $G(c, a/\epsilon)$ that can be used in the dynamic analysis. We plot the subcritical size particle distribution $\phi(r)$ along with the size distribution $f(r) = \frac{Be}{G} \frac{-(r-r_c)}{\sigma G}$ for the crystals that do not agglomerate in Figure I-A-1 taking $f(r) = \phi(r)$ for $r < r_c$.

We immediately note that this type of modeling accounts for the shape of particle size distribution data reported by Rosen & Hulburt.

Figure I-(A-1): Particle size distribution for system with area dependent nucleation and growth

$$f(r) = \frac{B^o}{\epsilon G_L} e^{\frac{-h_c a/\epsilon (r-r_o)}{G_L}} \quad ; r_o < r < r_c$$

$$f(r) = \frac{B}{G} e^{\frac{-(r-r_c)}{\sigma_G}} \quad ; r > r_c$$

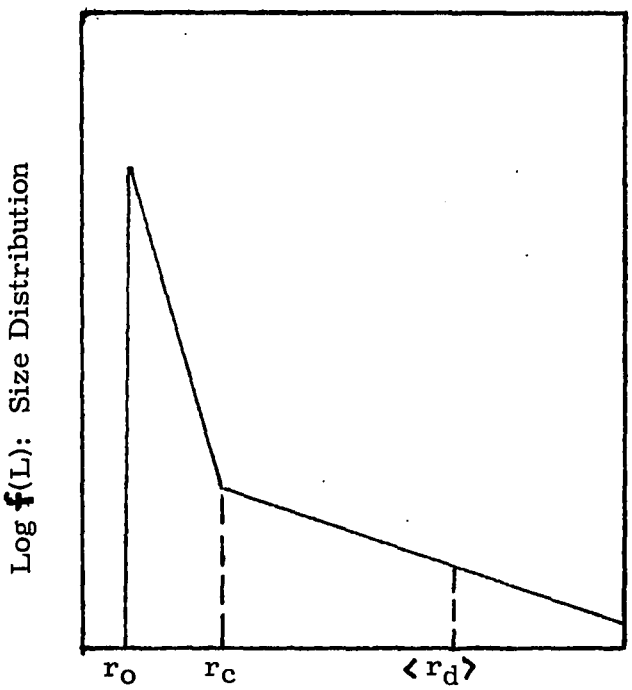

APPENDIX I-B

Uniqueness of Steady State for Area Dependence

The following set of conditions for I-(8) and I-(9) to have a unique solution are not necessary and sufficient conditions. They are, however, reasonably broad sufficient conditions which cover the cases we are studying. The conditions for unique solutions are:

a. $B(c, a/\epsilon)$ and $G(c, a/\epsilon)$ be strictly increasing functions of c vanishing at c_s;

I-(B-1) b. $B(c, a/\epsilon) \cdot G(c, a/\epsilon)^3$ be monotone decreasing* function of a/ϵ;

c. $G(c, a/\epsilon) \frac{a}{\epsilon}$ be strictly increasing function of a/ϵ, vanishing at $a/\epsilon = 0$, and finite as $a/\epsilon \sim \infty$.

The validity of I-(B-1) can best be seen by a graphical examination of I-(8) and I-(9), where working conditions of the crystallizer is such that

$$\rho > c_f > c_s$$

Based on I-(B-1) equation I-(8) expresses c as a strictly decreasing function of a/ϵ. This can best be visualized graphically. Figure I-(B-1) contains plots of each side of equation I-(8) versus c.

From the parametric variation in a/ϵ implicit in Figure I-(B-1), one may plot c versus a/ϵ. In Figure I-(B-2) c decreases for c_f at $a/\epsilon = 0$ to c_s as $a/\epsilon \sim \infty$

Based on I-(B-1) equation I-(9) expressed c as a monotone increasing function of a/ϵ. This may also be seen quite simply from a sketch of I-(9). Figure I-(B-3) is a sketch of each side of I-(9) for various values of a/ϵ.

Thus one can see c is a monotone increasing function of a/ϵ. (Or perhaps a constant in the case where B and G are not functions of a/ϵ. In Figure I-(B-4), c lies between c_s and c_f.

*"monotone decreasing" means simply "not increasing." It includes the situation where B and G do not depend on a/ϵ at all.

Figure I-B-1: Graphical Representation of equation (I-8); Right hand side and Left hand side of (I - 8) versus solute concentration with solid surface area concentration as a parameter

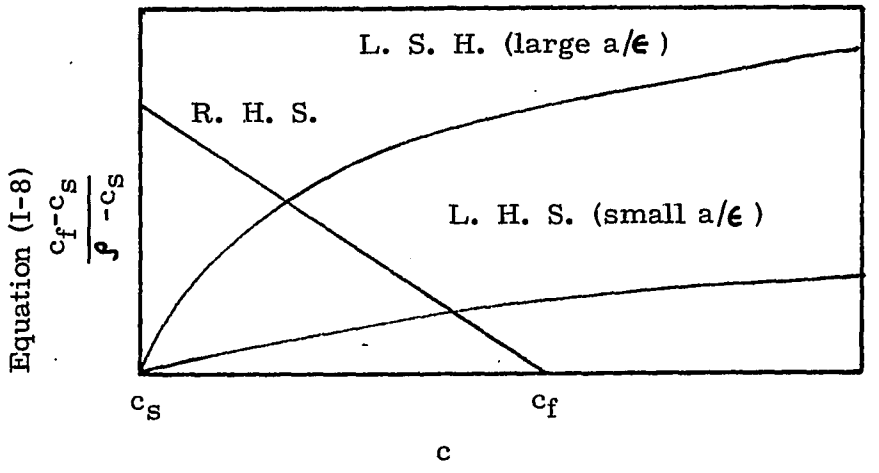

Figure I-(B-2): Graphical representation of locus of points from Figure I-B-1 in which R. H. S. = L. H. S.

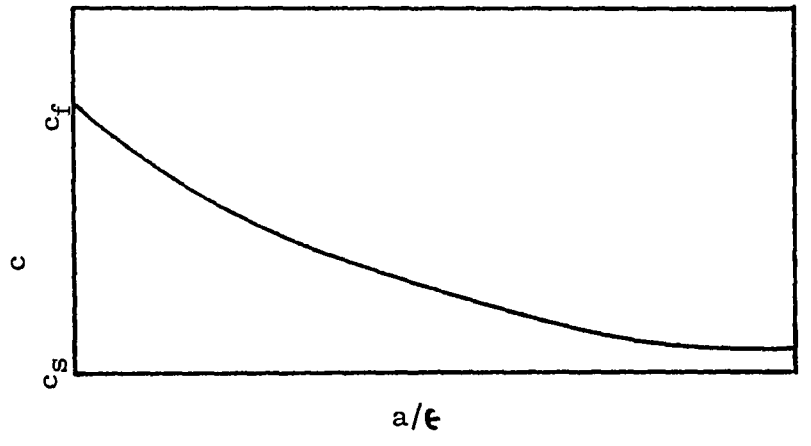

Figure I-B-3: Graphical representation of equation (I-9); Right hand side and Left hand side of (I-9) versus solute concentration with solids surface area concentration as a parameter.

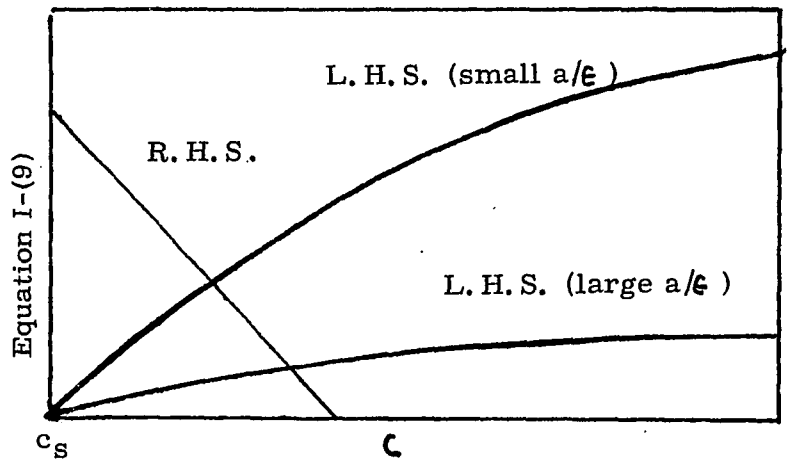

Figure I-(B-4) Graphical representation of locus of points from Figure I-(B-2) in which R. H. S. = L. H. S.

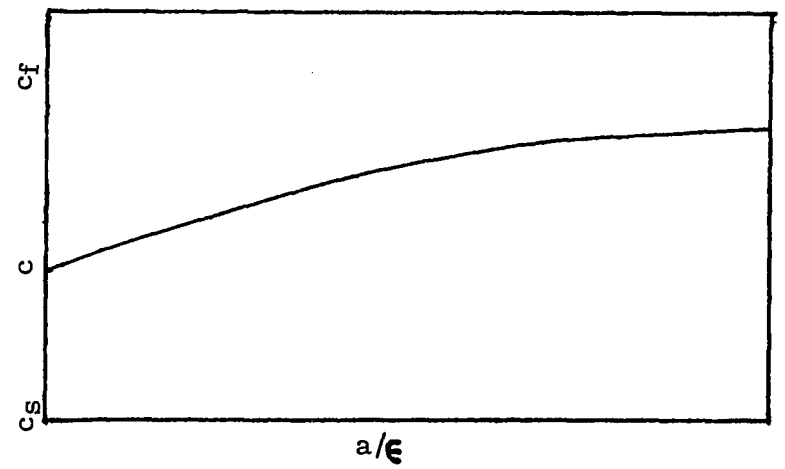

Thus one can see c is a monotone increasing function of α/ϵ. (Or perhaps a constant in the case where B and G are not functions of α/ϵ.) In Figure I-(B-4), c lies between c_s and c_f.

Figure I-(B-4) and Figure I-(B-2) which represent equations I-(9) and I-(8), respectively, obviously have a unique intersection. Hence, equations I-(9) and I-(8) have a unique solution under conditions I-(B-1).

To conclude this section, it is noteworthy to mention that I-(B-1) does not cover the limiting case where G is proportional to $1/(\alpha/\epsilon)$.

It is possible for one to modify condition I-(B-1) to cover this case. The following are the modified conditions:

a. $B(c, \alpha/\epsilon)$ and $G(c, \alpha/\epsilon)$ be strictly increasing functions of c_i vanishing as c_s.

b. $B(c, \alpha/\epsilon)$, $G(c, \alpha/\epsilon)^3$ be strictly decreasing functions of α/ϵ.

c. $G(c, \alpha/\epsilon)$ be a monotone increasing function of α/ϵ.

One can see that these conditions imply a unique solution of I-(8) and I-(9). Figure I-(B-2) now represents a simple monotone decreasing function of c between c_s and c_f. Figure I-(B-3) represents, however, a strictly increasing function of c from c_s at $\alpha/\epsilon = 0$ to c_f at $\alpha/\epsilon \sim \infty$ Hence, the curves represented in Figures I-(2) and I-(4) still have a unique intersection and therefore, the steady state solution is unique.

Uniqueness Conditions for Number Dependent Nucleation

(a) B(c,n) be a monotonically increasing function of c, equal to zero @ $c=c_s$ and be finite for $c \sim c_f$

(b) G(c) be a monotonically function of c, equal to zero @ $c=c_s$ and be finite for $c \sim c_f$

(c) If $B(c,n) = B(c) \cdot n$ then it is required that B(c) not be a constant. $B(c) = 1/\theta$ would then determine the system performance uniquely. If B(c) were constant, then the possibility of there being no steady state relation would exist.

If equation I-(10) can be inverted as $n = n(c, \theta)$, Figure I-(B-5) then becomes a graphical representation of I-(11) and the inversion of I-(10)

Figure I-B-5: Graphical representation of equation I-11 and the inversion of equation I-10 to give n as an explicit function of c.

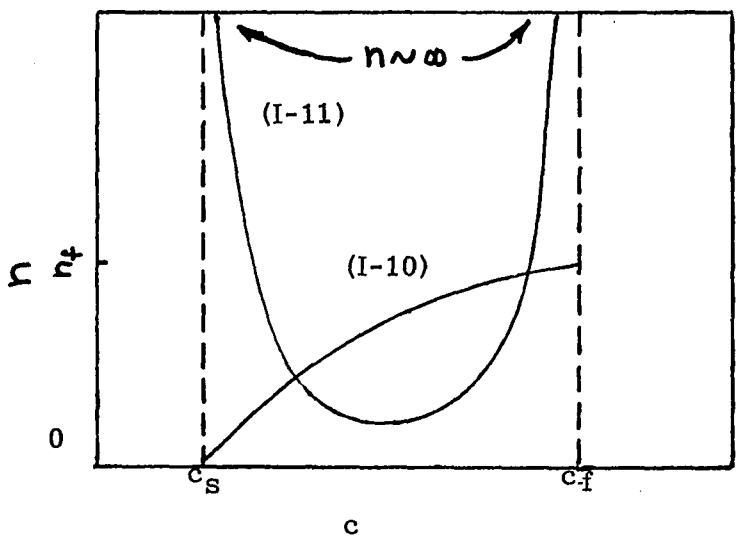

of I-(10). Note that in I-(11) $n \sim 0$ as $c \sim c_s$. and as $c \sim c_f$. The inversion of I-(10) requires $n \sim 0$ as $c \to c_s$. [$n(c_f, \theta)$ need not be the maximum of the inversion of I-(10)].

APPENDIX I-C

Linearized Stability Analysis: B(c, a/ϵ), G(c, a/ϵ)

We now linearize equations I-(12) and I-(13) about

$$\phi(t) = \phi + \delta\phi(t)$$
$$c(t) = c + \delta c(t)$$
$$f(r,t) = f(r) + \delta f(r,t)$$

where ϕ, c and f(r) refer to the steady state solutions. The $\delta\phi(t)$ $\delta c(t)$, and $\delta f(r,t)$ are regarded as small perturbations, so their squares and products may be neglected. The equations may now be written in terms of the perturbed variables:

$$\frac{d\delta\phi(t)}{dt} = -\frac{\delta\phi(t)}{\Theta}$$

$$\frac{\partial\delta f(r,t)}{\partial t} + G\frac{\partial\delta f(r,t)}{\partial r} + \frac{\delta f(r,t)}{\Theta} = -\left(\frac{\partial f(r)}{\partial r}\right)\cdot\delta G(t) \qquad ; r>0$$

$$G\cdot\delta f(r) = -f(r)\{G(t) + \epsilon\delta B(t) + B\delta\epsilon(t) \qquad ; r=0$$

where

$$\delta a(t) = 3K\int_0^\infty r^2\,\delta f(r,t)\,dr$$

$$\delta\epsilon(t) = -K\int_0^\infty r^3\,\delta f(r,t)\,dr$$

$$\delta G(t) = \frac{\partial G}{\partial c}\delta c(t) + \frac{\partial G}{\partial a/\epsilon}\delta\left\{\frac{a(t)}{\epsilon(t)}\right\}$$

$$\delta B(t) = \frac{\partial B}{\partial c}\delta c(t) + \frac{\partial B}{\partial a/\epsilon}\delta\left\{\frac{a(t)}{\epsilon(t)}\right\}$$

and from the steady state solution:

$$f(r) = \frac{\epsilon B}{G} e^{-\frac{r}{\Theta G}} \; ; \; \frac{df(r)}{dr} = -\frac{1}{\Theta G}\frac{\epsilon B}{G} e^{-\frac{r}{\Theta G}}$$

By consultation of the expression for $\delta\phi(t)$, $\delta c(t)$ can be expressed in terms of $\delta\phi(t)$ and $\delta\epsilon(t)$:

$$\delta c(t) = \frac{\delta\phi(t) + (\rho - c)\delta\epsilon(t)}{\epsilon}$$

By expanding the expressions for $\delta B(t)$ and $\delta G(t)$, in terms of $\delta a(t)$ and $\delta\epsilon(t)$ and using the expressions for $\delta c(t)$ in terms of $\delta\phi(t)$ and $\delta\epsilon(t)$ it is possible to rearrange the equations in terms of $\delta\phi(t)$, $\delta f(r,t)$, the moments of $\delta f(r,t) \cdots \delta a(t)$ and $\delta\epsilon(t)$ and parameters which are functions of the steady state operating conditions. The linearized equations become:

$$\frac{\partial \delta f(r,t)}{\partial t} + G\frac{\partial f(r,t)}{\partial r} + \frac{\delta f(r,t)}{\Theta} = \frac{1}{\Theta G}\frac{B}{G} e^{-\frac{r}{\Theta G}} \left\{ \begin{array}{l} \frac{\partial G}{\partial c}\delta\phi(t) + \frac{\partial G}{\partial a_{16}}\delta a(t) \\ + \left\{ (\rho - c)\frac{\partial G}{\partial c} - \frac{a}{6}\frac{\partial G}{\partial a_{16}} \right\}\delta\epsilon(t) \end{array} \right\}; \; r > 0$$

$$-G\,\delta f(r,t) = \left\{ \begin{array}{l} \left(\frac{B}{G}\frac{\partial G}{\partial c} - \frac{\partial B}{\partial c}\right)\delta\phi(t) + \left(\frac{B}{G}\frac{\partial G}{\partial a_{16}} - \frac{\partial B}{\partial a_{16}}\right)\delta a(t) \\ + \left\{ (\rho - c)\left(-\frac{\partial B}{\partial c} + \frac{B}{G}\frac{\partial G}{\partial c}\right) - \frac{a}{6}\left(\frac{B}{G}\frac{\partial G}{\partial a_{16}} - \frac{\partial B}{\partial a_{16}}\right) - B \right\}\delta\epsilon(t) \end{array} \right\}; \; r = 0$$

$$\frac{d\delta\phi(t)}{dt} = -\frac{\delta\phi(t)}{\Theta}$$

It is convenient at this point to introduce dimensionless variables to simplify the study on the linearized equations. Let the physical variables be replaced by dimensionless variables defined in the following manner:

physical	⟶	dimensionless
t		$\Theta \cdot t'$
r		$\Theta G \cdot r'$
$\delta f(r,t)$		$\frac{\epsilon B}{G} \cdot \delta f'(r,t)$
$\delta \phi(t)$		$6K \frac{\epsilon B}{G} (\Theta G)^4 (\rho - c) \delta \phi'(t)$

Note: In terms of the physical variables

$$\delta a(t) = 3K \int_0^\infty r^2 \delta f(r,t) dr$$

so that if one introduces the variable change:

$$\delta a(t) = 6K \epsilon \frac{B}{G} (\Theta G)^3 \delta a'(t)$$

then in terms of the new variables

$$\delta a'(t) = \int_0^\infty \frac{r^2}{2} \delta f(r,t) dr$$

Also, in the physical variables

$$\delta \epsilon(t) = -K \int_0^\infty r^3 \delta f(r,t) dr$$

so that introducing by the new variable

$$\delta \epsilon(t) = 6K \epsilon \frac{B}{G} (\Theta G)^4 \delta \epsilon'(t)$$

one may rewrite the new variable

$$\delta \epsilon'(t) = -\int_0^\infty \frac{r^3}{6} \delta f'(r,t) dr$$

The linearized equations may be rewritten in a dimensionless form. They become:

$$\frac{d\{\delta\phi'(t)\}}{dt} = -\{\delta\phi'(t)\}$$

$$\frac{\partial\{\delta f'(r',t)\}}{\partial t} + \frac{\partial\{\delta f'(r',t)\}}{\partial r'} + \{\delta f'(r',t)\} = e^{-r'}\cdot\{g\,\delta\phi'(t) + \nu\,\delta a'(t) + (g-\alpha\nu)\,\delta\epsilon(t)\};\quad r'>0$$

$$\delta f'(r',t) = (b-g-\nu)\,\delta\phi'(t) + (\beta-\nu)\,\delta a(t) + \{b-g-\alpha(\beta-\nu)\}\,\delta\epsilon(t);\quad r'=0$$

with the following dimensionless parameters:

$$\alpha = 6K\frac{B}{G}(\Theta G)^4 = \frac{1-\epsilon}{\epsilon}$$

$$\beta = \frac{a/\epsilon}{B}\frac{\partial B}{\partial a/\epsilon} = \frac{\partial \ln B}{\partial \ln a/\epsilon}$$

$$\gamma = \frac{a/\epsilon}{G}\frac{\partial G}{\partial a/\epsilon} = \frac{\partial \ln G}{\partial \ln a/\epsilon}$$

$$b = 6K\frac{B}{G}(\Theta G)^4\left[1 + \left(\frac{\rho-c}{c}\right)\left(\frac{c}{B}\frac{\partial B}{\partial c}\right)\right] = \left(\frac{1-\epsilon}{\epsilon}\right)\left(1 + \left(\frac{\rho-c}{c}\right)\frac{\partial \ln B}{\partial \ln c}\right)$$

$$g = 6K\frac{B}{G}(\Theta G)^4\left[\left(\frac{\rho-c}{c}\right)\left(\frac{c}{G}\frac{\partial G}{\partial c}\right)\right] = \left(\frac{1-\epsilon}{\epsilon}\right)\left(\frac{\rho-c}{c}\right)\frac{\partial \ln G}{\partial \ln c}$$

The stability analysis for the system is now based on the dimensionless equations. Here, we carry out a formal spectral analysis which we feel is free of some of the ambiguities of the customary Laplace transform methods. The dynamic equations have been put in a form so as to identify the linear operator $\mathcal{L}$

$$\frac{\partial}{\partial t'}\begin{Bmatrix} \delta\phi'(t) \\ \delta f'(r,t) \end{Bmatrix} = \mathcal{L}\begin{Bmatrix} \delta\phi'(t) \\ \delta f'(r,t) \end{Bmatrix}$$

A formal spectral analysis on $\mathcal{L}$ requires solving the associated eigen value problem

$$\mathcal{L}\begin{Bmatrix} \phi'(t) \\ \delta f'(r,t) \end{Bmatrix} = s\begin{Bmatrix} \delta\phi'(t) \\ \delta f'(r,t) \end{Bmatrix}$$

It should be clear that either $\delta\phi'(t)=0$ or $s = -1$ to fulfill the eigen value problem. Since we are only interested in what the analysis can tell us about possible instabilities, one may summarily set $\delta\phi'(t) = 0$. This leaves us with the equation rewritten in the form as:

$$s\delta f'(r) = -\frac{\partial \delta f'(r)}{\partial r} - \delta f'(r) + e^{-r}\{a_1\delta a' + \epsilon_1\delta\epsilon_1\}$$

$$\delta f'(0) = a_2\delta a' + \epsilon_2\delta\epsilon'$$

where:

$$a_1 = \gamma$$
$$\epsilon_1 = q - \alpha\gamma$$
$$a_2 = b - q - \alpha(\beta-\gamma)$$
$$\epsilon_2 = b - q - \alpha(\beta-\gamma)$$

are constructs of the dimensionless steady state parameters.

Conditions such that the above has a solution generates the characteristic equation. The upshot of these computations is to obtain the characteristic equation in terms of these parameters which depend on the steady state operating conditions. The characteristic polynomial is:

$$P(s) = s^4 + (4+g^*)s^3 + (6+4g^*)s^2 + (4+6g^*-m)s + (1+b^*+3g^*-m)$$

where:

$$b^* = b(1+\gamma) - \beta(g+a)$$
$$g^* = g - \gamma(a+1)$$
$$m = \beta - \gamma$$

} are parameters based on the steady state operating conditions

Application of the Routh-Hurwitz criteria to the aforementioned results in stability criteria for the system. These conditions are:

$$4+g^* > 0$$

$$20+16g^* + 4g^* + m > 0$$

$$(4+6g^*-m)(20+16g^*+4g^{*2}+m) - (4+g^*)^2(1+b^*+3g^*-m) > 0$$

$$1+b^*+3g^*-m > 0$$

Linearized Stability Analysis: B(c,n), G(c)

In this section we develop stability criteria for the operation of a continuous crystallizer with number dependent nucleation kinetics. We again rewrite the crystallizable material balance in terms of the total solute-crystal resource function. The dynamic equations are then:

$$\frac{\partial f(r,t)}{\partial t} + G\frac{\partial f(r,t)}{\partial r} = -\frac{1}{\Theta} f(r,t) \quad ; r > 0$$

$$G f(r,t) = B \quad ; r = 0$$

$$\frac{d\phi(t)}{dt} = \frac{c_i}{\Theta} - \frac{\phi(t)}{\Theta}$$

with

$$\phi(t) = \epsilon(t)\cdot c(t) + (1-\epsilon(t))\rho$$

$$n(t) = \int_0^\infty f(r,t)\,dr$$

$$\epsilon(t) = 1 - k\int_0^\infty r^3 f(r,t)\,dt$$

We now linearize the equations about their steady state solutions Taking

$$\phi(t) = \phi + \delta\phi(t)$$

$$c(t) = c + \delta c(t)$$

$$f(r,t) = f(r) + \delta f(r,t)$$

where ϕ, c and f(r) refer to the steady state solutions.

The $\delta\phi(t)$, $\delta c(t)$ and $\delta f(r,t)$ are regarded as small perturbations, so their squares and products may be neglected. The governing equations above may now be written in terms of the perturbed variables following similar rearrangement techniques as presented in the surface dependent case.

$$\frac{\partial \delta f(r,t)}{\partial t} + G\frac{\partial \delta f(r,t)}{\partial r} + \frac{1}{\Theta}\delta f(r,t) = \frac{B}{\Theta G^2} e^{-\frac{r}{\Theta G}} \left\{ \frac{\partial G}{\partial c}\left[\frac{\delta\phi(t) + (\rho - c)\delta\epsilon(t)}{\epsilon} \right] \right\} \; ; \; r > 0$$

$$G\,\delta f(r,t) = -\frac{B}{G}\left\{ \frac{\partial G}{\partial c}\left[\frac{\delta\phi + (\rho - c)\delta\epsilon}{\epsilon} \right] \right\} + \frac{\partial B}{\partial c}\left\{ \left[\frac{\delta\phi + (\rho - c)\delta\epsilon}{\epsilon} \right] + \frac{\partial B}{\partial n}\delta n \right\} \; ; \; r = 0$$

$$\frac{d\,\delta\phi(t)}{dt} = \frac{\delta\phi_0(t)}{\Theta} - \frac{\delta\phi(t)}{\Theta}$$

It is again convenient to introduce dimensionless variables to simplify the study on the linearized equations. Let the physical variables be replaced by dimensionless variables defined in the following manner:

physical	⟶	dimensionless
$\delta f(r,t)$		$\frac{B}{G} \cdot \delta f'(r,t)$
r		$\Theta G \cdot r'$
t		$\Theta \cdot t'$
$\delta\phi(t)$		$\alpha\epsilon(\rho - c)\,\delta\phi'(t)$

The linearized equations may be rewritten in a dimensionless form. They become:

$$\frac{d\{\delta\phi'(t)\}}{dt} = -\{\delta\phi'(t)\}$$

$$\frac{\partial \delta f'(r,t)}{\partial t} + G\frac{\partial f'(r,t)}{\partial r} + \delta f'(r,t) = e^{-r}\{q\,\delta\phi'(t) + g\,\delta\epsilon'(t)\} \; ; \; r > 0$$

$$\delta f'(r,t) = (q - b)\,\delta\phi'(t) + b_n\,\delta n'(t) + (b - g)\,\delta\epsilon'(t) \; ; \; r = 0$$

where:

$$\alpha = \frac{1+\epsilon}{6}$$

$$b = \alpha\left(\frac{\rho-c}{c}\right)\frac{\partial \ln B}{\partial \ln c}$$

$$g = \alpha\left(\frac{\rho-c}{c}\right)\frac{\partial \ln B}{\partial \ln c}$$

$$b_n = \frac{\partial \ln B}{\partial \ln n}$$

Following the method outlined in the surface dependent section, we can again extract a linear operator and carry out the spectral analysis. We again note that either $\delta\phi'(r) = 0$ or $s = -1$ to fulfill the eigen value question for this system. We are then left with the equation in the following form:

$$\frac{d\,\delta f'(r)}{dr'} + (s+1)\,\delta f(r) = g\,\delta\epsilon'\,e^{-r'} \quad ; \quad r'>0$$

$$\delta f'(r) = (b-g)\,\delta\epsilon' + b_n\,\delta n' \quad ; \quad r'=0$$

with

$$\delta n' = \int_0^\infty \delta f'(r)\,dr$$

$$-\delta\epsilon' = \int_0^\infty \frac{r^3}{6}\,\delta f'(r)\,dr$$

The characteristic equation can then be written as the following polynomial:

$$P(s) = s^4 + (4+g-b_n)s^3 + (6+4g-b_n(3+g))s^2 + (4+6g-3b_n(1+g))s + (b+(1-b_n)(1+3g)) = 0$$

Application of the Routh-Hurwitz criteria to the above results in stability criteria for the system. These conditions are:

$$4+g-b_n > 0$$

$$\{(4+g-b_n)(6+4g-b_n(3+g)) - (4+6g-3b_n(1+g))\} > 0$$

$$\left\{\begin{array}{l} 4+6g-3b_n(1+g)\left(\{4+g-b_n\}\{6+4g-b_n(3+g)\} - \{4+6g-3b_n(1+g)\}\right) \\ \quad -(b+(1+3g)(1-b_n)(4+g-b_n)^2 \end{array}\right\} > 0$$

$$\{(1+3g)(1-b_n)+b\} > 0$$

APPENDIX I-D

The characteristic polynomial representing the system is:

$$P(s) = s^4 + (4+g^*)s^3 + (6+4g^*)s^2 + (4+6g^*-m)s + (1+b^*+3g^*-m)$$

By application of the Routh-Hurwitz criteria one may obtain directly the conditions that the system will be stable if and only if:

$$4+g^* > 0$$

$$20+16g^*+4g^{*2}+m>0$$

I-(D-1) $$(4+6g^*-m)(20+16g^*+4g^{*2}+m) - (4+g^*)^2(1+b^*+3g^*-m) > 0$$

$$1+b^*+3g^*-m > 0$$

It is possible through rearrangement of (D-1) to represent the stability conditions in a form which can be more clearly interpreted.

To begin with, it is possible to rewrite the first two inequalities:

I-(D-1)

a - $$g^* > -4$$

b - $$(g^*+2)^2 > -\left(\frac{4+m}{4}\right)$$

Note that condition (D-2b) is vacuous for $m = -2$. The last two conditions may be rewritten as:

I -(D-2c, d) $$-(3g^*+1-m) < b^* < \left\{ \frac{21g^{*3}+(87-3m)g^{*2}+(128-2m)g^*+64-m^2}{(g^*+4)^2} \right\}$$

At this point it is clear that the first two inequalities show a range for g* and the last two show stable limits on b* for all values of the parameters.

Thus, in order to define the stable regions in the (b*, g*) plane with m as a parameter, one must be careful in applying the results obtained from developing the results of the Routh-Hurwitz criteria.

Although it is possible when $m < -4$ for $b^*_1 = (3^* + - m)$ and

$$b_2^* = \left\{ \frac{21g^{*3} + (87-3m)g^{*2} + (120-21m)g^* + 64 - m^2}{(g^*+4)^2} \right\}$$

to have three intersections, it can be shown that the entire set of stability criteria contains conditions that require $g^* >$ constant (i.e. a function of m only and is the rightmost intercept of (b^*_1, b^*_2). Hence one need only be concerned in the (b^*, g^*) plane with values of b^*, g^* for $g^* >$ a value.

One may verify these facts by rearrangement of the stability condition

$$b^*_1 < b^* < b^*_2$$

Recalling that multiplying all terms in an inequality by a positive factor or adding a quantity to all the terms in the inequality does not change the nature of the inequality, one may simplify the presentation by multiplying the inequalities on b^* by $(g^* + 4)^2$ a positive constant since g^* is real and subtracting $-(3g^* + 1-m)\ (g^* + 4)^2$ from each term in the inequality. One now has the following inequality:

$$0 < \Psi^*(b^*, g^*, m) < P(g^*, m) \; ; \; g^* \geq -m$$

where:

$$\Psi^*(b^*, g^*, m) = (g^*+4)^2 \left(3g^* + 1 - m + b^* \right)$$

$$P(g^*, m) = 24g^{*3} + (112-4m)g^{*2} + (184-10m)g^* + 80 - 16m - m^2$$

That is to say, the stable region is bounded by those values of $\Psi^*(b^*, g^*, m)$ which lie below the cubic polynomial $P(g^*, m)$ and above zero. It can be shown that conditions I-(D-2a, b) result in a stability requirement that for g^* is greater than a constant in which the constant is > -2.

A final simplification can be made by recognizing that conditions

I -(D-2b)

$$g^* > -2 + \sqrt{-\left(\frac{m+4}{4}\right)}$$

and

$$g^* > -2 - \sqrt{-\left(\frac{m+4}{4}\right)}$$

are zeros of the polynomial $P(g^*, m)$. Thus, $P(g^*, m) = 0$, which is a stability region limit of I-(D-3) has the roots

$$g_1^* = -2 + \sqrt{-\left(\frac{m+4}{4}\right)}$$

$$g_2^* = -2 - \sqrt{-\left(\frac{m+4}{4}\right)}$$

$$g_3^* = -\frac{4}{3} - \frac{2}{3}\left(\sqrt{-\left(\frac{m+4}{4}\right)}\right)^2$$

Thus the stability boundary $P(g^*, m)$ can have either a single real root or three roots depending on whether or not $-\left(\frac{m+4}{4}\right)$ is greater than zero (i.e. $m < -4$).

Note: for $m = -4$ one root is a repeated root = $g^* = -2$.

Thus, $P(g^*, m)$ will take on one of the following forms depending on the parameter m.

For $m < -4$, $P(g^*, m)$ will be of the following form: (See Figure I-D-1)

In Figure I- D-1 , the region that lies between g_2^* and g_3^* will be unstable independent of which root is larger. If $g_3^* > g_2^*$ condition I-D-26^b requires $g^* < g_2^*$ and $g^* > g_1^*$. Hence, the region above the axis to the right of g_2^* will be unstable. $g_2^* > g_3^*$ occurs only when $m < -20$ and in this region $g^* < -4$. By condition I-D-2a, this region is unstable.

Thus for $m < -4$., one has one stable region bounded by $g^* > -2+\sqrt{-\left(\frac{m+4}{4}\right)}$ lying below $P(g^*, m)$ and above zero.

When $m > -4$, the only real root of $P(g^*, m) = 0$ is g_3^*, and thus the stable region is clearly bounded by $g^* > +2/3 \cdot \left(2 - \left(\sqrt{-\left(\frac{m+4}{4}\right)}\right)^2\right)$ lying below $P(g^*, m)$ and above zero. See Figure I- D-2 .

When $m = -4$, the stability region also has one stable region. See Figure I-(D-3) is a sketch of this limiting case.

Figure I-(D-1): Locus of stable region for area dependent nucleation and growth kinetics with m<-4.

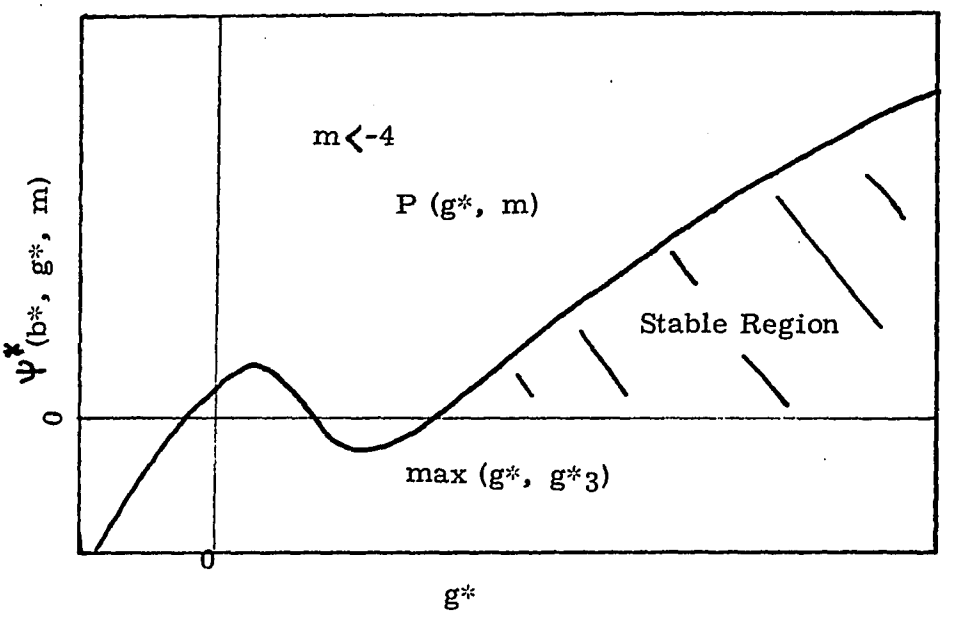

Figure I-D-2: Locus of stable region for area dependent nucleation and growth kinetics with $m > -4$

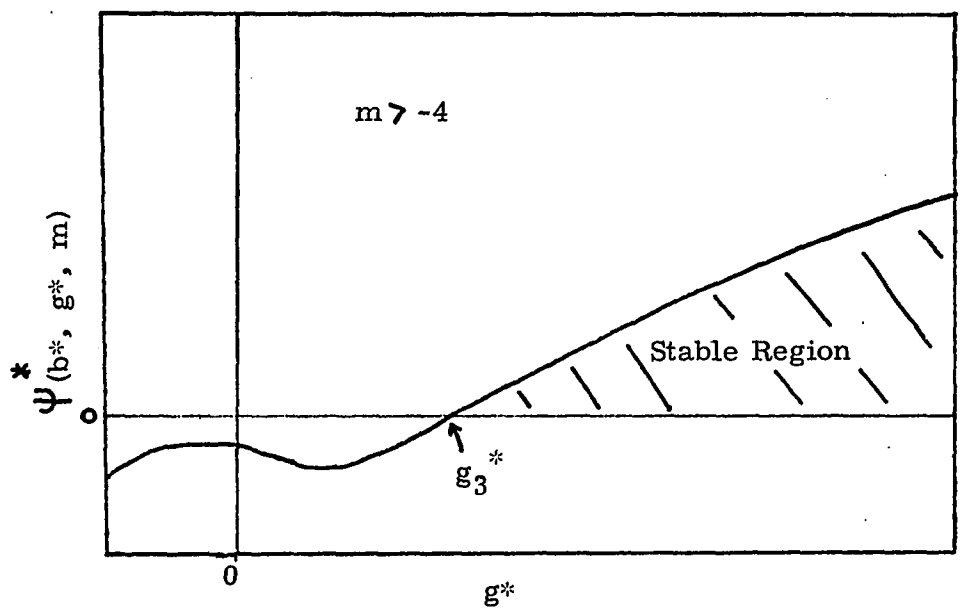

Figure I-D-3: Locus of stable region for area dependent nucleation and growth kinetics with m= -4.

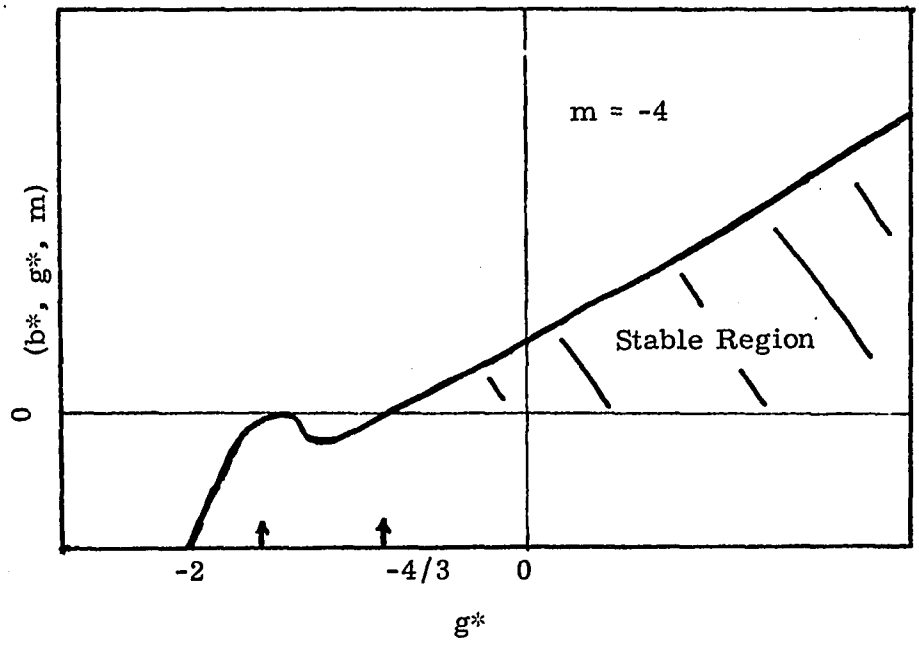

Thus, based on these results which are illustrated in Figures I- (D- 1, 2, 3,), one may be clear that the inequality I- D-3 is of the same nature as I-D-2e, d and, therefore, plots of I- D-2c, d in the (b*, g*) plane similarly have a single stable region with a lower bound:

$g^* > g_1^*$; $m \leq -5$

$g^* > g_3^*$; $m \geq -5$

APPENDIX II-A

The other mechanism for particle formation to be considered here shall be referred to as the averaged coalescence model. This model is physically similar to the macroradical coalescence mechanism previously mentioned.

In the averaged coalescence model, subcritical particles are generated as initiator molecules decompose to form primary free radicals. The primary free radicals grow by monomer addition. They may coalesce with one another forming a cluster of larger size, and the growing radicals and cluster may be captured by existing stable particles. Termination does not affect the number of subcritical particles as it is taken to occur only after coalescence of radicals or subcritical clusters has brought radicals into contact. The name "averaged coalescence model" refers to the fact that in setting up the governing differential-integral equation for the size distribution of subcritical clusters, the growth rate of individual clusters by monomer polymerization is taken to be the liquid phase average growth rate independent of cluster size. i.e., The volumetric growth rate G_a of a subcritical cluster in the averaged coalescence model is equal to $k_{pL} M_L \nu_m$, the volumetric increase due to monomer polymerization per growing free radical in the cluster of size V, times the number of radicals in a cluster of size V, R(v).

$$G_a = k_{pL} M_L \nu_m R(v)$$

The number of radicals in a cluster of size V, R(v), is taken equal to the liquid phase average, independent of cluster size.

$$R(v) = \frac{\text{total number of radicals in liquid}}{\text{total number of subcritical clusters}} = \frac{\int r_L(x)dx}{\int \phi(v)dv} = \frac{\lambda_{oL}}{n_o}$$

Thus, the growth rate of clusters may be taken to be: $G_a = k_{pL} M_L \nu_m \frac{\lambda_{oL}}{n_o}$

Nucleation of a stable precipitated particle occurs when a subcritical cluster grows past the critical size by monomer polymerization or when coalescence of two subcritical polymer clusters forms a cluster above the critical nuclei size. In order to compute the nucleation rate for the averaged coalescence model, one first needs to set up the equation governing the size distribution of subcritical clusters based on this model. Let $\phi(V)$ be the number of subcritical aggregates lying in the volumetric size range V, V + dV per unit liquid volume. The equation governing ϕ (v) is written as:

II-(A-1) $$\frac{\partial\{\epsilon\phi(v)\}}{\partial t} + G_a \frac{\partial\{\epsilon\phi(v)\}}{\partial v} = \mathcal{R}\cdot 2k_z I\epsilon\cdot\delta\left(v-\frac{v_z}{2}\right) - \frac{1}{\theta}\epsilon\phi(v) - h_a\phi(v) + \epsilon\beta\cdot\left\{\frac{1}{2}(\phi * \phi)(v) - \phi(v)\int_0^{V_c}\phi(z)dz\right\} - C(V)$$

where $$G_a = k_{pl} M_c \nu_M \frac{\int r_z(x)dx}{\int \phi(z)dz}$$

and $$C(V) = \epsilon\cdot G_a\cdot\phi(V)\,\delta(v-v_c) + \epsilon\frac{\beta}{2}\int_0^V \phi(z)\phi(v-z)dz\;\Delta(V-V_c)$$

The left-hand side of equation II-(A-1) represents the accumulation of clusters at size V and the averaged growth rate of clusters past the size V respectively. The first term on the right-hand side represents the fact that subcritical clusters are formed at half the molecular volume of the initiator upon decomposition of the initiator molecules. The next two terms represent disappearance of clusters at size V due to outflow from the reactor and capture by stable precipitated particles respectively. The next term represents the total rate at which clusters below size V form clusters at size V via coalescence. The next term represents the rate at which clusters at size V disappear due to coalescence with clusters of all sizes. The last term represents the fact that as clusters grow past the critical size or coalesce to form aggregates above V_c, they are taken to immediately precipitate out as stable particles.

The nucleation rate B, based on the averaged coalescence model, may therefore be computed directly by integrating $C(\bar{V})$ over all $\bar{V}$ above V_c, i.e., the number of stable particles formed per unit reactor volume is

$$\epsilon \cdot B = \int_{V_c}^{\infty} c(v)\,dV$$

or rather

$$B = G_c\,\phi(V_c) + \frac{\beta}{2}\int_{V_c}^{2V_c} dV \cdot \int_{V-V_c}^{V_c} \phi(z)\,\phi(V-z)\,dz$$

where the upper limit $2V_c$ on the coalescence integral is due to the fact that the largest nuclei which can be formed from a population of particles of sizes up to V_c is $2V_c$.

The equations determining the radical and polymer size distributions must be written slightly different from that formulated for the pure coalescence model. In the averaged coalescence model there is a finite probability of a radical or polymer at any size leaving the liquid phase as a growing cluster nucleates a stable solid particle. However, this contribution is virtually always negligible as are the equivalent terms in the preceeding models.

The expression for the particle growth rate G used in the previous formulation is also used here. The same form results from the fact that it does not matter how one computes the growth rate of stable particles based on the capture of clusters. That is, if one takes the total contribution of the clusters or the individual contribution of the growing radicals and terminated polymer models. Mathematically, this is verified by the fact that

$$\int v\,\phi_V\,dV = \int \left(\frac{v_I}{2} + v_m x\right) r_L(x)\,dx + \int (v_I + v_m x)\,P_L(x)\,dx$$

It is again possible to write a closed set of dynamic equations in terms of I, M_L, M_S, $r_L(x)$, r_s, $P_L(x)$, $\phi(v)$ and f where B, G, a, and ϵ are expressed as implicit functions of the reactor variables. The equations

governing the dynamic behavior of precipitation polymerization reactors based on the averaged coalescence model are essentially equivalent in form as those given on page (14).51

For the averaged coalescence model the nucleation sensitivities may be considered in a similar fashion as for the pure coalescence model. Using the expressions obtained in the steady state analysis to compute the nucleation sensitivities for the quasi steady state results in equation II-A-2

$$B = B_g + B_c = G_a \phi(V_c) + \frac{\beta_c}{2} \int_{V_c}^{2V_c} dv \int_{v-V_c}^{V_c} \phi(z)\phi(v-z)\,dz$$

where:

$$\phi(v) = P_a e^{-\tau_a \frac{v}{V_c}} \frac{I_1(\sigma_a v)}{\sigma_a v}$$

$$P_a = 4 k_\phi^2 \frac{I}{M_L} \frac{\left(-1+\sqrt{1+\omega/(2k_\phi^2)}\right)}{\left(-1+\sqrt{1+\omega}\right)}$$

$$\sigma_a = \sqrt{\frac{2k_\phi^2 \omega}{\beta^2 m_2}} \left(\frac{a/\epsilon}{M_L}\right) \left(\frac{-1+\sqrt{1+\omega/(2k_\phi^2)}}{-1+\sqrt{1+\omega}}\right)$$

$$\tau_a = \sqrt{1+2k_\phi^2/\omega} \cdot \sigma_a$$

$$k_\phi = \sqrt{R_r/(\beta_c \beta^2 m_2)}$$

Explicit expressions for the values of the $\frac{\partial \ln B_g}{\partial \ln \gamma}$'s are obtained by direct differentiation of $B_g = G_a \cdot \phi(V_c)$ in the following form:

$$\frac{\partial \ln B_g}{\partial \ln \gamma} = \frac{\partial \ln G_a}{\partial \ln \gamma} + \frac{\partial \ln P_a}{\partial \ln \gamma} + \left[\sigma_a V_c \cdot \frac{I_0(\sigma_a V_c)}{I_1(\sigma_a V_c)} - 2\right] \frac{\partial \ln \sigma_a}{\partial \ln \gamma} - \frac{\tau_a \partial \ln \tau_a}{\partial \ln \gamma}$$

Expressions for the values of the $\frac{\partial \ln B_c}{\partial \ln \gamma}$'s are obtained from the complex collision integrals.

$$\frac{\partial \ln B_c}{\partial \ln \gamma} = 2 \cdot \left\{ \frac{\partial \ln P_a}{\partial \ln \gamma} + \left(\langle S(v) \rangle - 1\right) \frac{\partial \ln \sigma_a}{\partial \ln \gamma} - \tau \left\langle \frac{v}{V_c} \right\rangle \frac{\partial \ln \tau_a}{\partial \ln \gamma} \right.$$

where $\langle S(v) \rangle$ and $\left\langle \frac{v}{V_c} \right\rangle$ are weighted integrals in the same form as those in equations ( ) where $S(v)$ in this case is simply

$$S(v) = \sigma_a v \frac{I_0(\sigma_a v)}{I_1(\sigma_a v)}$$

compared to their integral ratio in the pure coalescence model.

P_a, σ_a, τ_a, and G_a are continuous differentiable functions of M_L, I, and a/ϵ. It is possible to compute their logarithmic derivatives analytically. Substituting these values into the expressions for the nucleation sensitivities for the averaged coalescence model results in the following:

$$\frac{\partial \ln B_q}{\partial \ln M_L} = T_a - \sigma_a V_c - 2$$

$$\frac{\partial \ln B_q}{\partial \ln I} = 1 + \left(\frac{\sigma_a V_c}{2} - 1\right)(1 - \lambda_a + \lambda_a') - \frac{T_a}{2}\left(\frac{\omega_a}{1+\omega_a} + \lambda_a' - \lambda_a\right)$$

$$\frac{\partial \ln B_q}{\partial \ln q_\epsilon} = (\sigma_a V_c - 2)(\lambda_a - \lambda_a') - T_a \cdot \left(\frac{1}{1+\omega_a} + \lambda_a - \lambda_a'\right)$$

$$\frac{\partial \ln B_c}{\partial \ln M_L} = 2 + T_a \cdot \left\langle \frac{V}{V_c} \right\rangle - 2\langle S(V) \rangle$$

$$\frac{\partial \ln B_c}{\partial \ln I} = (\lambda_a - \lambda_a') - \frac{T_a}{2}\left\langle \frac{V}{V_c} \right\rangle \left(\frac{\omega_a}{1+\omega_a} + \lambda_a' - \lambda_a\right) + \langle S(V) \rangle (1 - \lambda_a + \lambda_a')$$

$$\frac{\partial \ln B_c}{\partial \ln q_\epsilon} = 2(\lambda_a' - \lambda_a) - T_a \left\langle \frac{V}{V_c} \right\rangle \left(\frac{1}{1+\omega_a} + \lambda_a - \lambda_a'\right) + 2\langle S(V) \rangle (\lambda_a - \lambda_a')$$

where: $\omega_a = \dfrac{\omega}{2k_\phi^2}$

$$\lambda_a = \frac{\omega}{(-1+\sqrt{1+\omega})\sqrt{1+\omega}}$$

$$\lambda_a' = \frac{\omega_a}{(-1+\sqrt{1+\omega_a})\sqrt{1+\omega_a}}$$

BIBLIOGRAPHY

The bibliography for sections I and II are listed separately on the following pages.

Literature Cited - I

1 - Anshus, B.E. and Ruckenstein, E. Chem. Eng. Sci. vol. 28 (1973) pp. 501-513.

2 - Baker, C.G.J. and Bergounou, M.A. Can. J. of Chem Eng. vol. 52 (April, 1974).

3 - Bauer, L.G., Larson, M.A. and Dallons, V.J. Chem Eng. Sci. vol. 29 (1974) pp. 1253-1261.

4 - Bennett, R.C., Fieldelman, H. and Randolph, A.D. Chem. Eng. Prog. vol. 69, no. 7 (July, 1973) pp. 86-93.

5 - Bero, M. and Leczkowski. Przemysl Chemiczny vol. 44, no. 5 (1965 pp. 269-271.

6 - Canning, T.F. Chem Eng. Prog. Symp. Sec. 110, vol. 67 pp. 74-80.

7 - Clontz, N.A. and McCabe, W.L. Chem. Eng. Prog. Symp. Ser. 110, vol. 67 pp. 6-17.

8 - Clontz, N.A., Johnson, R.T., McCabe, W.L. and Rousseau, R.W. Ind. Eng. Chem. Fund. vol. 11, no. 3 (1972) pp. 368-373.

9 - Desai, R.M., Rachow, J.W. and Timm, D.C. AIChE J. vol. 20, no. 1 (Jan. 1974) pp. 43-49.

10 - Finn, R.K. and Wilson, R.E. Agr. Food Chem. vol. 2, no. 2 (1954) p. 66.

11 - Gershberg, D.B. and Longfield, J. E. Paper presented at Symp. 45th AIChE meeting N.Y. (1961); Preprints no. 10.

12 - Glassner, A. Mat. Res. Bull. vol. 8 (1973) pp. 413-422.

13 - Greene, R. and Poehlein, G.W. "Methyl methacrylate polymerization in a continuous stirred tank reactor -- multiple steady states and possible cyclic conversion." Dept. Chem. Eng. Lehigh University Sept. 1972.

14 - Gunn, J.D. and Murphy, M.S. Chem. Eng. Sci. vol. 27 (1972) pp. 1293-1313.

15 - Han. C.D. and Shinnar, R. AIChE J. vol. 14, no. 4 (July, 1968) pp. 612-619.

16 - Johnson, R.T., Rousseau, R.W. and McCabe, W.L. AIChE Symp. Ser. 68 (1972) p. 121.

17 - Lal, D.P., Mason, R.E. and Strickland-Constable, R.F. J. Cryst. Growth vol. 5, no. 1 (1969).

18 - Lei, S.J., Shinnar, R. and Katz, S. AIChE J. vol. 17, no. 6 (Nov. 1971) pp. 1459-1470.

19 - Lei, S.J., Shinnar, R. and Katz, S. Chem. Eng. Prog. Symp. Ser. 110 vol. 67 (1971) pp. 129-144.

20 - Liss, B., Shinnar, R. and Katz, S. "Dynamic Behavior of Precipitation Polymerization Reactors." 163rd Annual Meeting A.C.S., Boston, 1972.

21 - Liss, B., Shinnar, R., Katz, S., Shonshine, R. and Klepfer, J. "Nucleation Models for Precipitation Polymerization." To be published.

22 - Liu, Y. and Botsaris, G.D. AIChE J. vol. 19, no. 3 (May, 1973) pp. 510-516.

23 - Margolis, G., Sherwood, T.K., Brian, D.L.T. and Serofim, A.F. Ind. Eng. Chem. Fund. vol. 10, no. 3 (1971) pp. 439-452.

24 - Matz, G. Chemie-Ingr-Tech. vol. 42, no. 18 (1970) p. 442.

25 - Moyers, C.G. and Randolph, H.D. AIChE J. vol. 19, no. 6 (Nov. 1973) pp. 1089-1104.

26 - Mullin, T.W. Crystallization. CRC Press, 2nd ed., 1972. p. 168

27 - Nyvlt, J. and Mullin. J.W. Chem. Eng. Sci. vol. 25 (1970) p. 431.

28 - Omi, S., Shiraishi, Y., Sato, H. and Kubota, H. J. of Chem. Eng. of Japan vol. 2, no. 1 (1969) pp. 64-70.

29 - Omi, S., Veda, T. and Kubota, H. J. of Chem. Eng. of Japan vol. 2, no. 2 (1969) pp. 193-198.

30 - Omi, S., Veda, T. and Kubota, H. J. of Chem. Eng. of Japan vol. 4, no. 1 (1971) pp. 50-54.

31 - Ottens, E.D.K. and deJong, E.J. Ind. Eng. Chem. Fund. vol. 12, no. 2 (May, 1973) pp. 179-184.

32 - Ottens, E.D.K., Janse, A.H. and deJong, E.J. J. of Cryst. Growth vol. 13, no. 14 (1972) pp. 500-505.

33 - Randolph, A.D., Beer, G.L. and Keener, J. p. AIChE J. vol. 19, no. 6 (Nov. 1973) pp. 1140-1149.

34 - Randolph, A.D. and Cise, M.D. AIChE J. vol. 18, no. 4 (July, 1972) pp. 798-806.

35 - Randolph, A.D. and Larson M.A. Theory of Particulate Processes. Academic Press, N.Y., 1971.

36 - Randolph, A.D. and Larson, M.A. AIChE J. vol. 11 (1965).

37 - Randolph, A.D. and Larson, M.A. AIChE J. vol. 8, no. 5 (1962) p. 639.

38 - Rosen H.N. and Hulbert, H.M. Chem. Eng. Prog. Symp. Ser. 110 vol. 67 pp. 18-26.

39 - Saeman. AIChE J. vol. 2, no. 1 (1956) p. 107.

40 - Saeman and Miller. Chem. Eng. Prog. vol. 43, no. 12 (1947) p. 667.

41 - Suzuki, A., Ho, N.F.H. and Higuchi, W.I. J. of Colloid & Interface Sci. vol. 29, no. 3 (1969) pp. 552-564.

42 - Sherwin, M.B., Shinnar, R. and Katz, S. AIChE J. vol. 13, no. 6 (Nov. 1967) pp. 1141-1154.

43 - Sherwin, M.B., Shinnar, R. and Katz, S. Chem. Eng. Prog. Symp. Ser. vol 65, no. 95 (1969) pp. 75-89.

44 - Thomas, W.M. and Mallison, W,C. Petrol. Refin. no. 5 (1961) p. 211

45 - Timm, D.C. and Larson, M.A. AIChE J. vol. 14, no. 3 (May, 1968) pp. 452-457.

46 - Youngquist, G.R. and Randolph, A.D. AIChE J. vol. 18, no. 2 (March, 1972) pp. 421-429.

47 - Youngquist, G.R., Estrin, T. and Sung. AIChE J.

48 - Hulburt, H. and Katz, S. Chem. Eng. Sci. vol. 191 (1964) p. 555.

Literature Cited - II

1. Bero, M. and Laczkowski. Pryzemysl Chemiczny vol. 44, no. 5 (1965) p. 269.

2. Thomas, W. M. and Mallison, W. C. Petrol. Refin. vol. 40, no. 5 (1961) pp. 211-216.

3. Fitch, R., Presonil, M. and Sprick, K. Journal of Polymer Science Part C, No. 27 (1969) pp. 95-118.

4. Fitch, R. and Isai, C. Polymer Colloids. Plenom Press, N.Y., 1971, p. 73.

5. Sherwin, M.B., Shinnar, R. and Katz, S. AIChE J. vol, 13, no. 3 (Nov. 1967) p. 1141.

6. Thomas, W.M., Gleason, E.H. and Mino J. Journal of Polymer Science no. 24 (1957) pp. 43-56.

7. Dainton, F.S., Saeman, et al. J. of Polymer Science vol, 34 (1959) pp. 209-228.

8. Klepfer, J. Sonshine, R. and Shinnar, R. Presentation at 65th National AIChE Symposium (May, 1969)

9. Baxendale.

10. Liss, B., Shinnar, R. and Katz, S. Paper Presented at 67th Annual AIChE Meeting (Dec. 1974).

11. Liss, B., Shinnar, R. Katz, S., Shonshine, R. and Klepfer, J. "Nucleation Models for Precipitation Polymerization." Paper to be Published.

12. Goldstein, R. R. and Amundson, N.R. Chem. Eng. Sci. vol 20 (1965) pp. 195, 449, 477, 501.

13. Roe, C.P. I & EC vol. 60, no. 9 (Sept. 1968) p. 20.

14. Hulbert, H. and Katz, S. Chem. Eng. Sci. vol. 191 (1964) p. 555.

15. Greene, R. and Poehlein, G.W. "Methyl-methacrylate polymerization in a continuous stirred tank reactor -- multiple steady states and possible cyclic conversion." Dept. Chem Eng. Lehigh University, Sept. 1972.

16. Randolph, A.D. and Larson, M,A, Theory of Particulate Processes. Academic Press, N.Y., 1971.

VITA

Barry Liss was born March 6, 1946 in The Bronx, New York. He graduated from James Monroe High School in June, 1962. He went to C. C. N. Y. in the fall of 1962 and graduated in June, 1967 with a B. E. (Chemical). He continued at C. C. N. Y. working towards a M. E. (Chemical) and simultaneously worked part-time for Chem Systems, Inc., N. Y. He was married to Cyndee Rosen on March 17, 1968. Melanie Liss was born on March 13, 1970.

He worked under Stanley Katz and Reuel Shinnar completing his dissertation in the spring of 1975. On August 1, 1974, he joined Chemico in New Products Development Division and proceeded to contribute to the response to the R. F. P. for a Clean Boiler Fuel Program from O. C. R. Since award of the contract, he has been transferred to Coalcon Company and is working as a senior process engineer.